Apport des techniques De caractérisation 3D Pour l'étude de la propagation des fisssures de fatigue.

J-Y Buffiere … *et beaucoup d'autres*!

Université de Lyon
INSA-Lyon
MATEIS CNRS UMR5510

Co-authors

N. Limodin, M. Herbig, , J. Adrien, I. Serrano, J. Lachambre

W. Ludwig,	**INSA Lyon/ MATEIS**
A. Gravouil, J. Réthoré,	**INSA Lyon/LAMCOS**
E.Ferrié	**INP Grenoble/SIMAP**
H. Proudhon	**ENSMP/CdM**
S. Roux, F. Hild	**E.N.S. Cachan/LMT**
P. Cloetens, E. Boller, J. Baruchel	**ESRF ID 19**

Why 3D imaging of fatigue cracks?

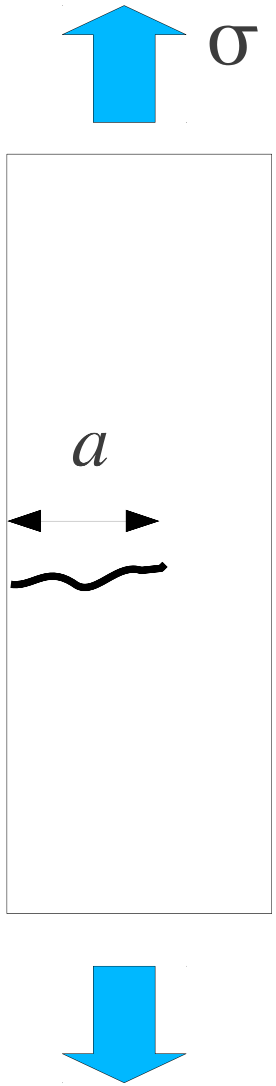

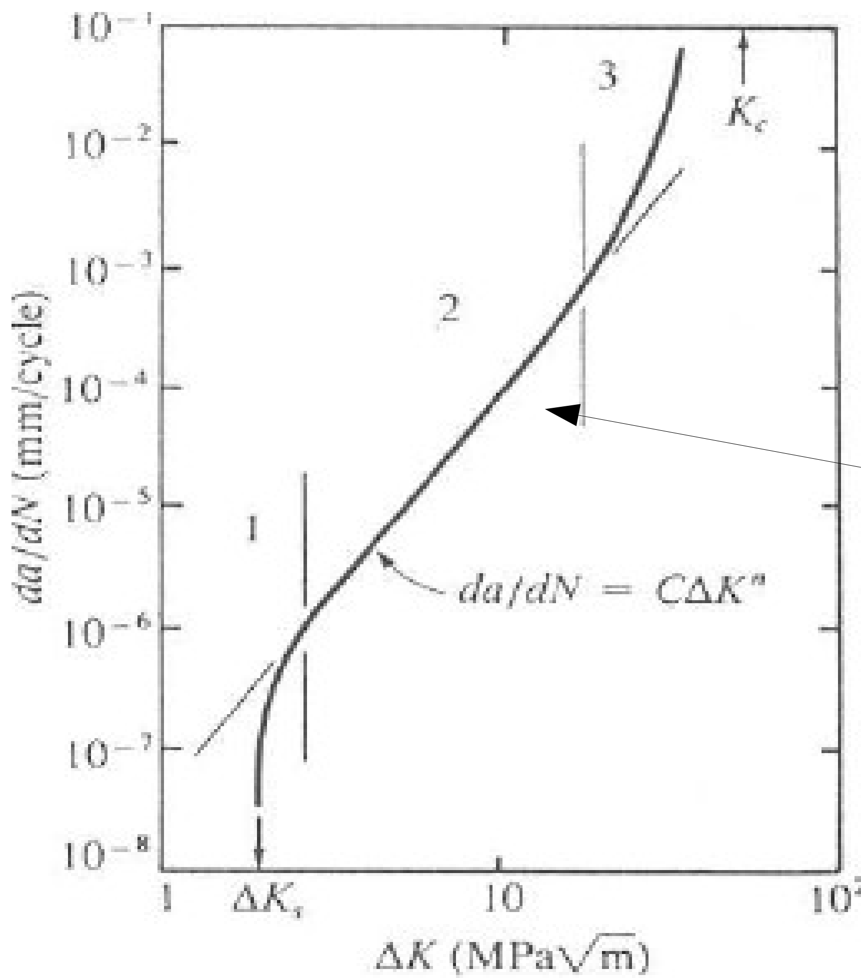

ΔK_{th}

Long cracks
Paris law
$da/dN = C\Delta K^m$

$K \sim \sigma\sqrt{a}$

Why 3D imaging of fatigue cracks?

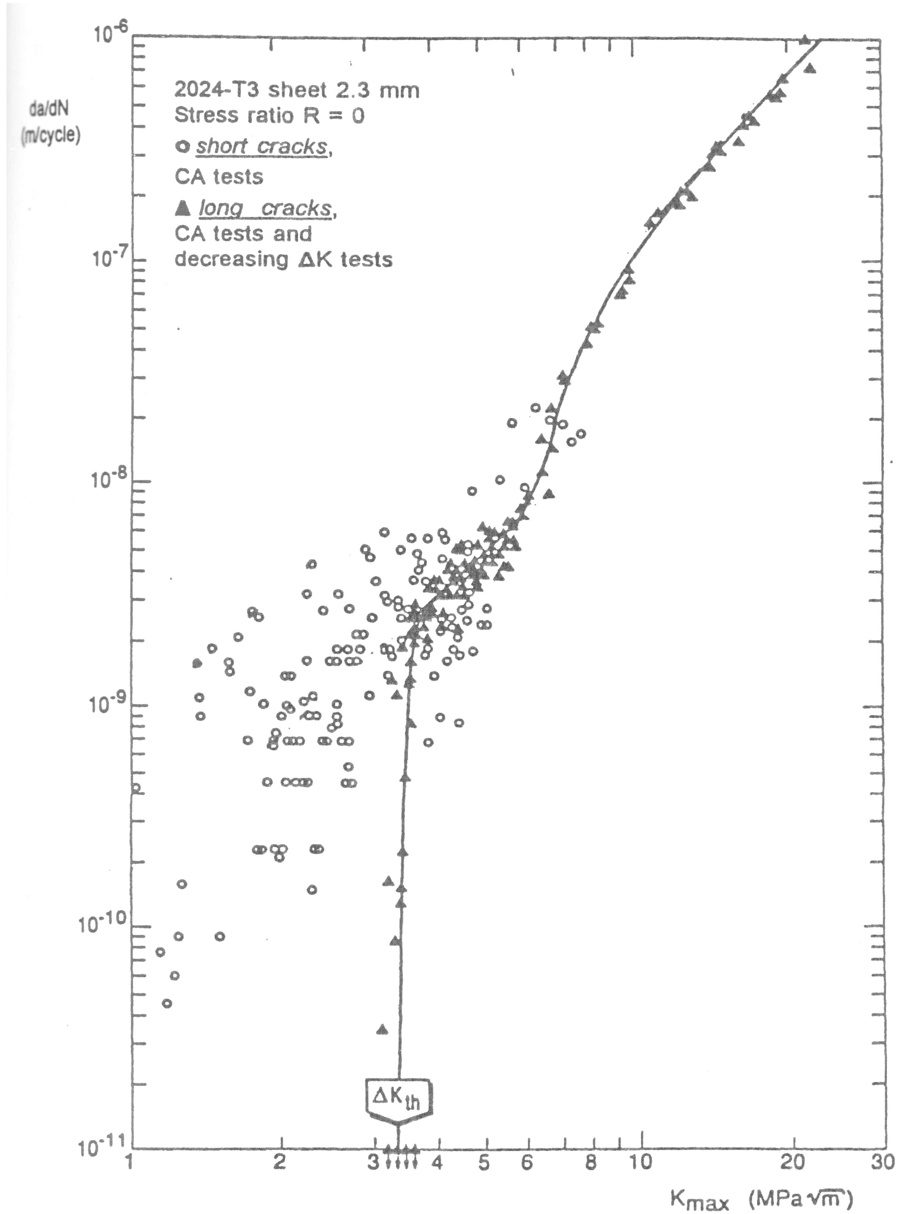

Why 3D imaging of fatigue cracks?

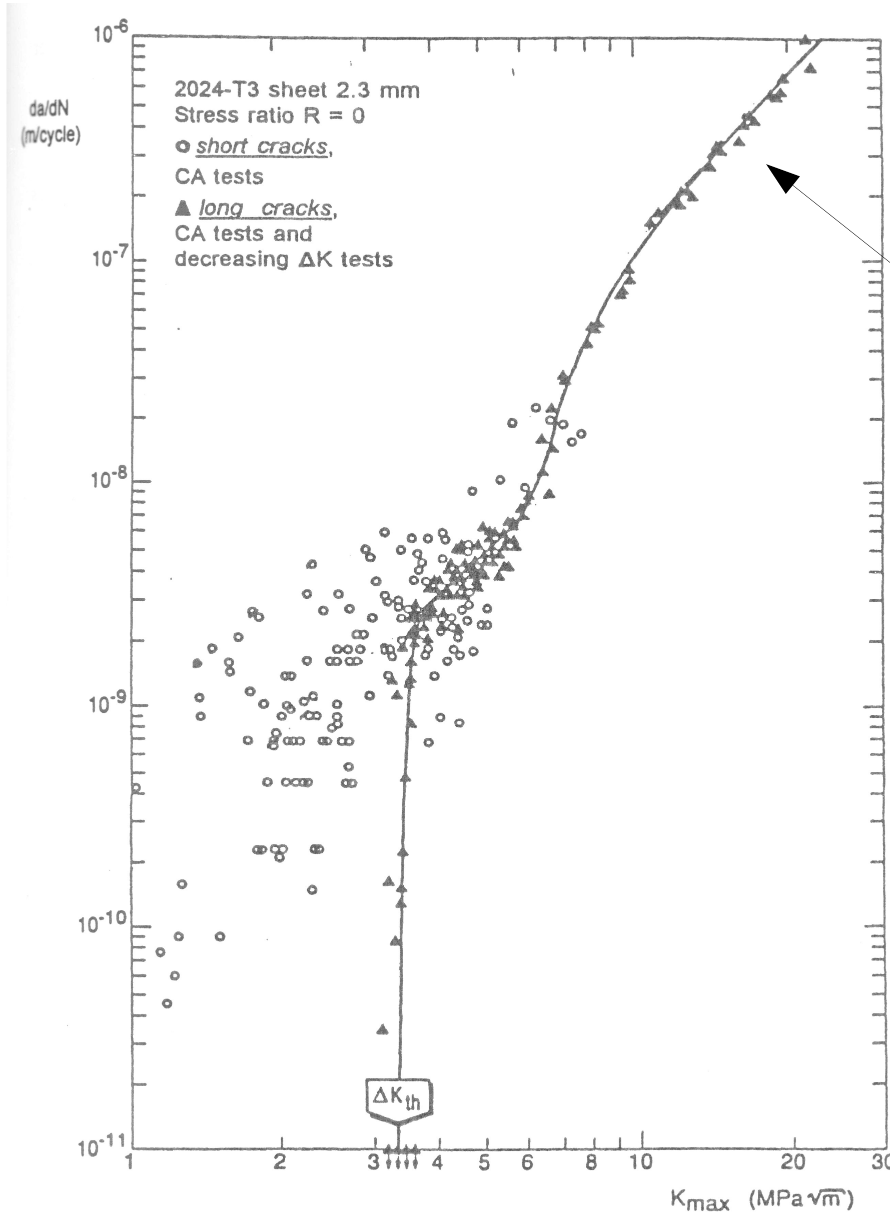

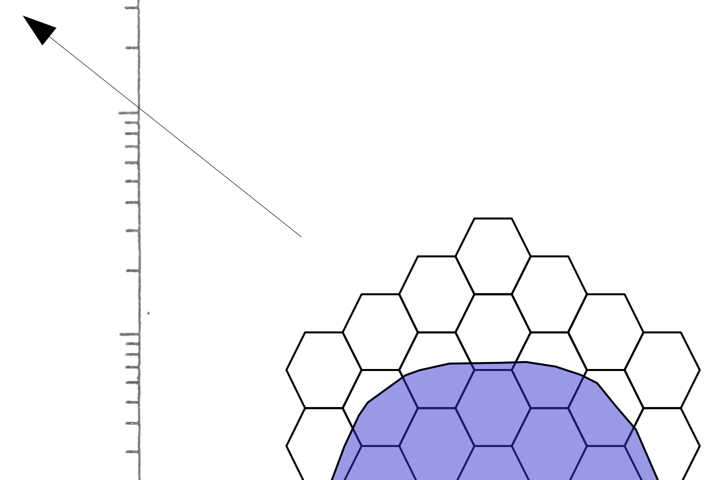

Why 3D imaging of fatigue cracks?

Short cracks

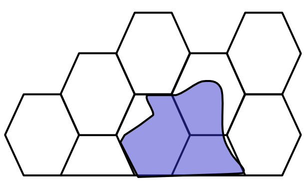

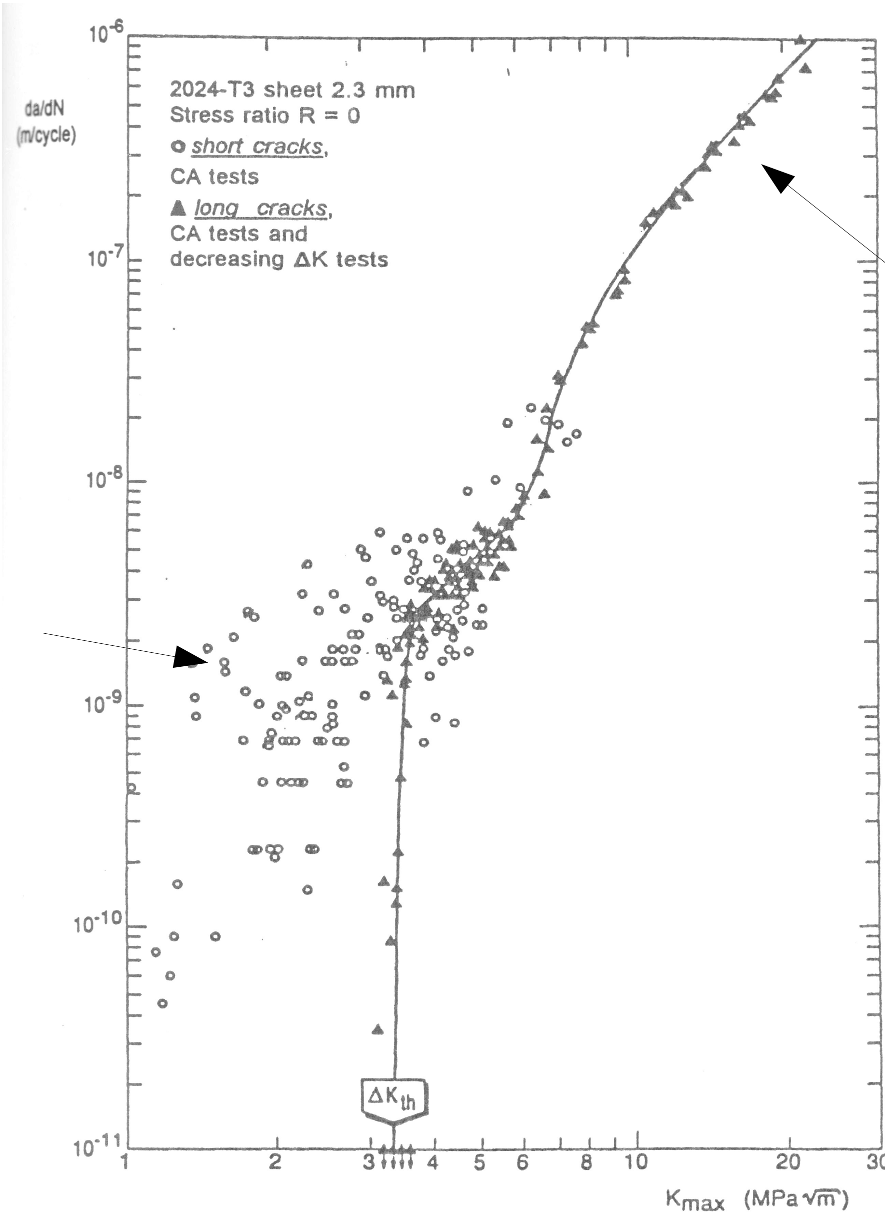

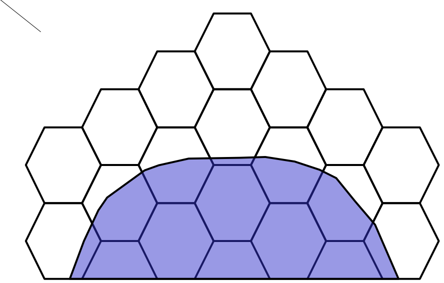

Looking at cracks in 3D: the different techniques

- Stiffness

(Ravichandran and larsen 1992)

- Potential drop

(Enmark et al. Jal Nucl. Mater 1992)

- Beach marking (environment, overloads...)

(Nadot et al. 1997)

- Serial polishing (mechanical, FIB …)

(Clément et al. 1984, Schaef 2011)

- 3D imaging

(Ludwig et al. 2003)

Looking at cracks in 3D: the different techniques

- Stiffness

→ 3D shape asumption, not accurate for short cracks

- Potential drop

→ not accurate for short cracks, no info on 3D shape

- Beach marking (environnement, overloads...)

→ influence on growth rate

- Serial polishing (mechanical, FIB …)

→ destructive, limited area

- 3D imaging (X ray tomography)

→ accuracy, availability

Outline

- ✗ Experimental set ups for tomography
- ✗ The resolution *v.s.* size dilemma
- ✗ Short cracks and the local crystallography
  - ✗Ti results
  - ✗Mg results
- ✗ Limits - What's next?

Principle of X ray tomography

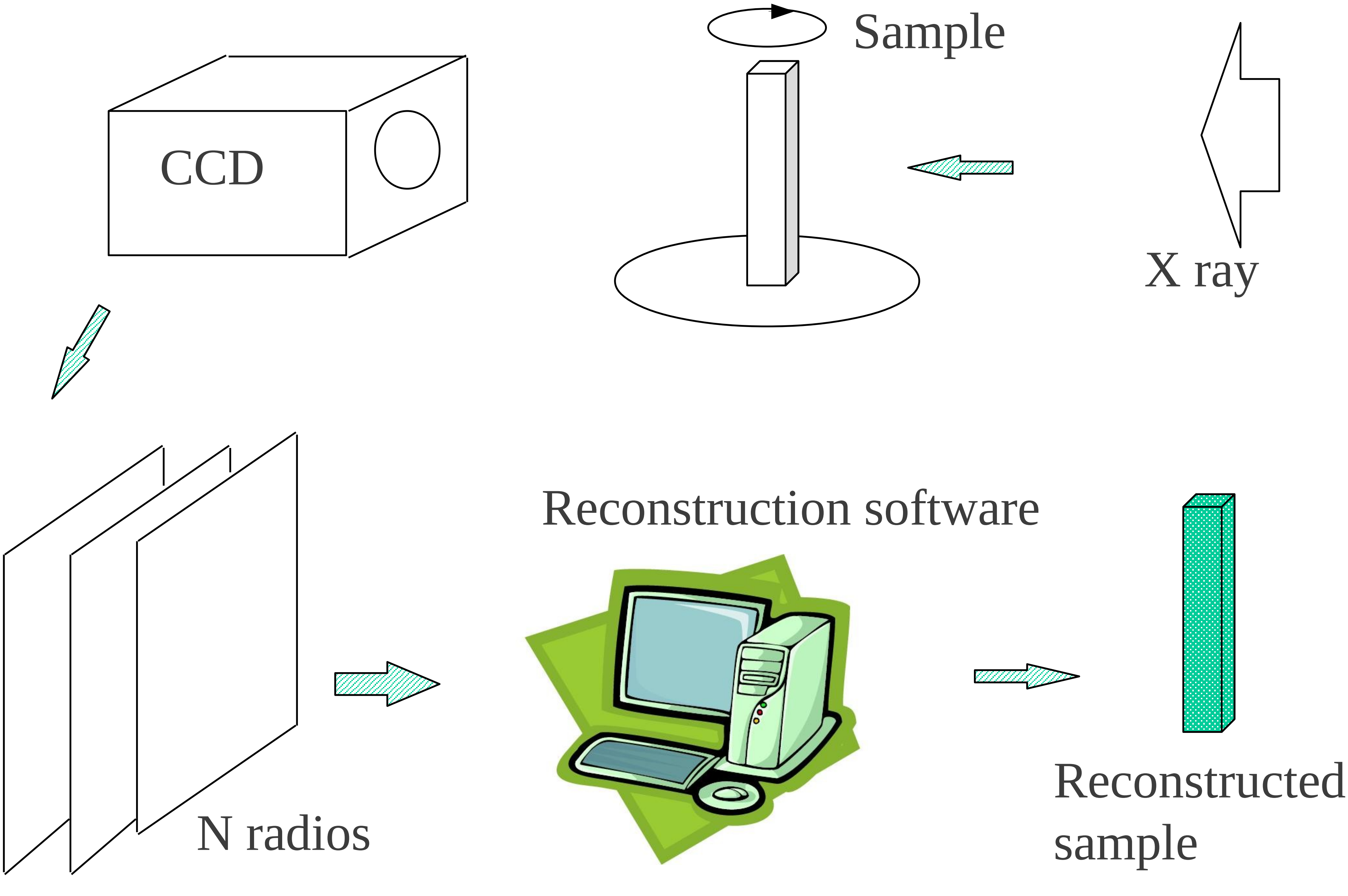

Synchrotron radiation

ESRF
Grenoble France

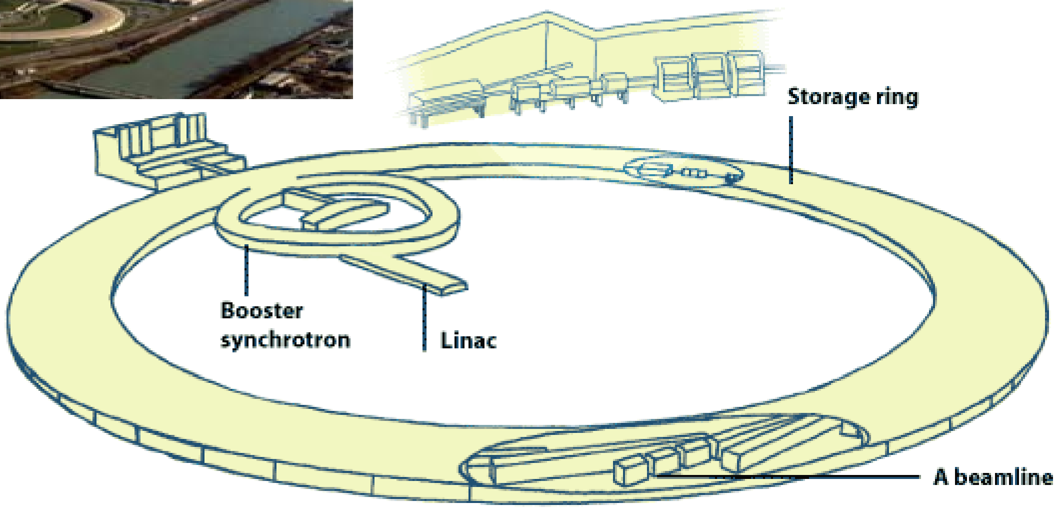

Beamlines:
ID19, ID15, BM05, ID22

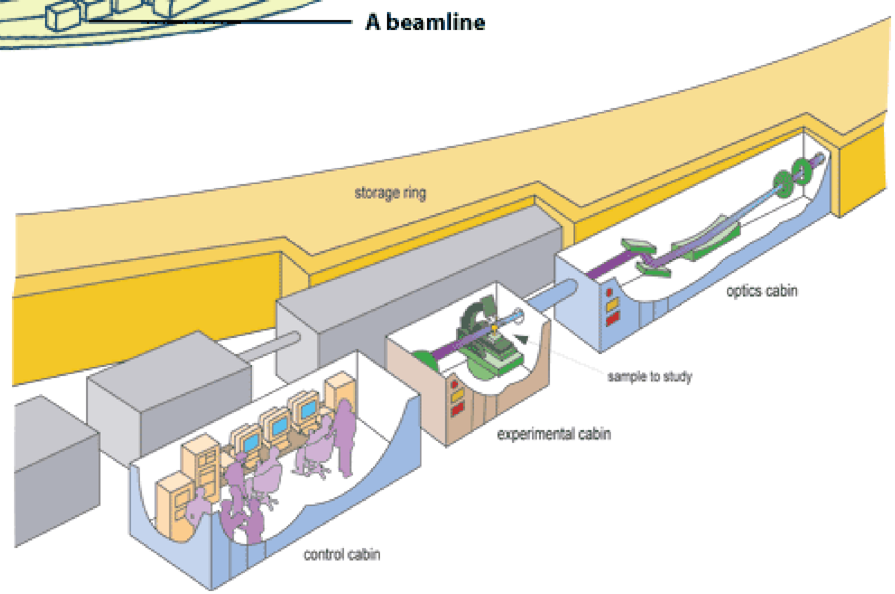

Experimental Setup at ID19

- Long distance (145 m)

→ coherence (phase contrast)

- Multilayer monochromator:
  $\Delta\lambda / \lambda \sim 10^{-2}$
- High resolution detector system
  14 bit, 1024^2 and 2048^2 CCD,
  60 ms readout, 1 μm.
- Dedicated μ-tomography set-up
- Sample environment: fatigue
  machine, cold cell, furnace, …

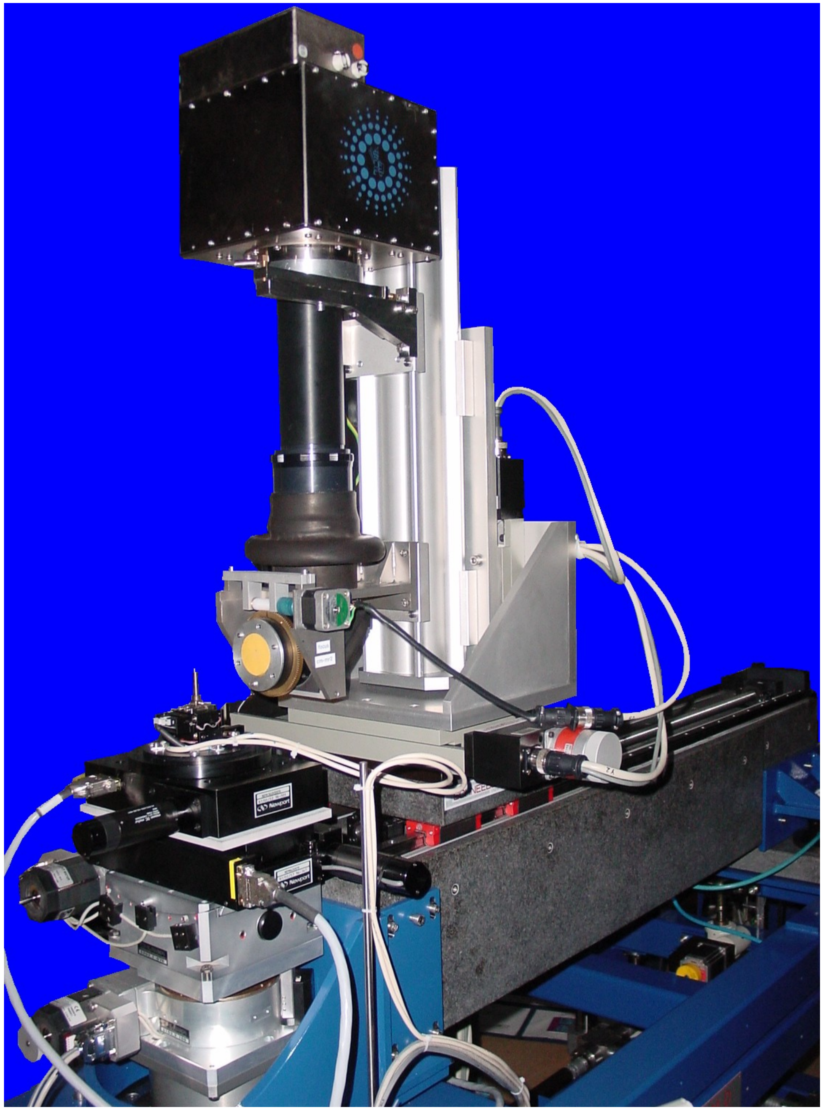

In situ fatigue

- Enables in situ cycling between scans
- Polymer tube
- Maximum load 2000 N
- Tension/Tension
- Cyclic frequency 25 Hz

5 cm

Resolution vs Sample size

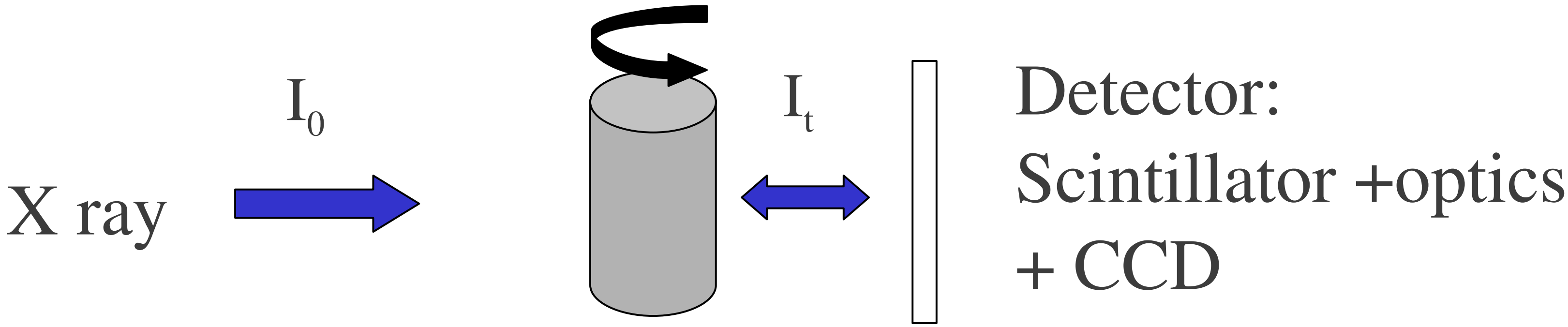

- Parallel beam $\rightarrow$ no enlargement
- Resolution ~ 2 * voxel size
- Crack tip $\rightarrow$ voxel size ~ 1 µm
- Sample size < CCD size $\rightarrow$ section < 1 mm^2

3D microstructural effects

Short cracks

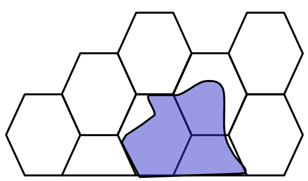

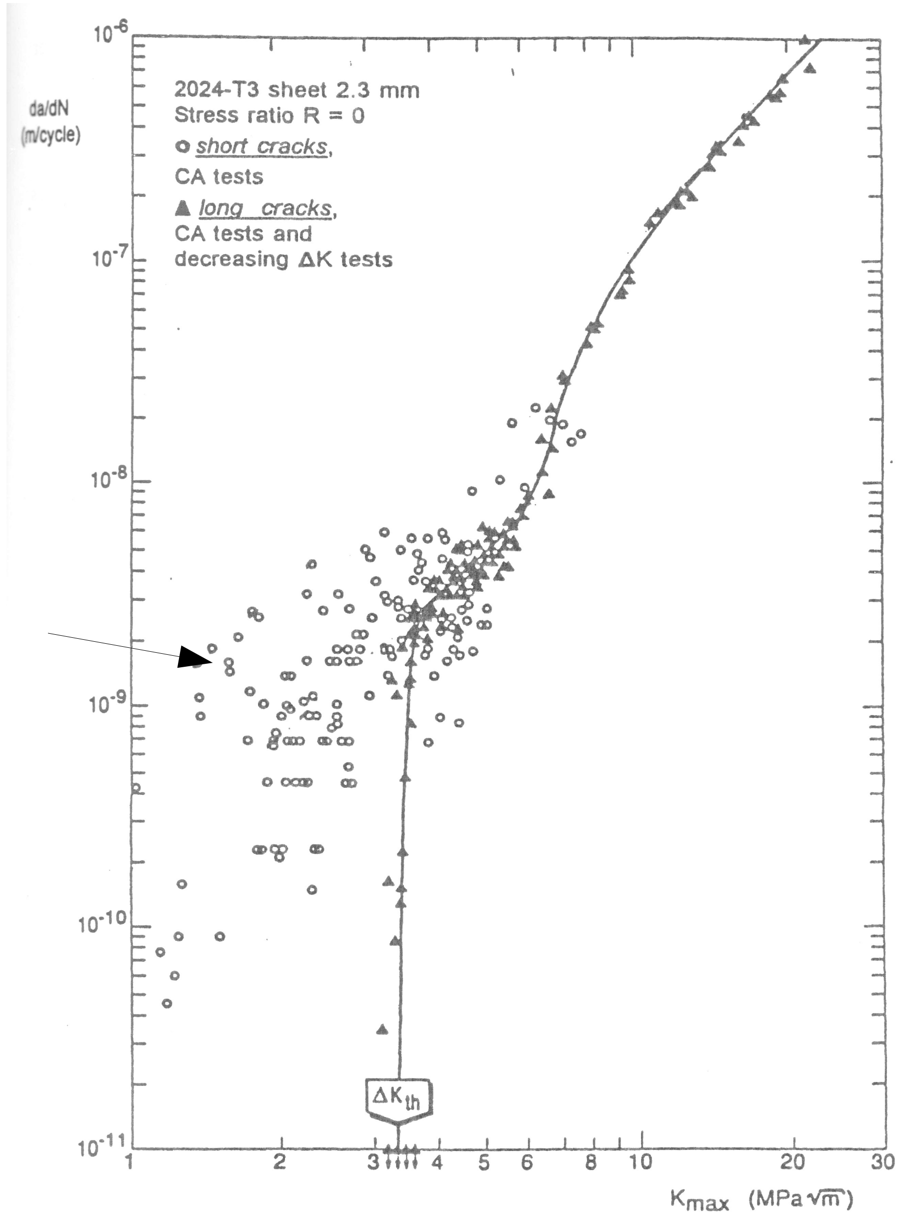

Short cracks *v.s.* microstructure

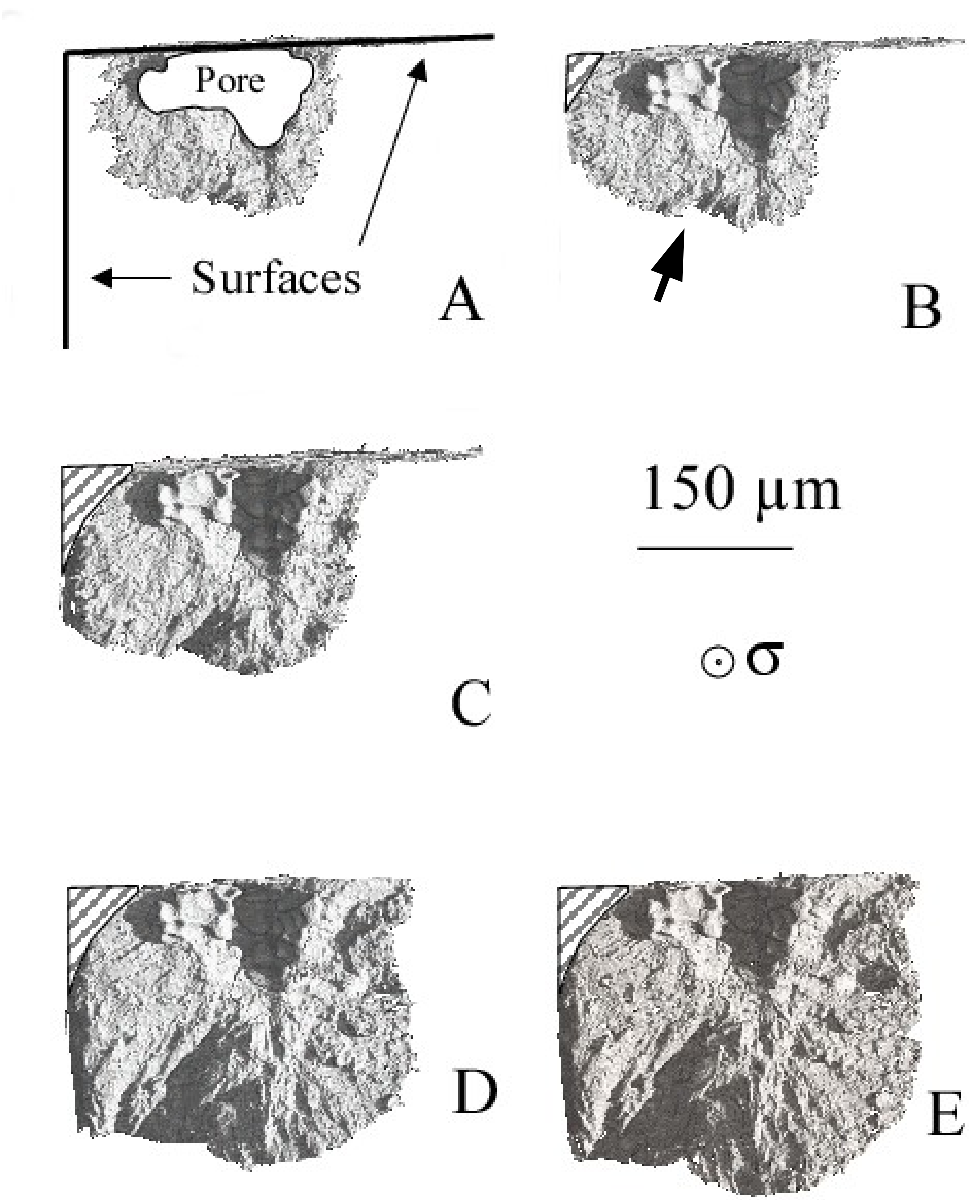

- Cracks initiate at the pore/surface intersection
- Local deviations of the crack front → grain boundaries?

Cast Al alloy grain size ~ 300 µm

Fatigue cracks *v.s.* grain boundaries

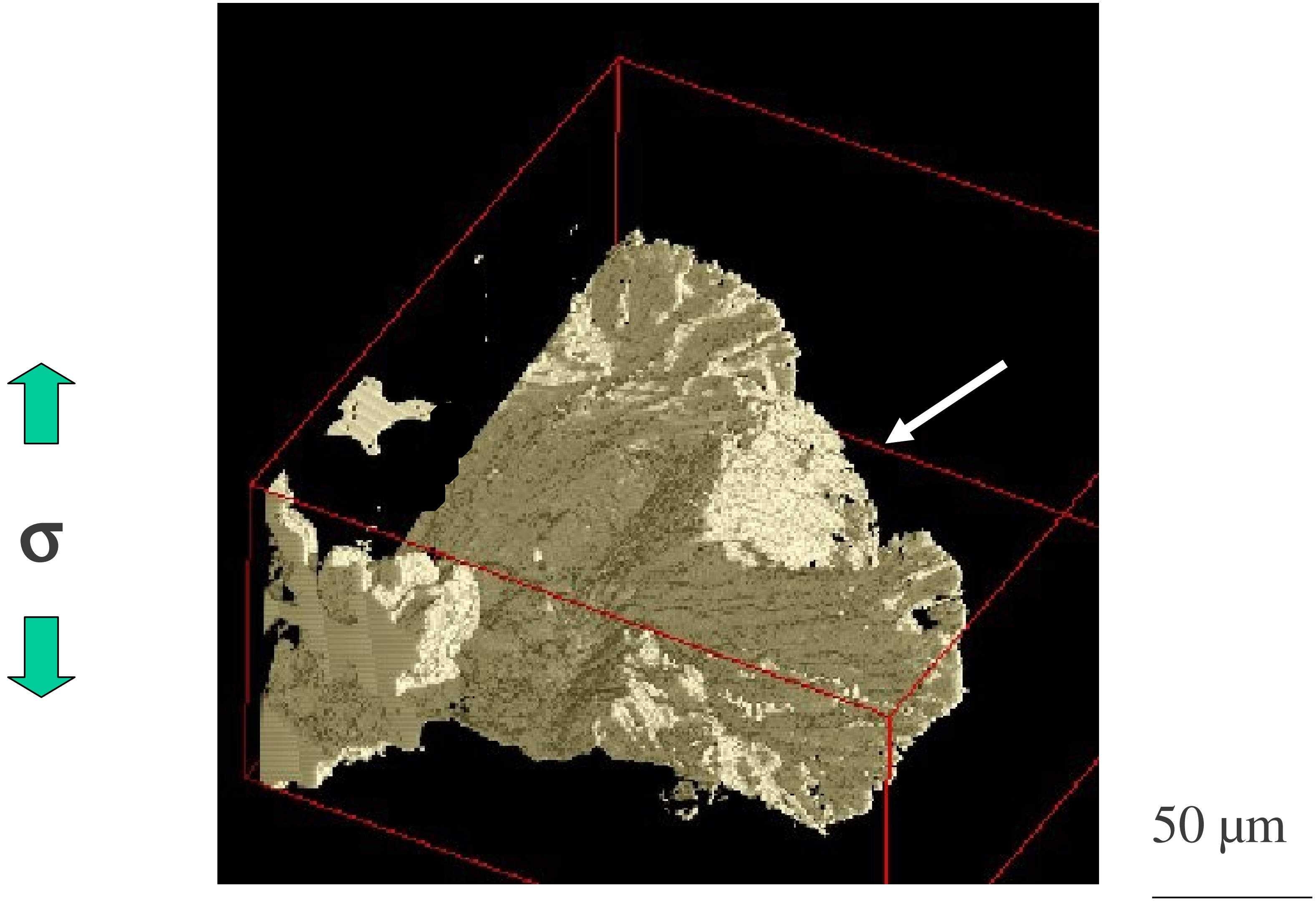

Cast Al alloy grain size ~ 300 μm

Fatigue cracks *v.s.* grain boundaries

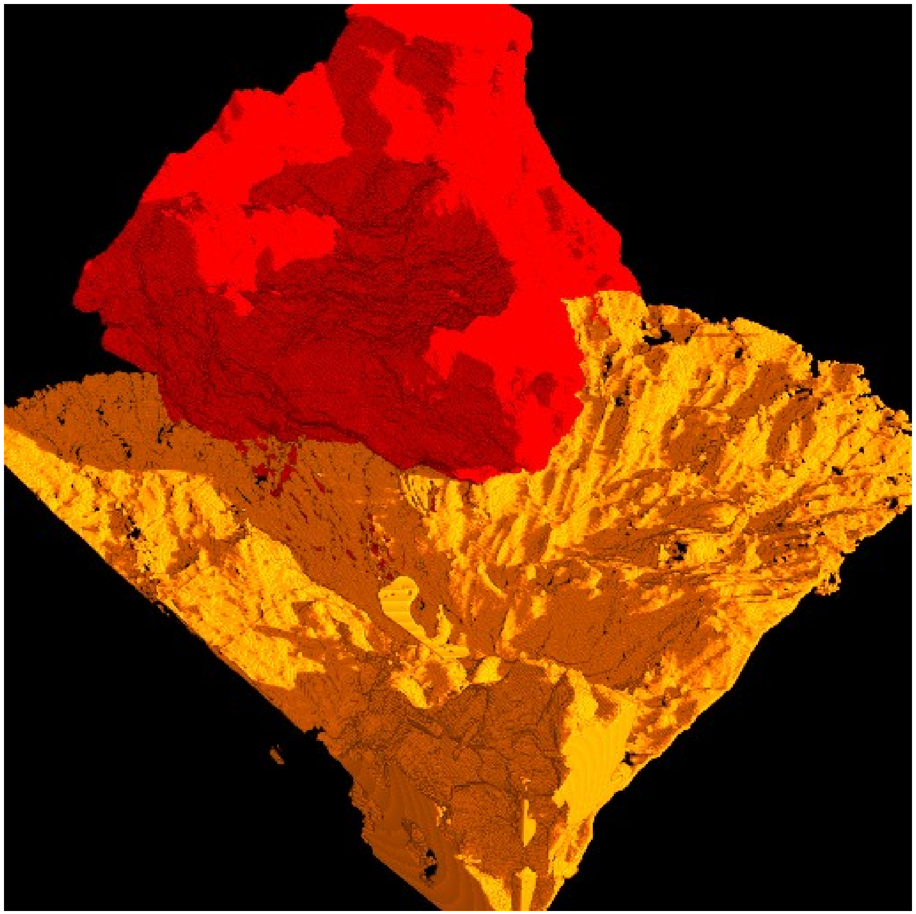

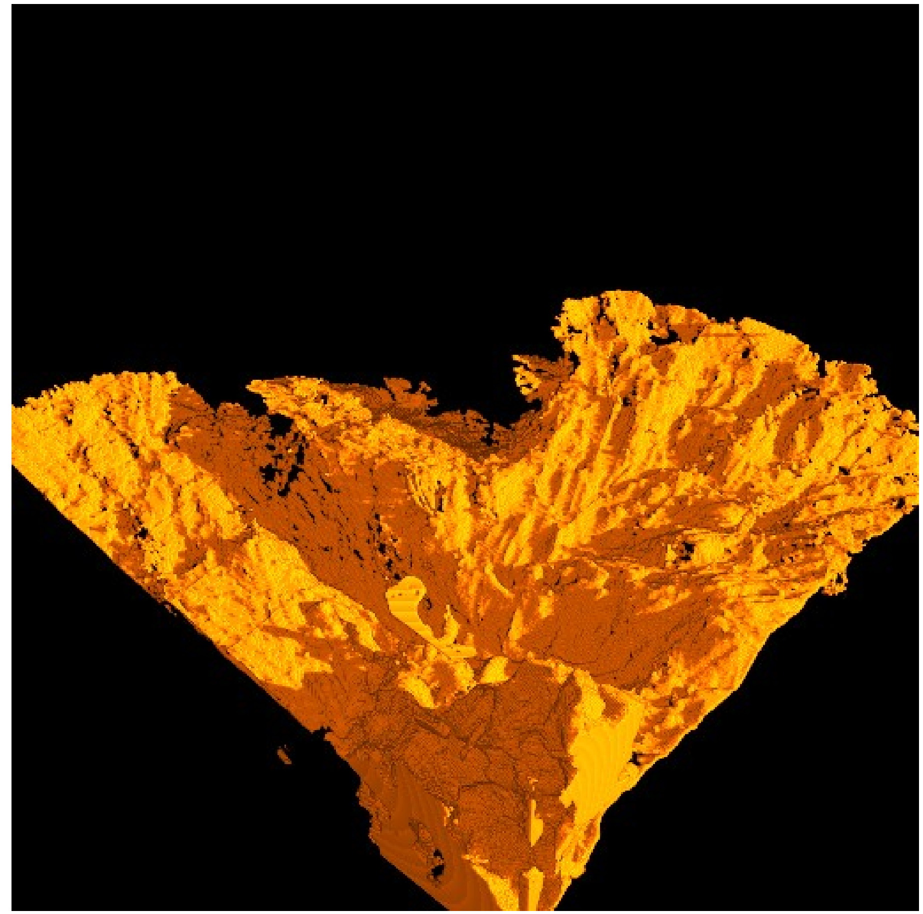

100 µm

Ludwig et al. Acta Mater 2003.

Fatigue cracks *v.s.* grain boundaries

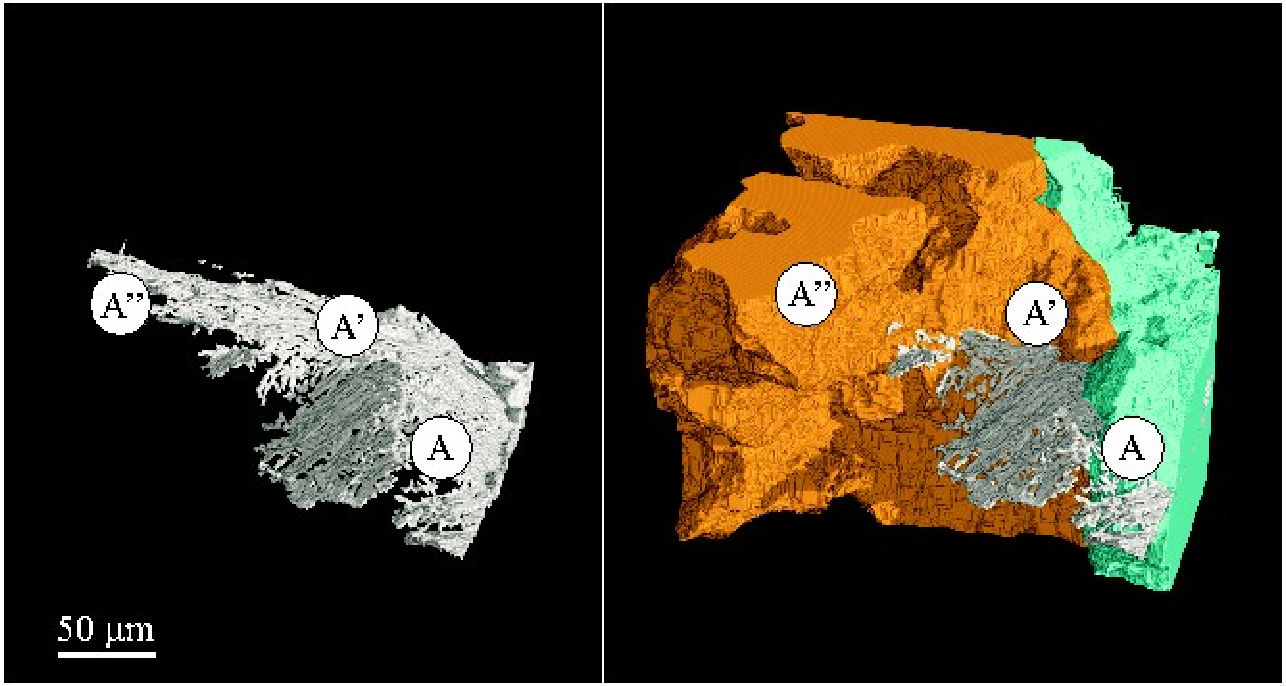

Local crystallography: key factor

Ludwig et al. Acta Mater 2003.

Fatigue cracks *v.s.* grain boundaries

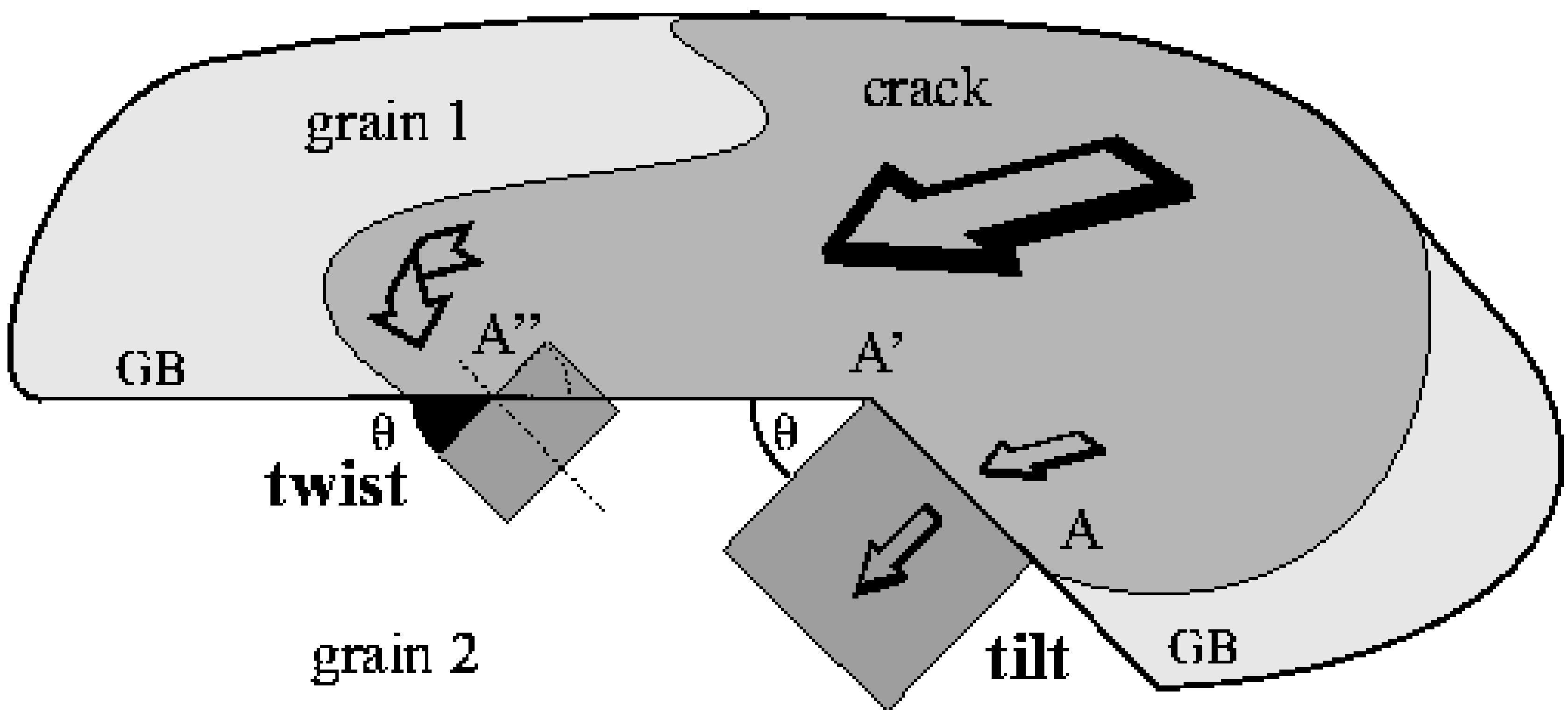

Tilt vs twist mechanism

Ludwig et al. Acta Mater 2003.

Limitations

- Ga works only for Al alloys
- Destructive and only provides grain shape
- Modelling requires the knowledge of local crystallography

→Diffraction Contrast Tomography

DCT: the method

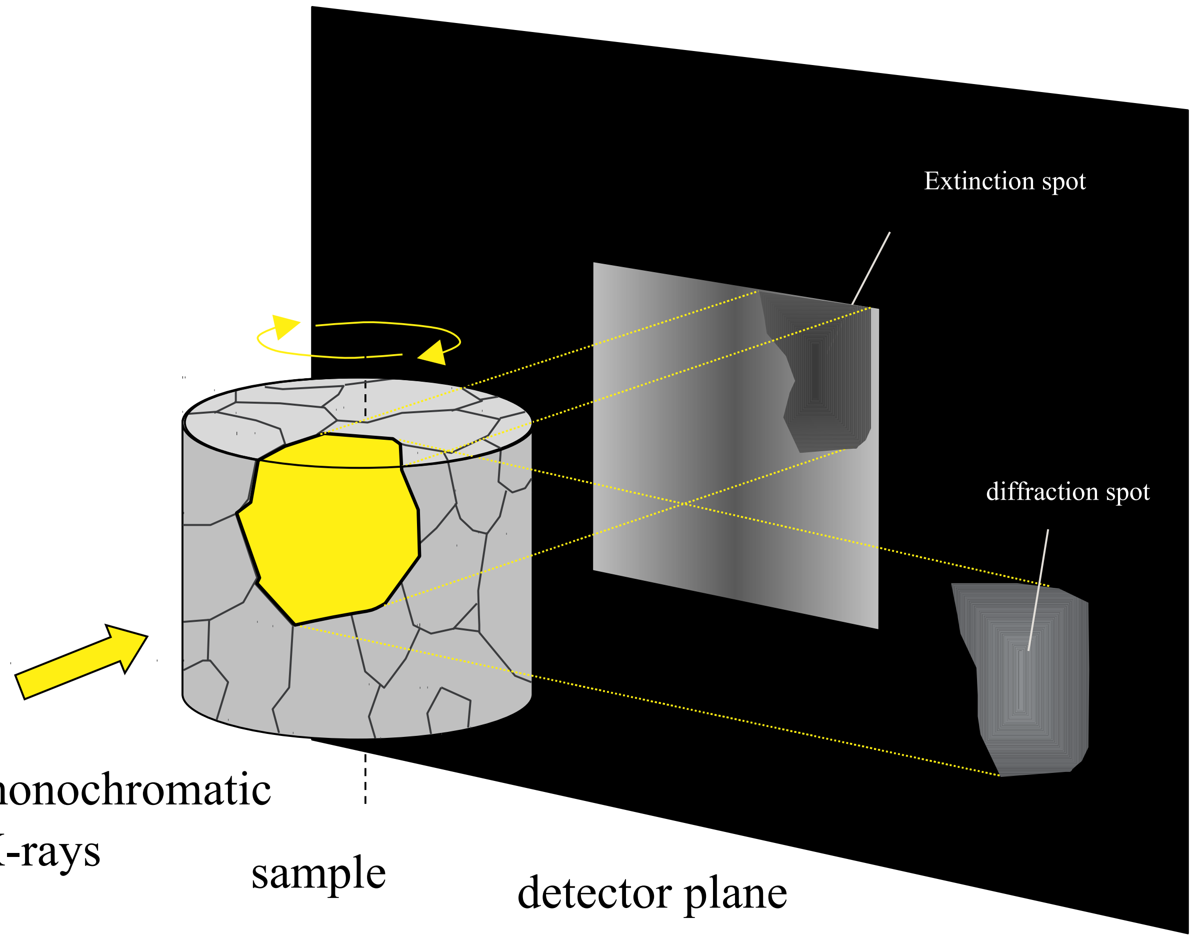

DCT raw data

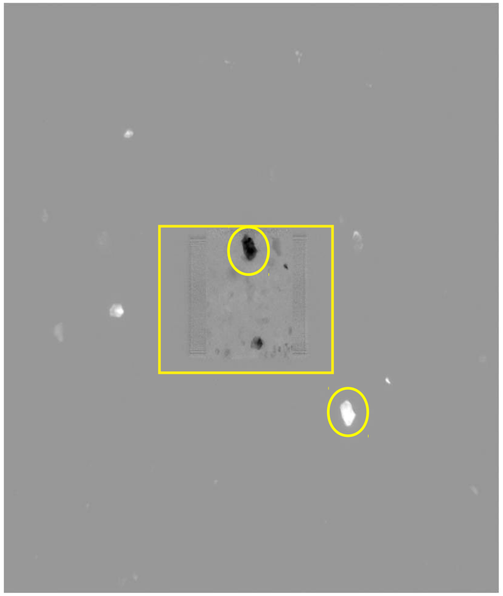

Pixel size 2.4 µm, ID11 (high flux)
Sample with 1000 grains
→ *ca.* 80 000 diffraction spots
on 7200 images

Ludwig et al. R.S.I. 2009

DCT on Ti alloy

*

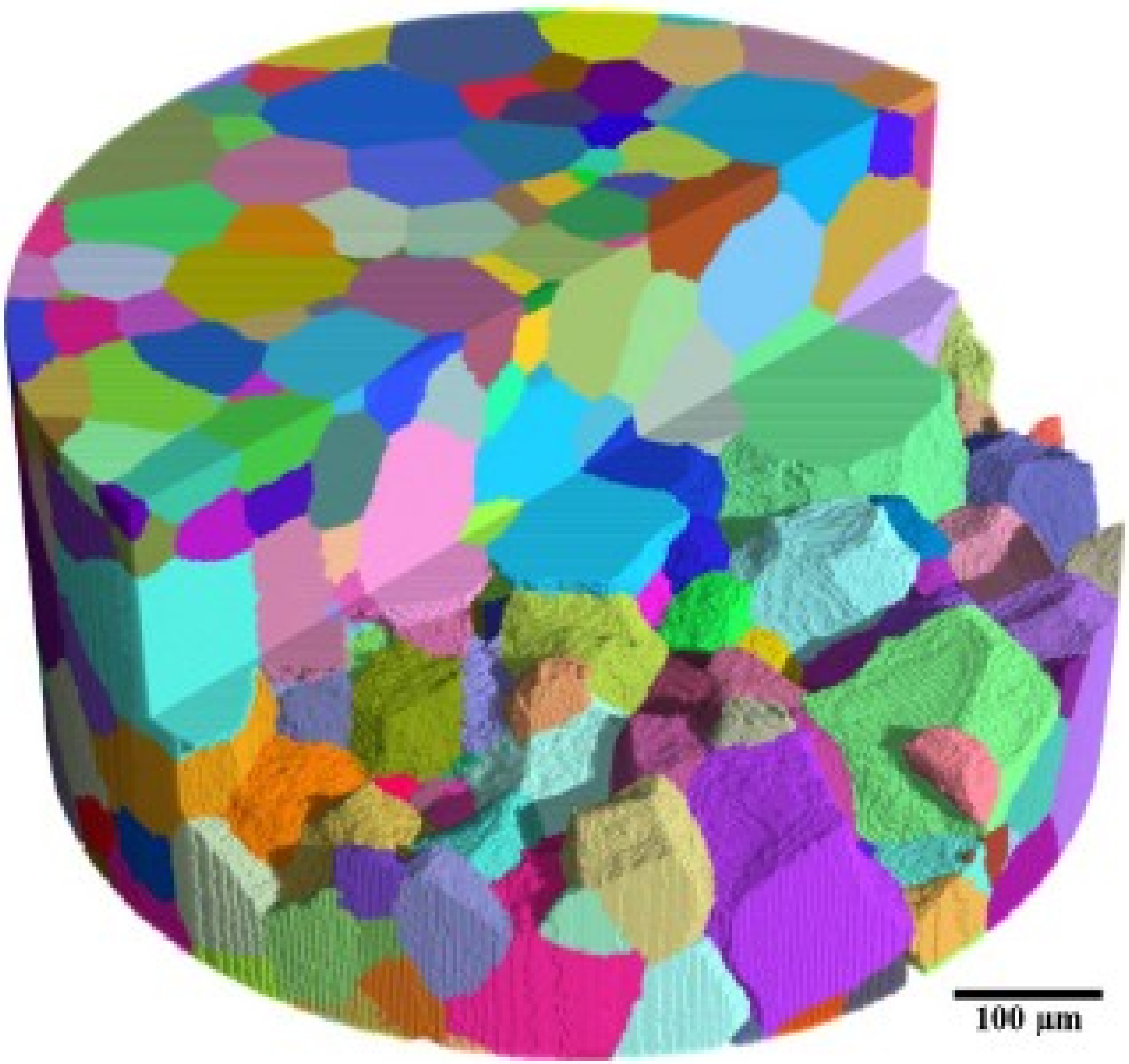

Metastable β-titanium alloy
'Timet®21S'
Chemical composition:
15 wt% Mo, 3 wt% Nb

1008 grains

Evaluation of DCT

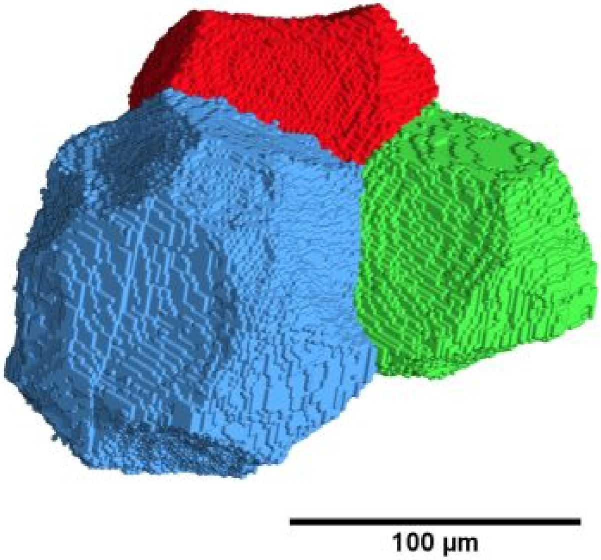

DCT grain cluster

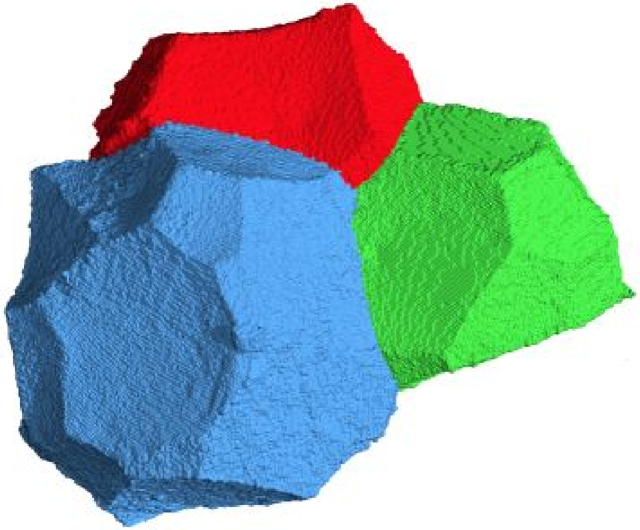

PCT grain cluster

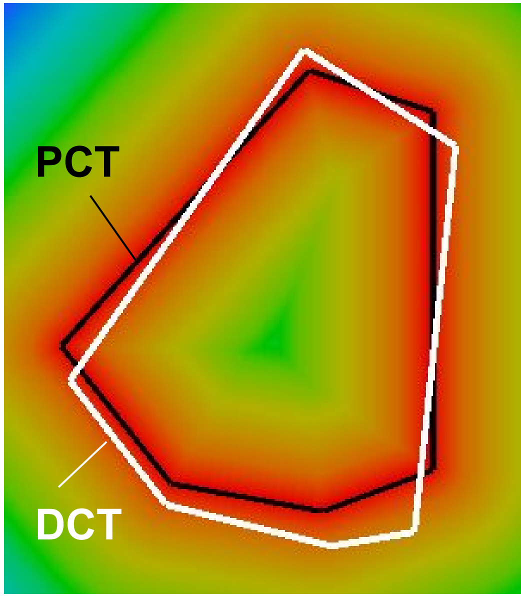

Principle of error calculation

Comparison of grain boundaries as reconstructed from DCT with real grain boundaries
→2.6 µm average error for 55 µm grains
→DCT accurate enough to be trusted

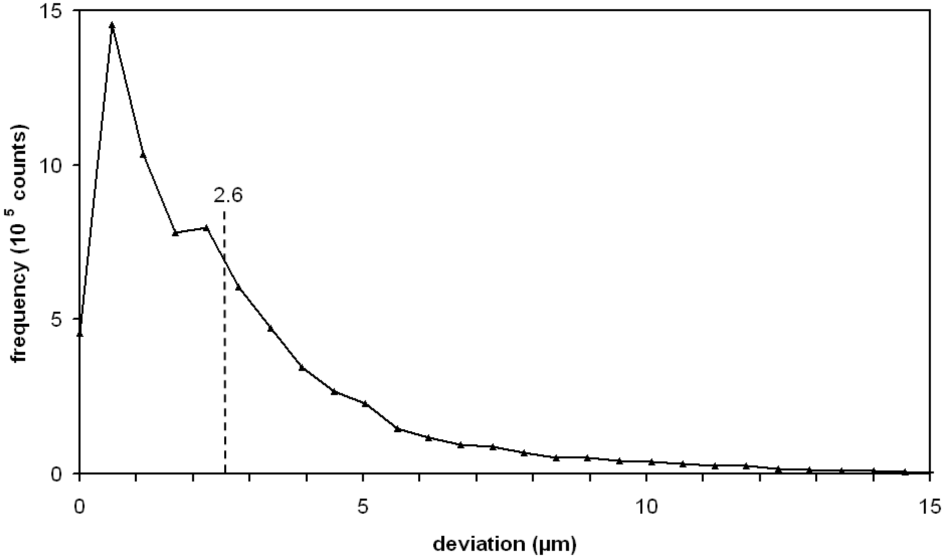

3DXTSM – Data Acquisition

Diffraction Contrast Tomography :
Non-destructive characterization of grain orientation and grain shape

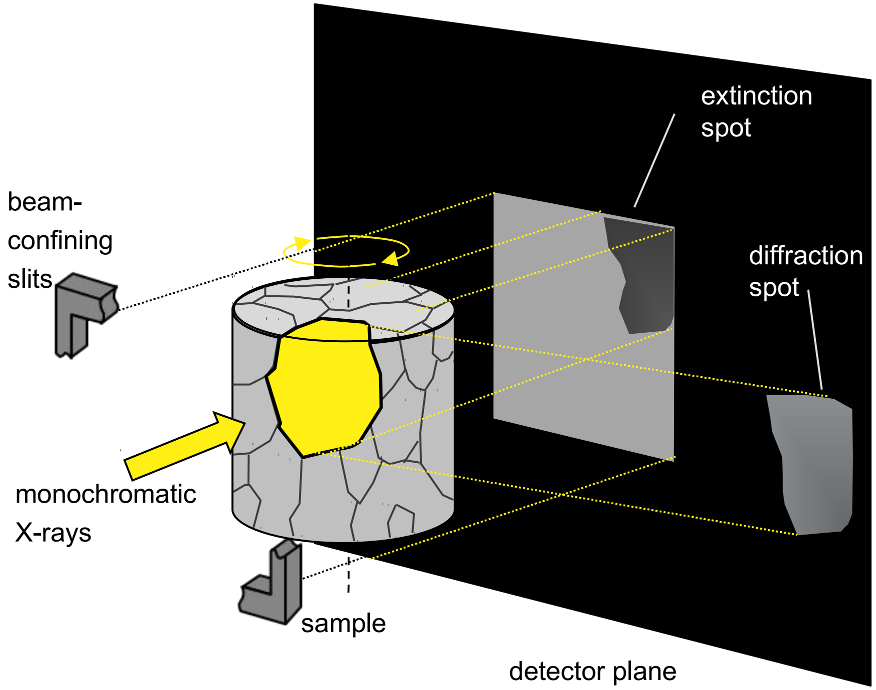

- pixel size 1.4 µm

Phase Contrast Tomography :
Phase contrast makes fine crack parts visible

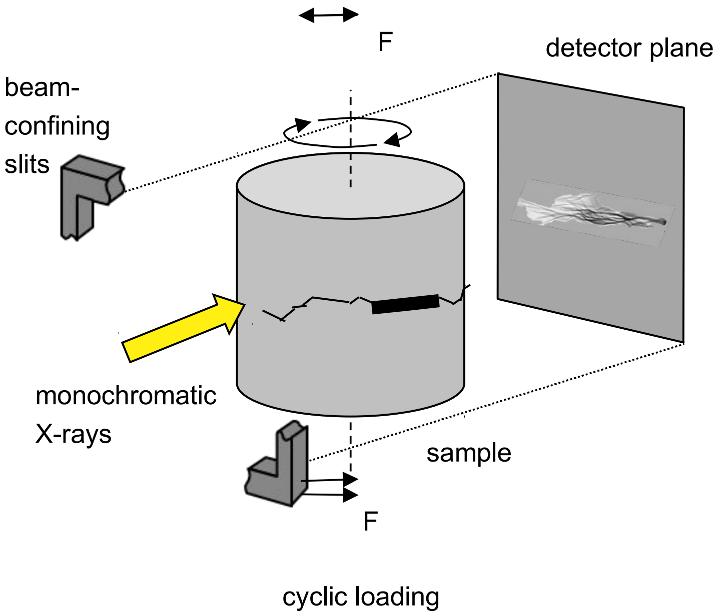

- pixel size 0.7 µm
- interrupted *in-situ* measurement

3DXTSM – Experimental Details

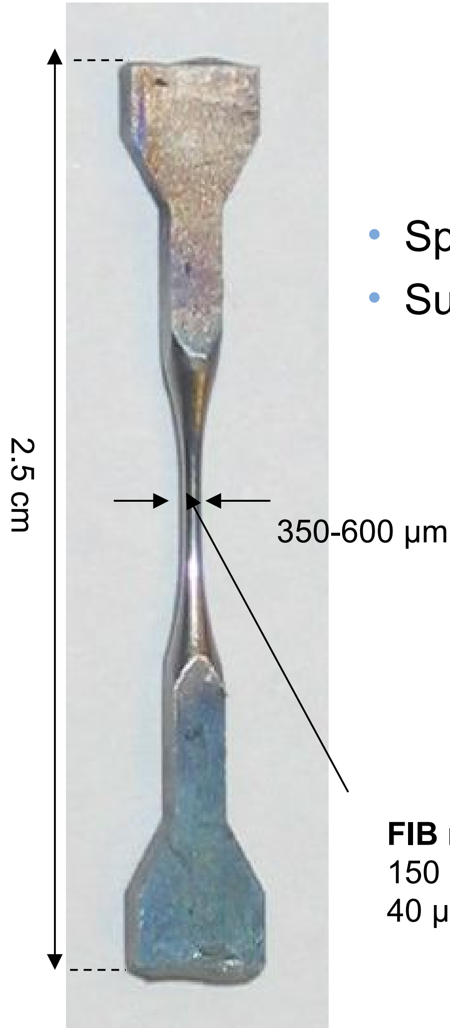

- Spark erosion cut
- Surface polished

FIB notch:
150 µm length,
40 µm depth

- Load: 10.6-318 MPa
- Cyclic frequency 25 Hz

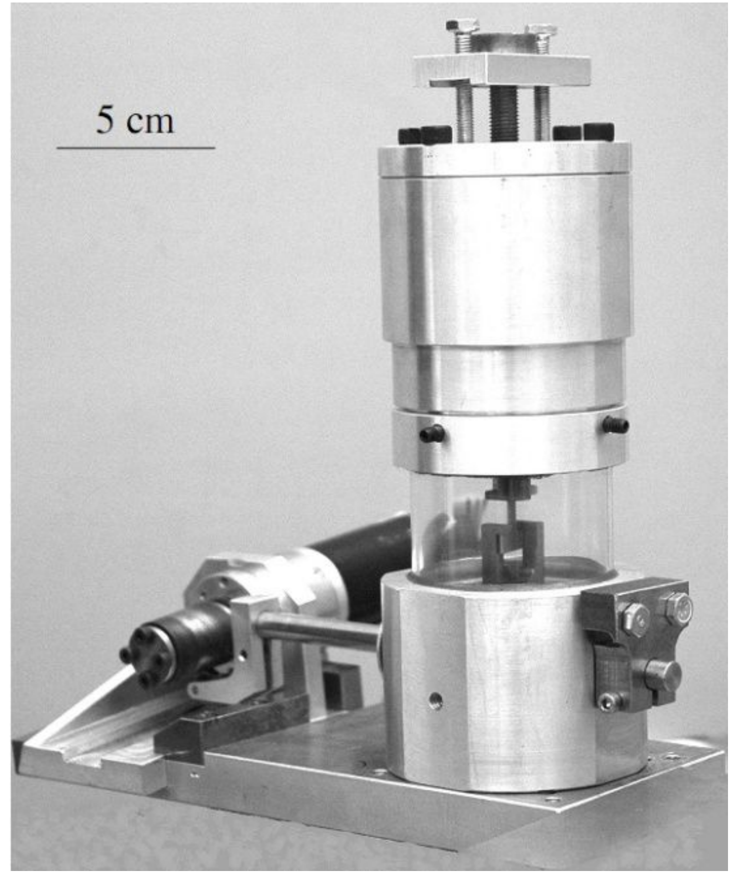

[Buffière et al. Mat.Sc. Tech. 2006]

3DXTSM – Volume Registration

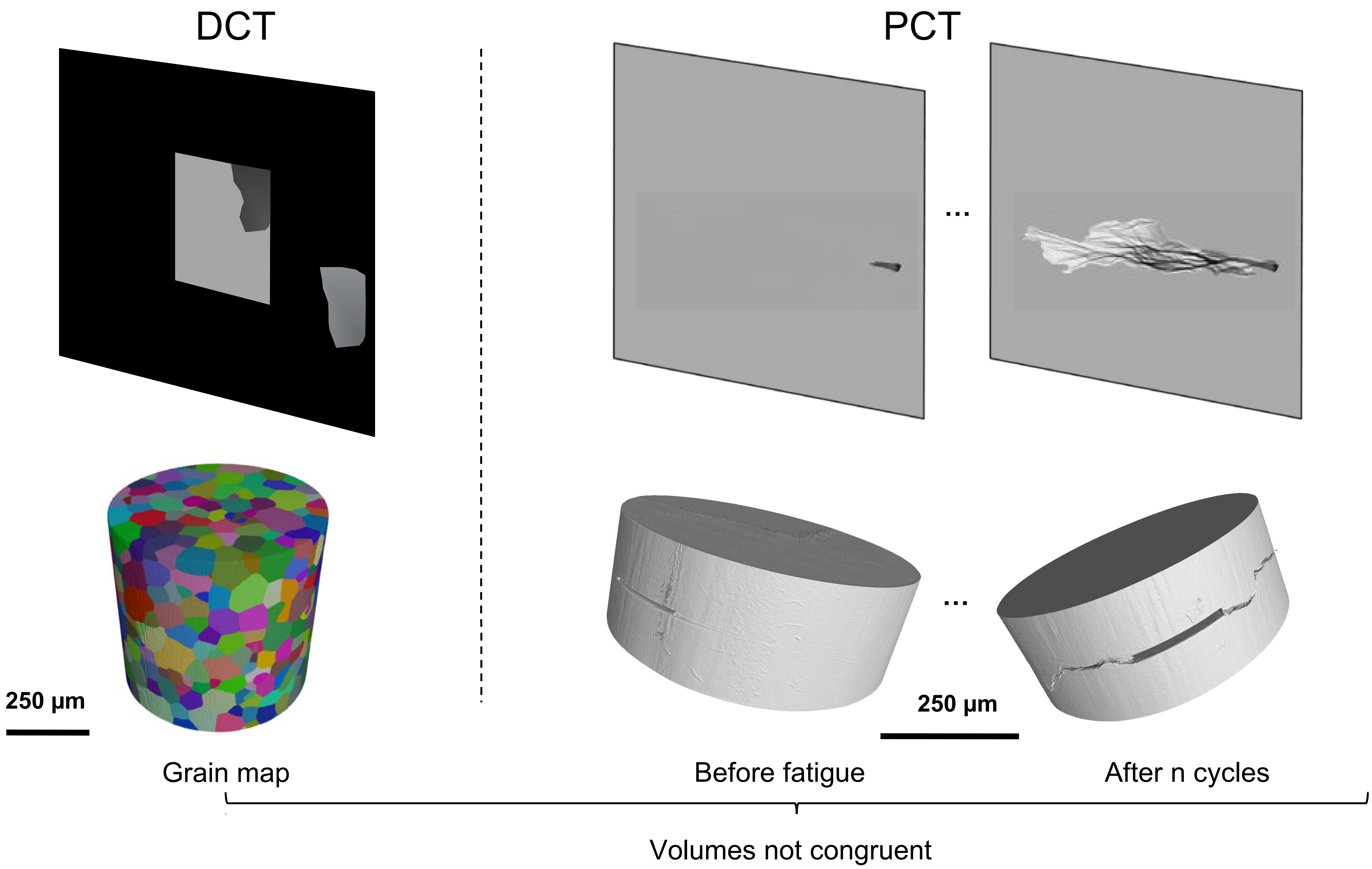

3DXTSM – Oversampling

Original

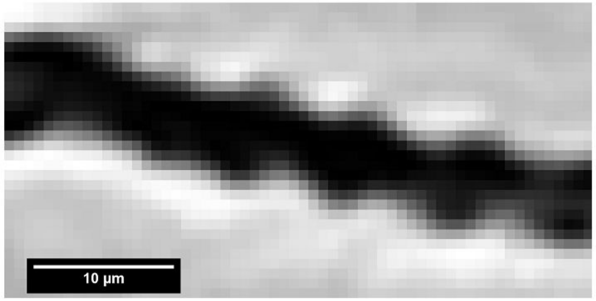

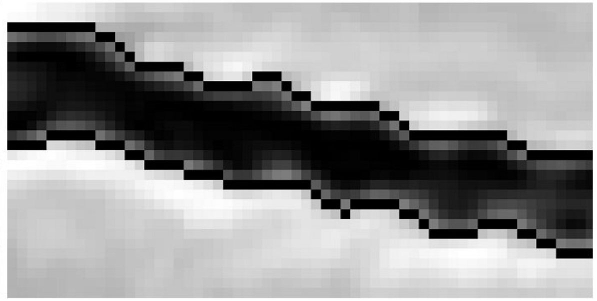

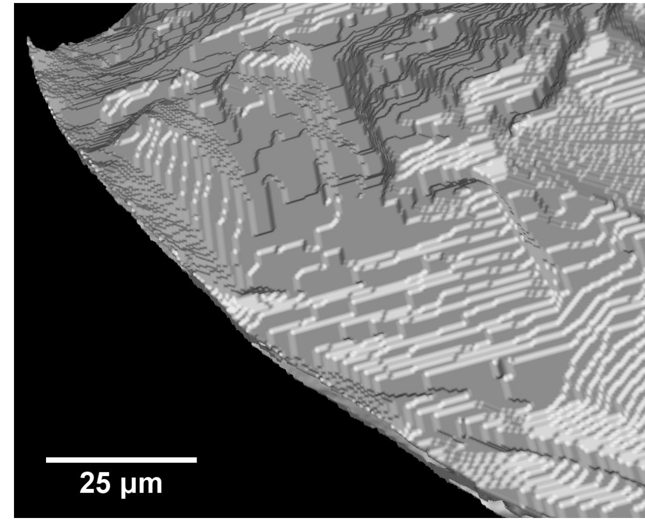

Cross-section through reconstructed volume

Cross-section with outline of segmented crack

3D rendering of segmented crack

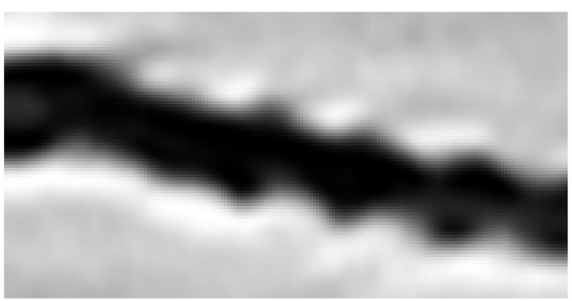

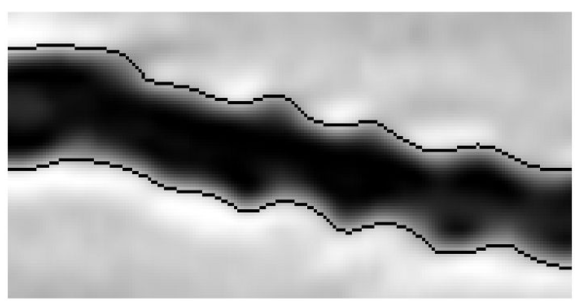

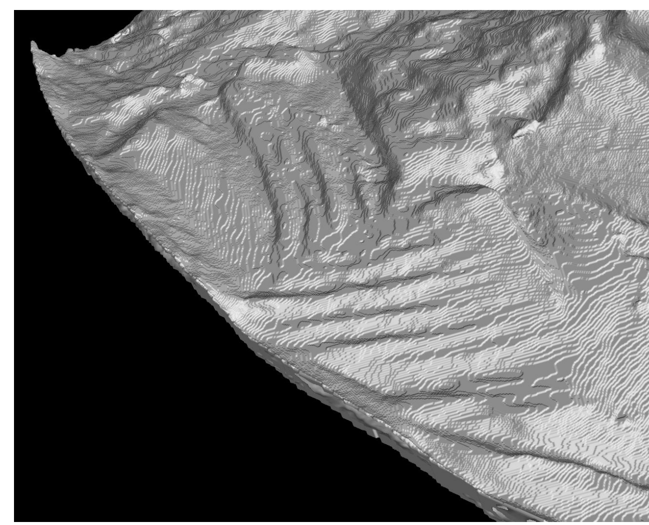

Oversampled

3DXTSM – Voxels → Mesh

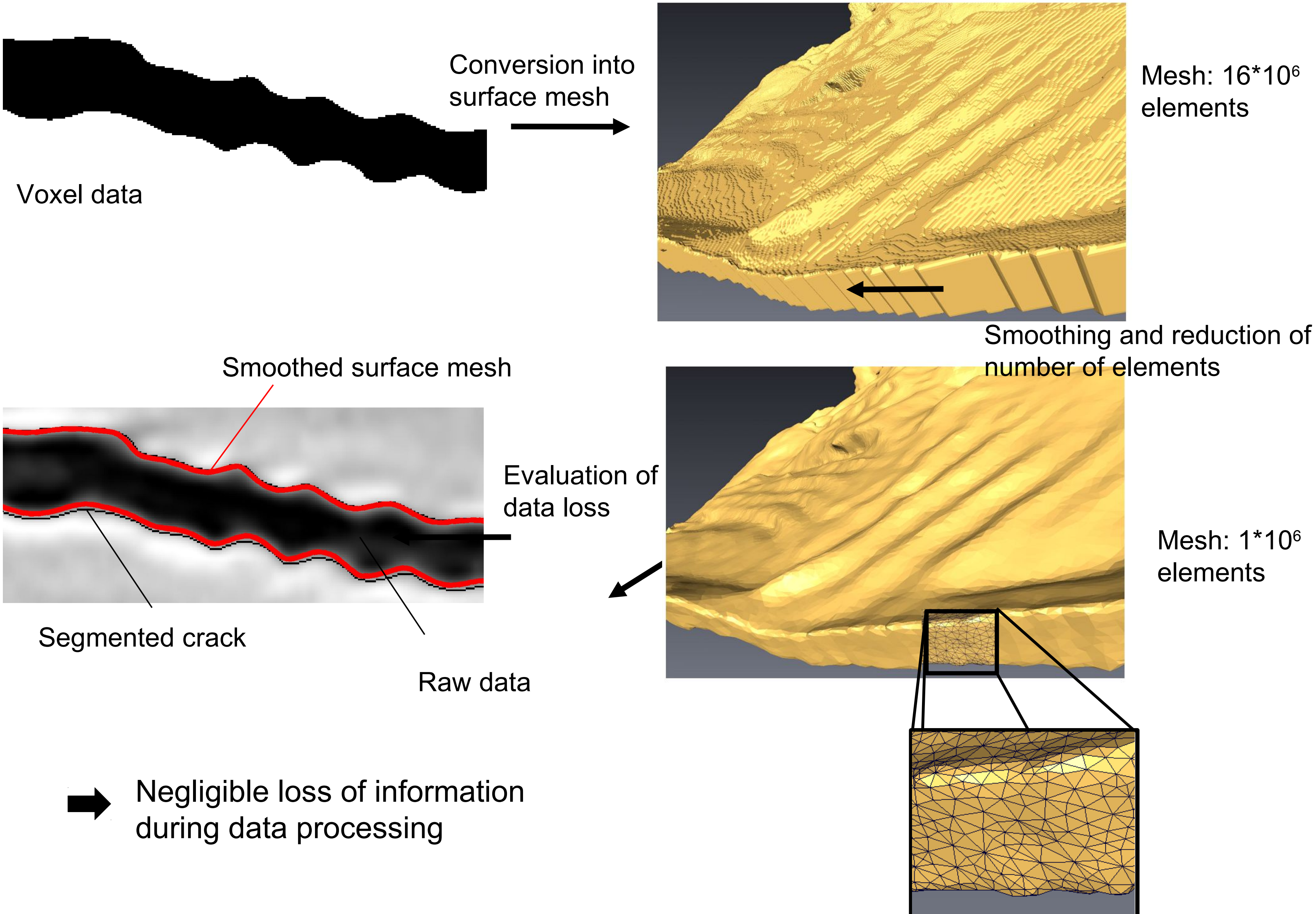

➡ Negligible loss of information during data processing

3DXTSM - Data Structure

- Physical orientation
- Grain affiliation
- Crystallographic orientation
- Propagation stage
- Local crack growth rate

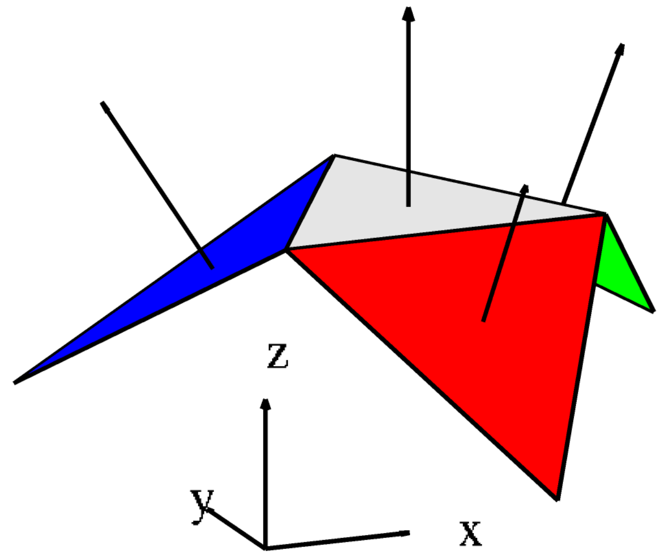

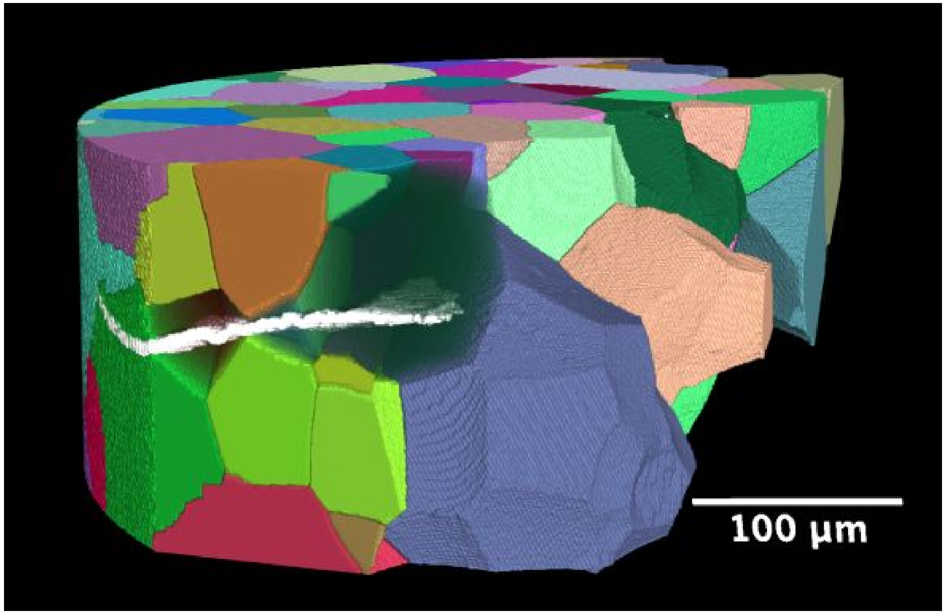

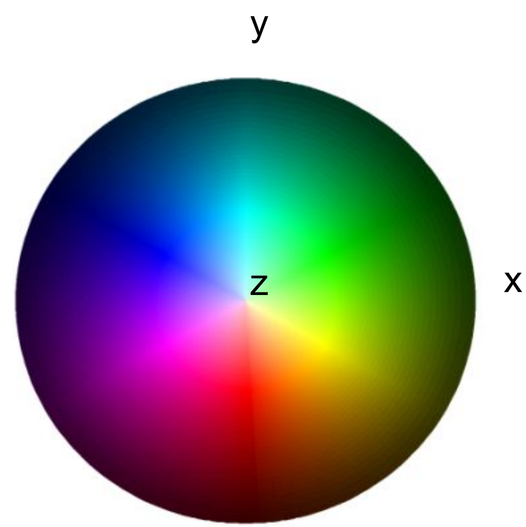

Studied samples

sample "VST":

- Near β-titanium (bcc) alloy 'VST55531'
- Ti-5Al-5V-5Mo-3Cr-1Zr
- 2 h / 843 °C, air cooled
- Grain size ~ 65 μm
- Single growth stage analyzed at 110 k cycles

sample "21S":

- Metastable β-titanium (bcc) alloy 'Timet®21S'
- Ti-15Mo-3Nb-3Al-.2Si
- 2 h / 850 °C, quenched in water
- Grain size ~ 55 μm
- 26 stages between 45 k and 75.5 k cycles

Studied samples

sample “VST”:

- Near β-titanium (bcc) alloy ‘VST55531’
- Ti-5Al-5V-5Mo-3Cr-1Zr
- 2 h / 843 °C, air cooled
- Grain size ~ 65 μm
- Single growth stage analyzed at 110 k cycles

sample “21S”:

- Metastable β-titanium (bcc) alloy ‘Timet®21S’
- Ti-15Mo-3Nb-3Al-.2Si
- 2 h / 850 °C, quenched in water
- Grain size ~ 55 μm
- 26 stages between 45 k and 75.5 k cycles

In situ fatigue

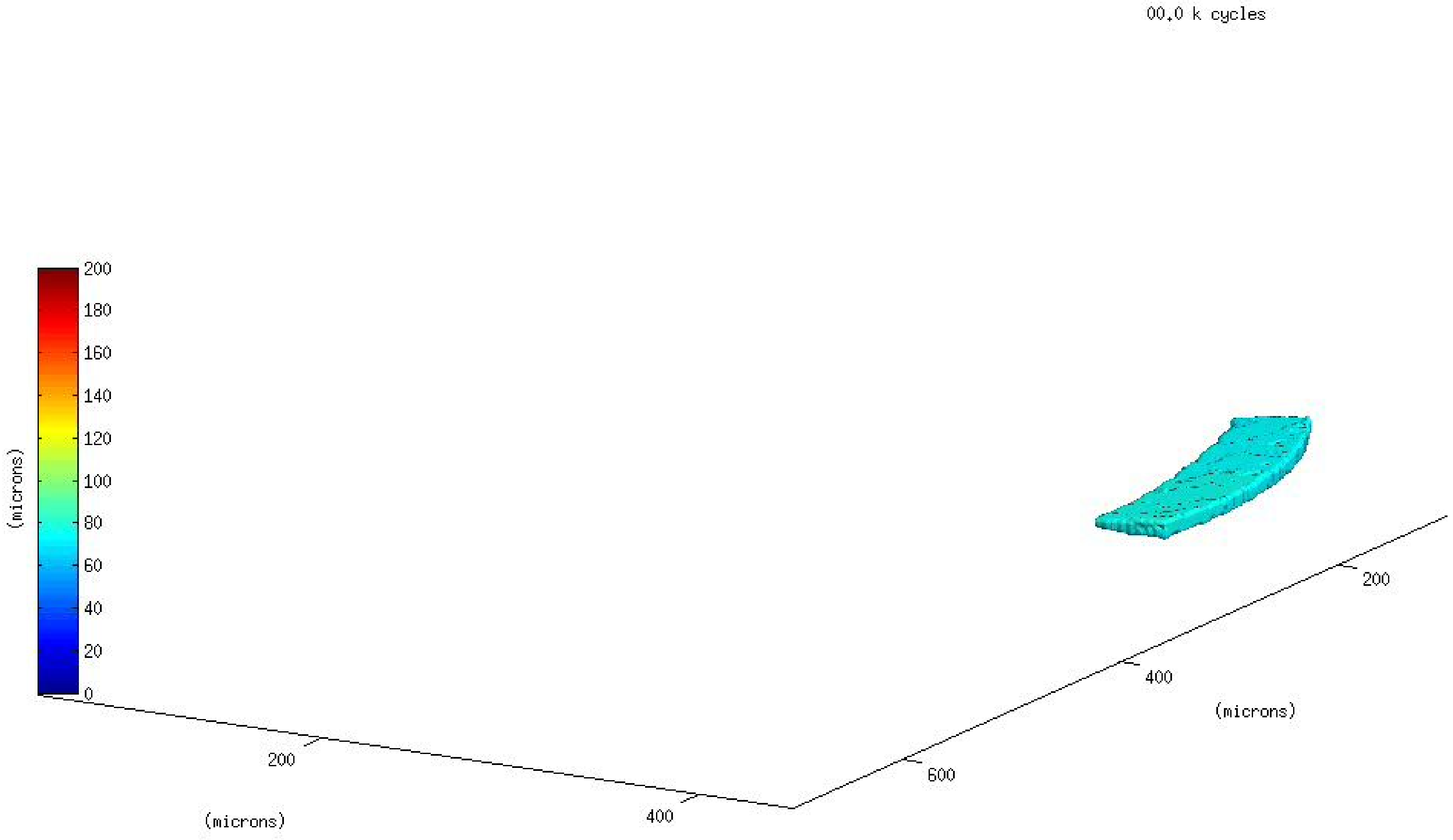

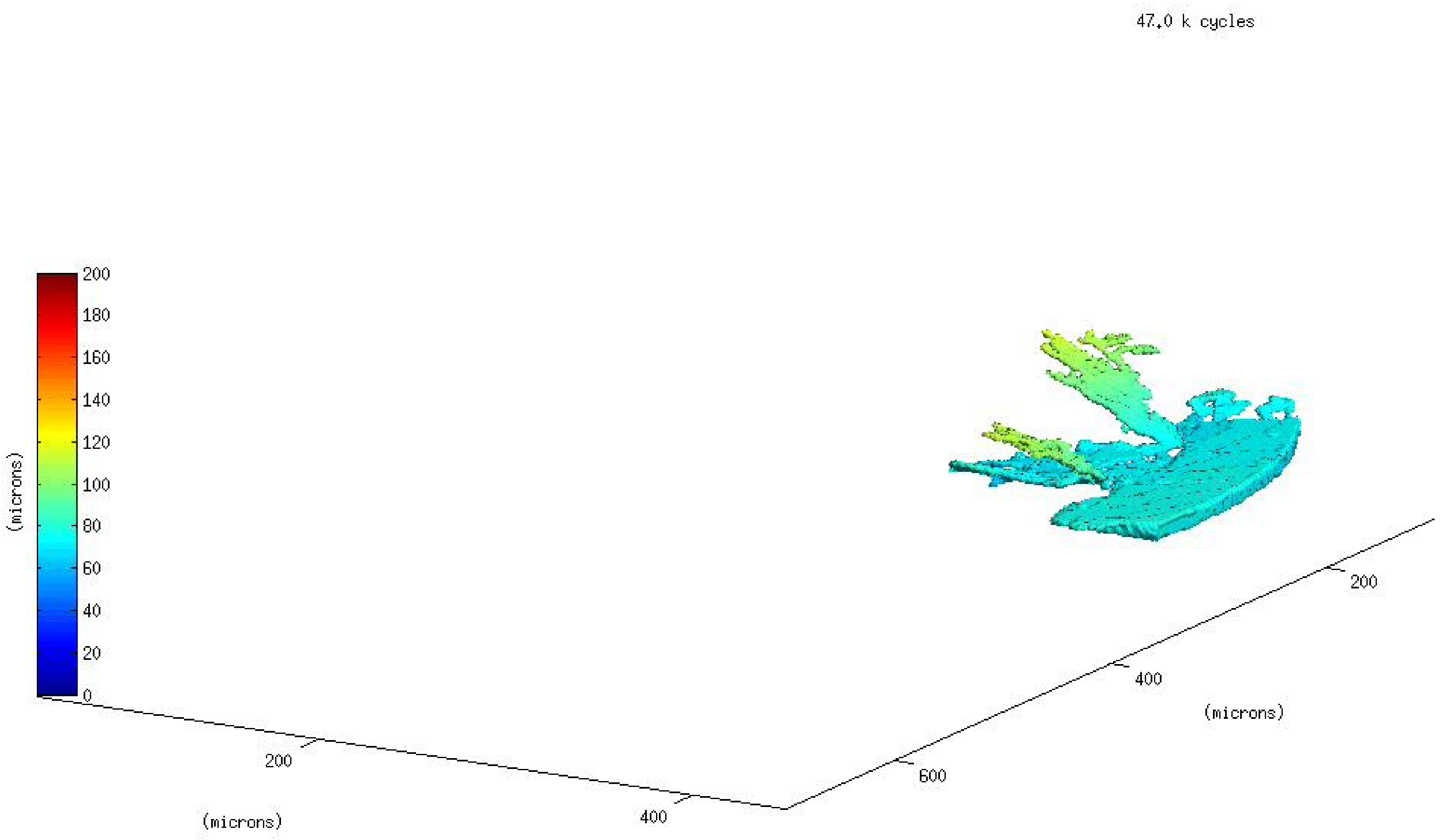
47.0 k cycles
200
180
160
140
120
100
80
60
40
20
0
(microns)
200
400
(microns)
200
400
600
(microns)

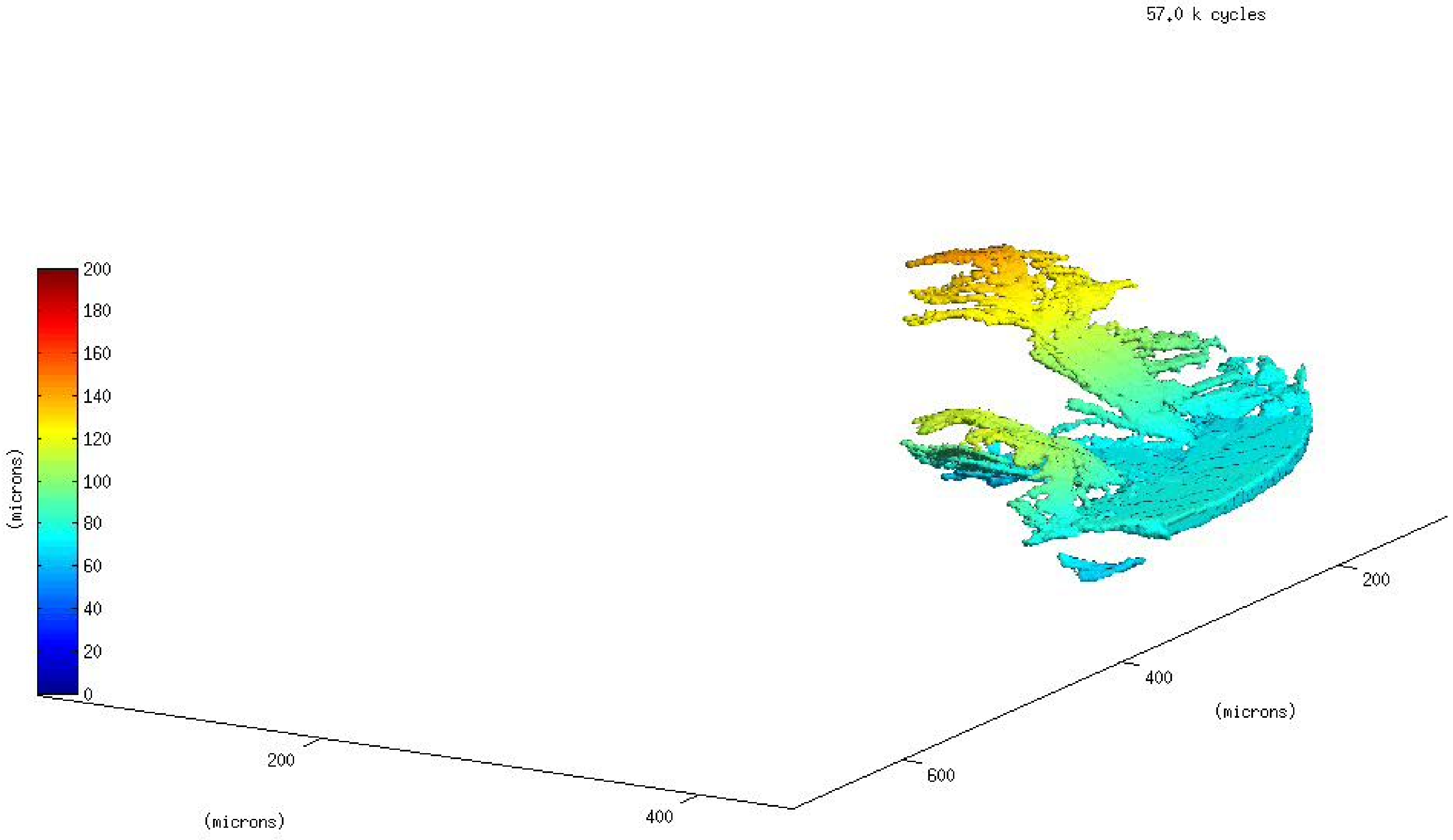
57.0 k cycles
200
180
160
140
120
100
80
60
40
20
0
(microns)
200
400
(microns)
200
400
600
(microns)

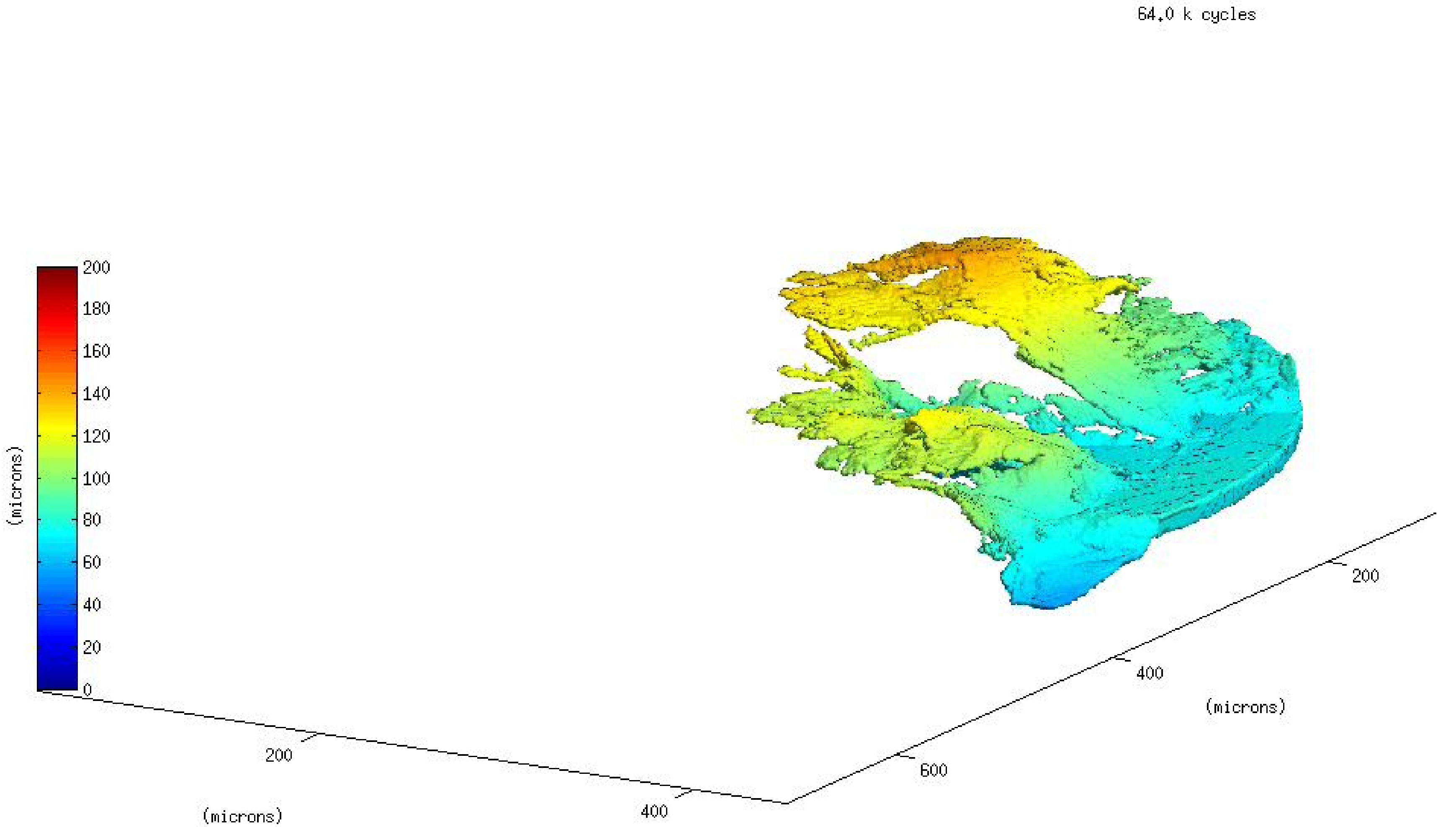

64.0 k cycles
200
180
160
140
120
100
80
60
40
20
0
(microns)
200
400
(microns)
200
400
600
(microns)

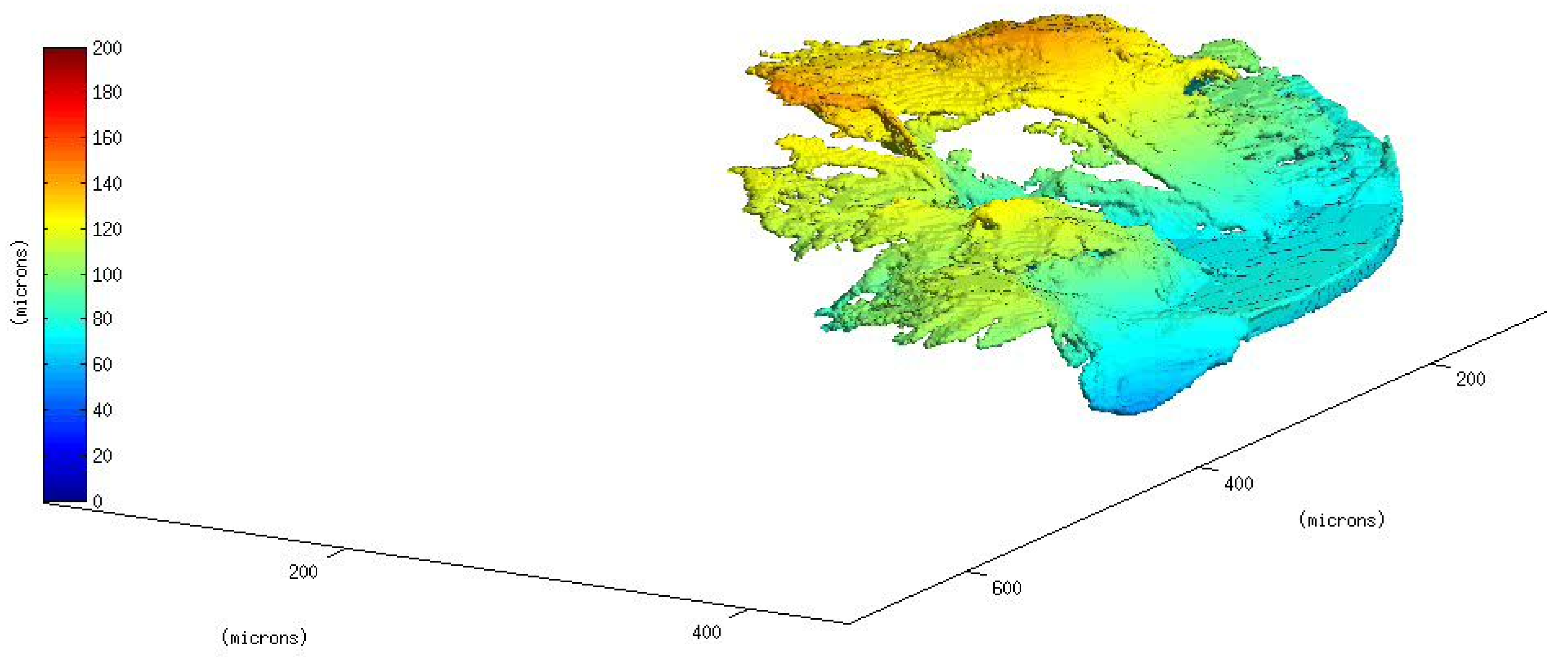
68.0 k cycles
200
180
160
140
120
100
80
60
40
20
0
(microns)
200
400
(microns)
200
400
600
(microns)

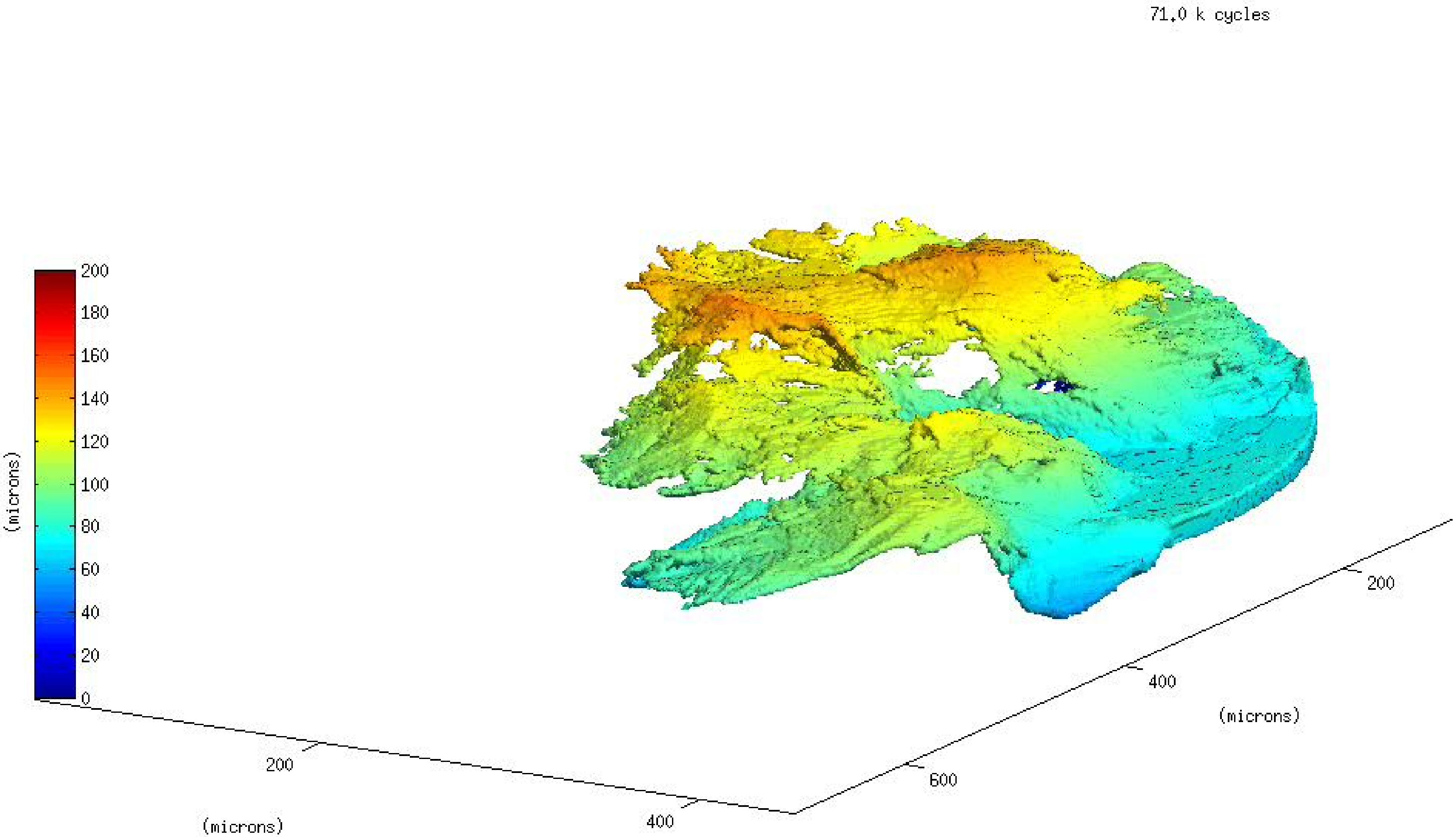

71.0 k cycles
200
180
160
140
120
100
80
60
40
20
0
(microns)
200
400
(microns)
200
400
600
(microns)

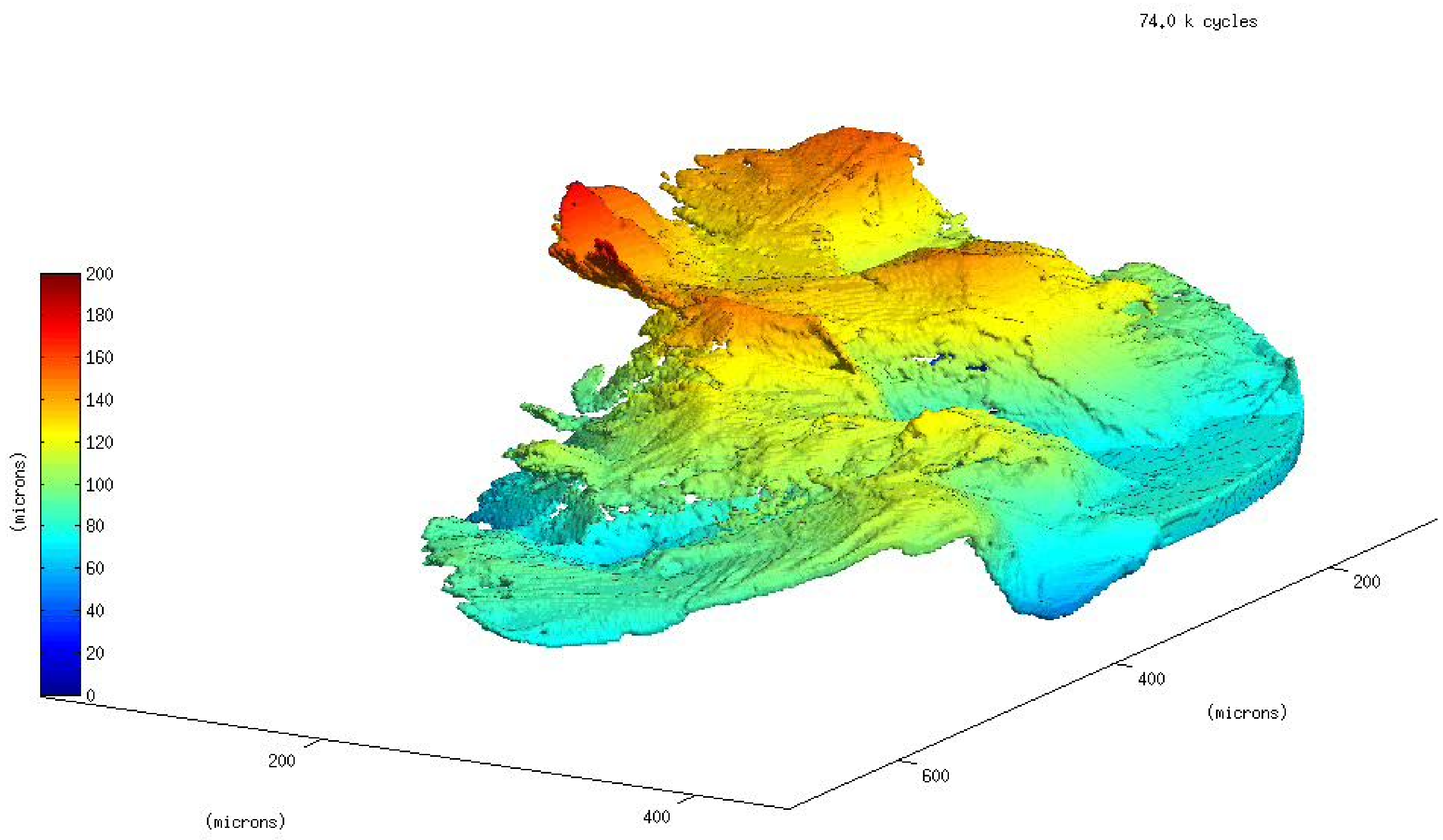
74.0 k cycles
200
180
160
140
120
100
80
60
40
20
0
(microns)
200
400
(microns)
200
400
600
(microns)

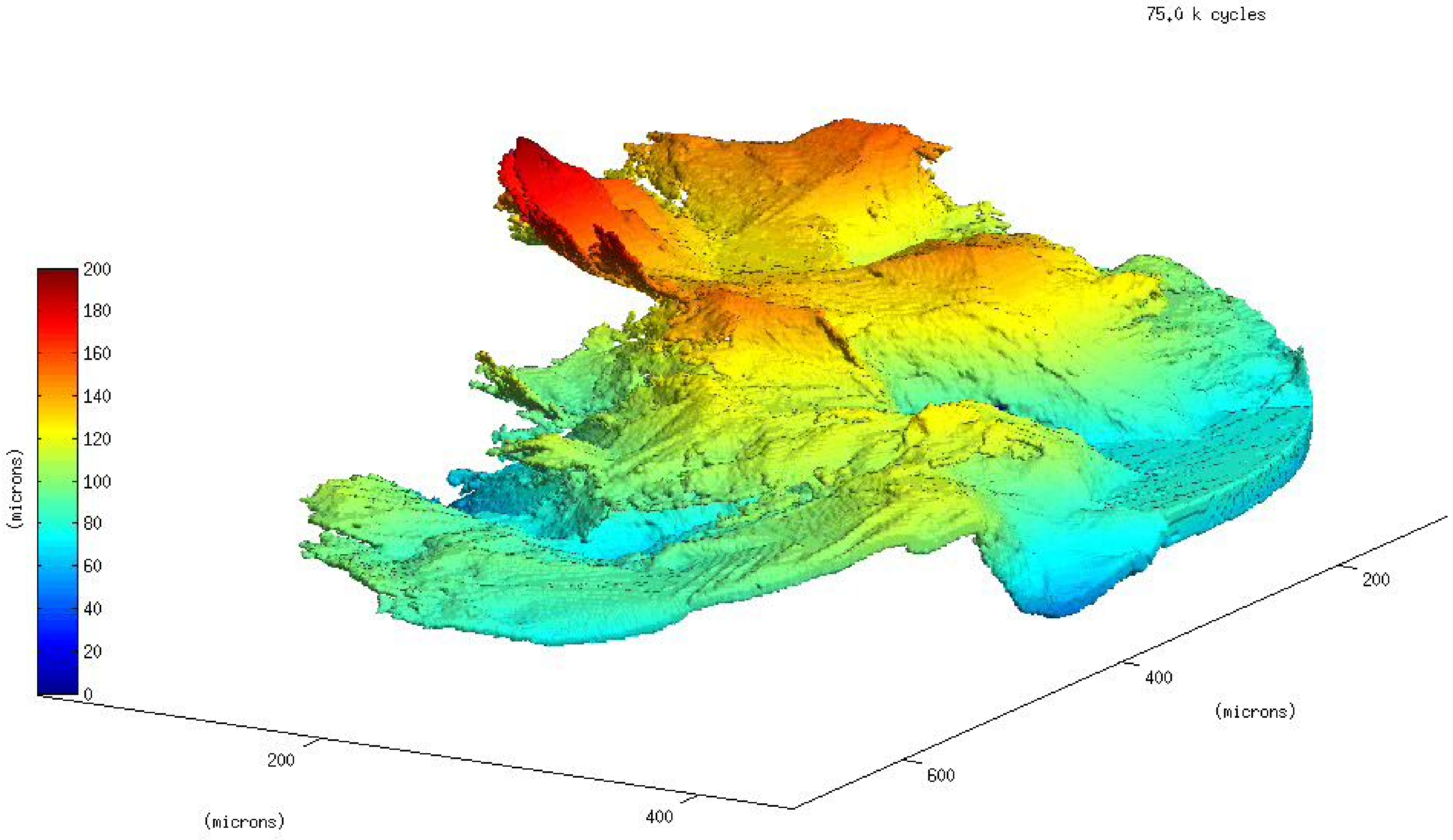

75.0 k cycles
(microns)
200
180
160
140
120
100
80
60
40
20
0
200
400
(microns)
200
400
600
(microns)

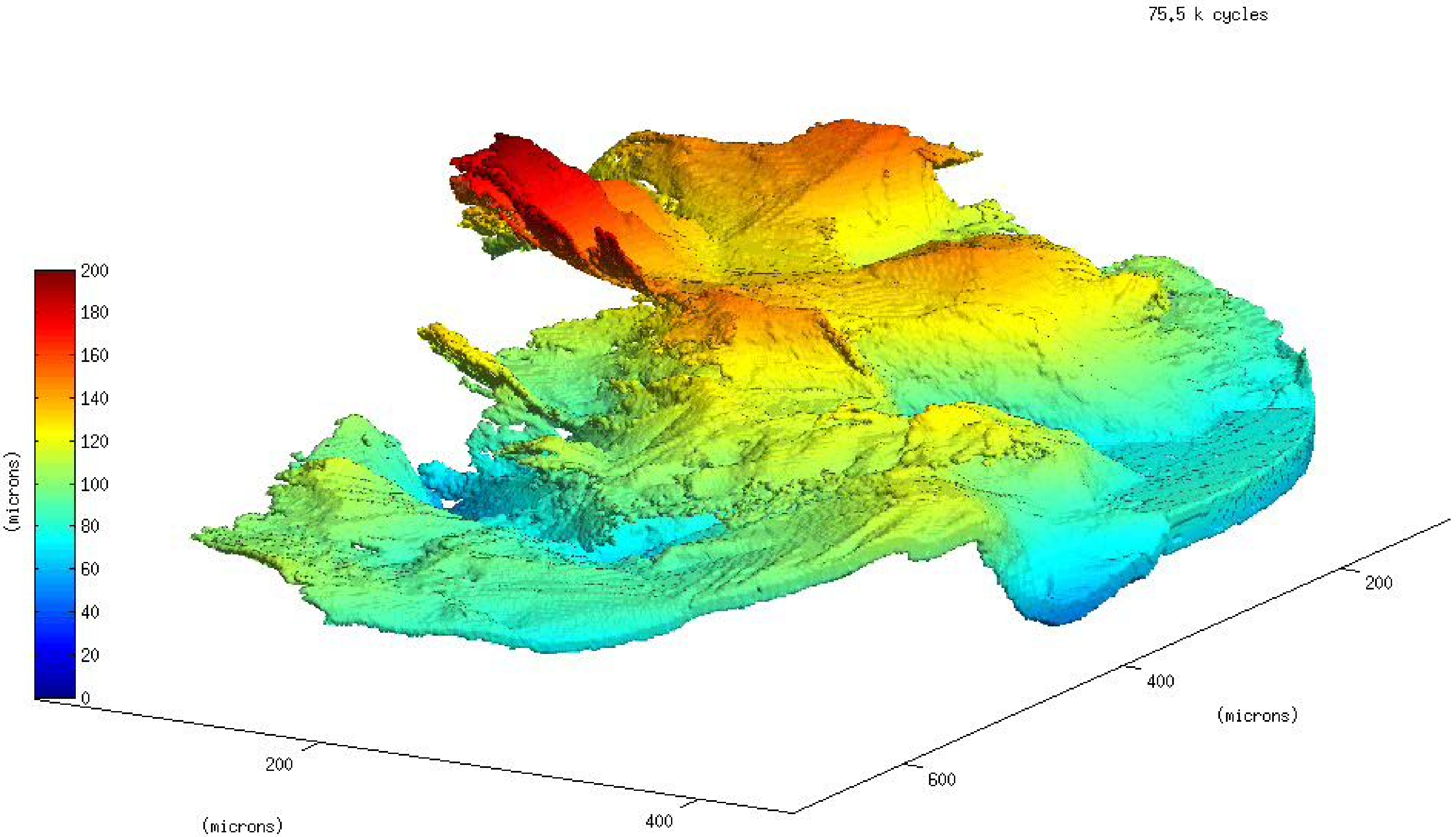
75.5 k cycles
200
180
160
140
120
100
80
60
40
20
0
(microns)
200
400
(microns)
200
400
600
(microns)

In situ fatigue

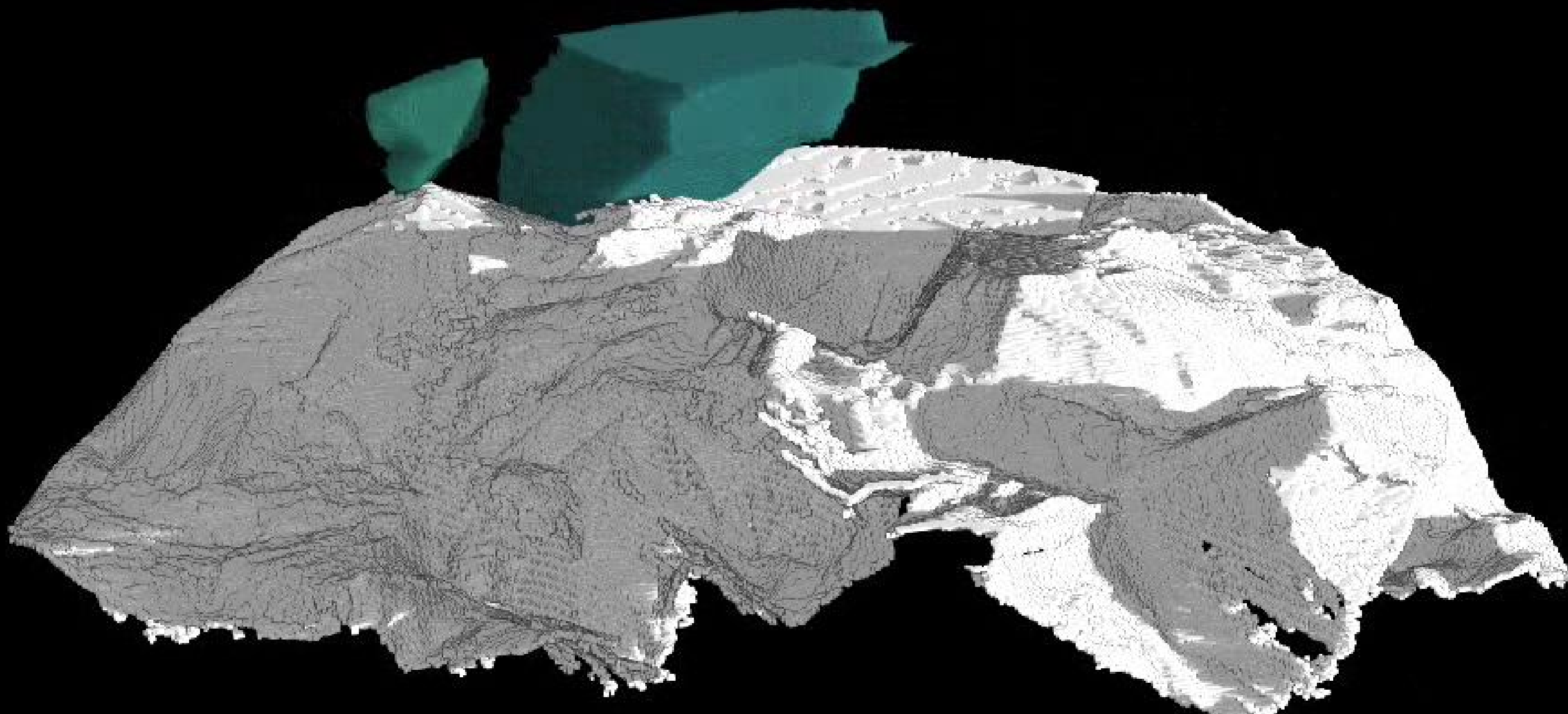

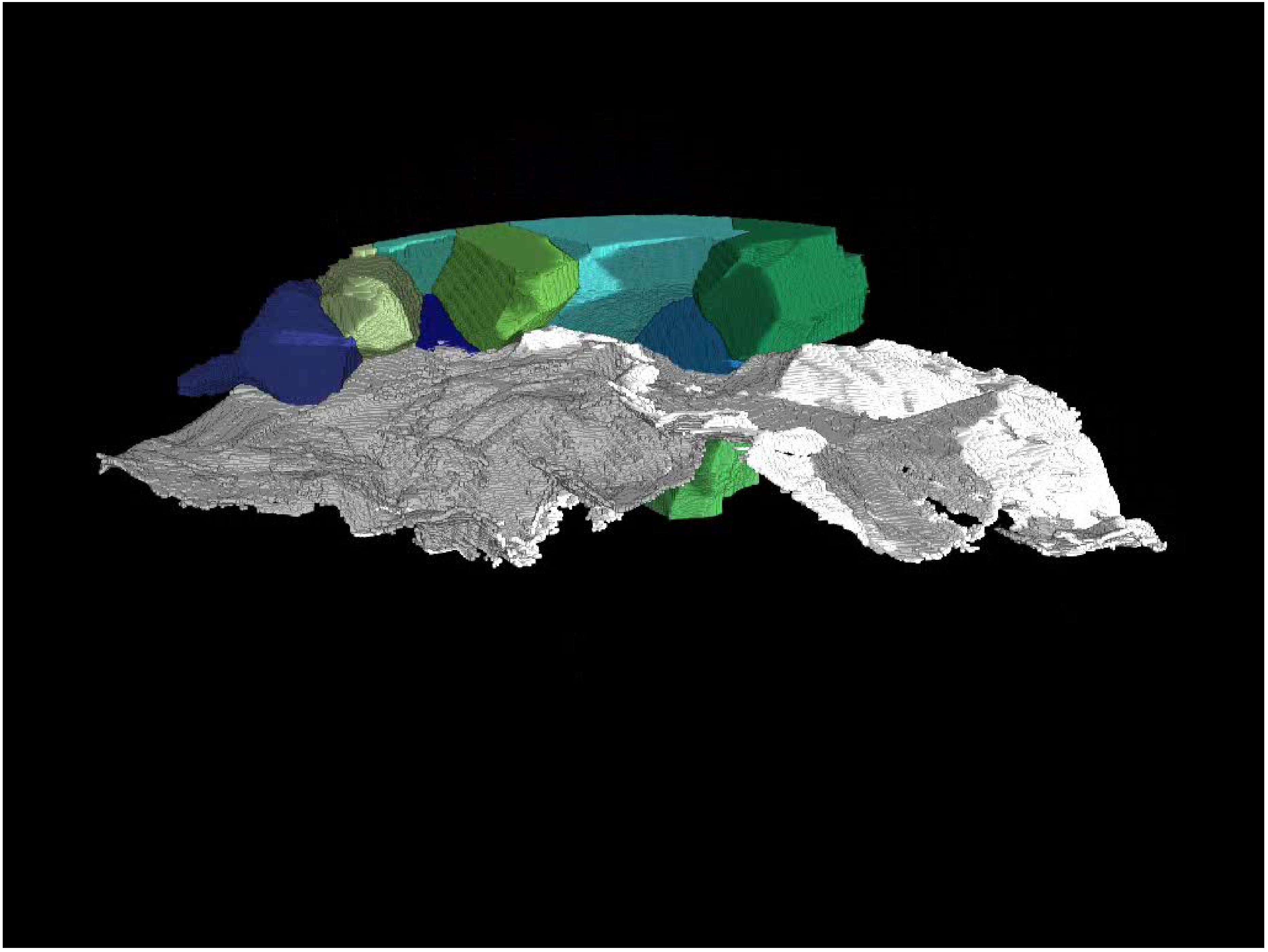

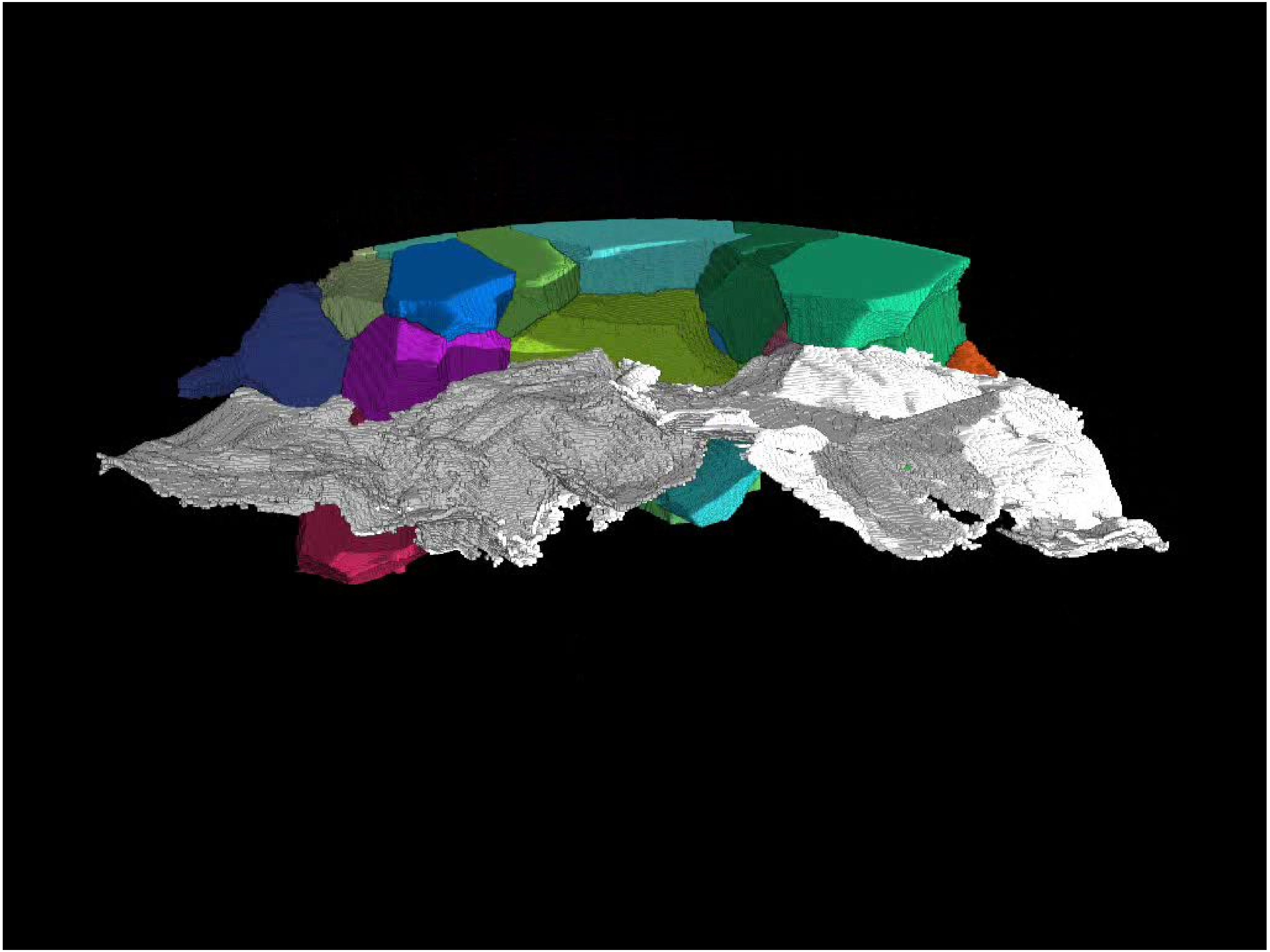

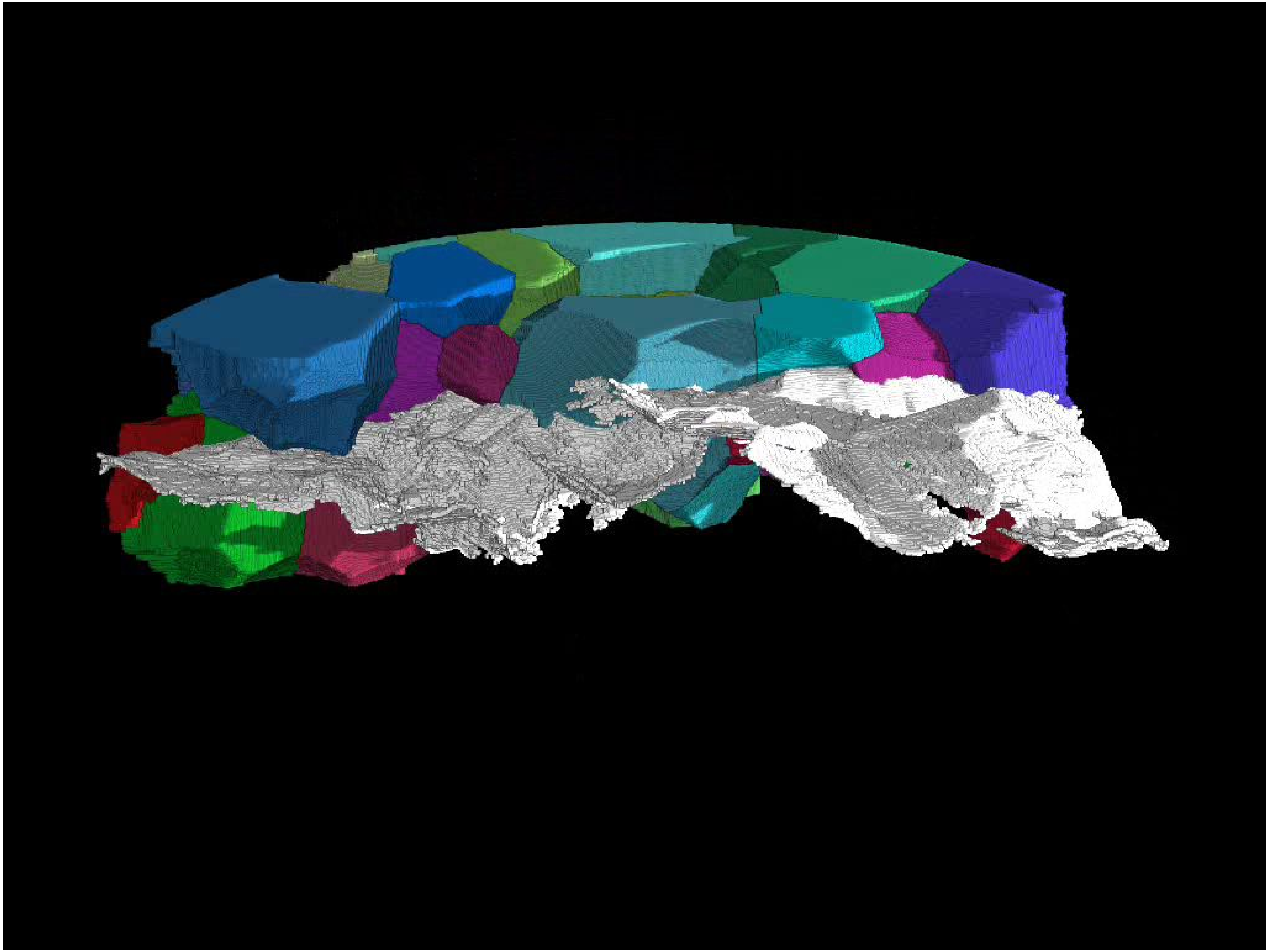

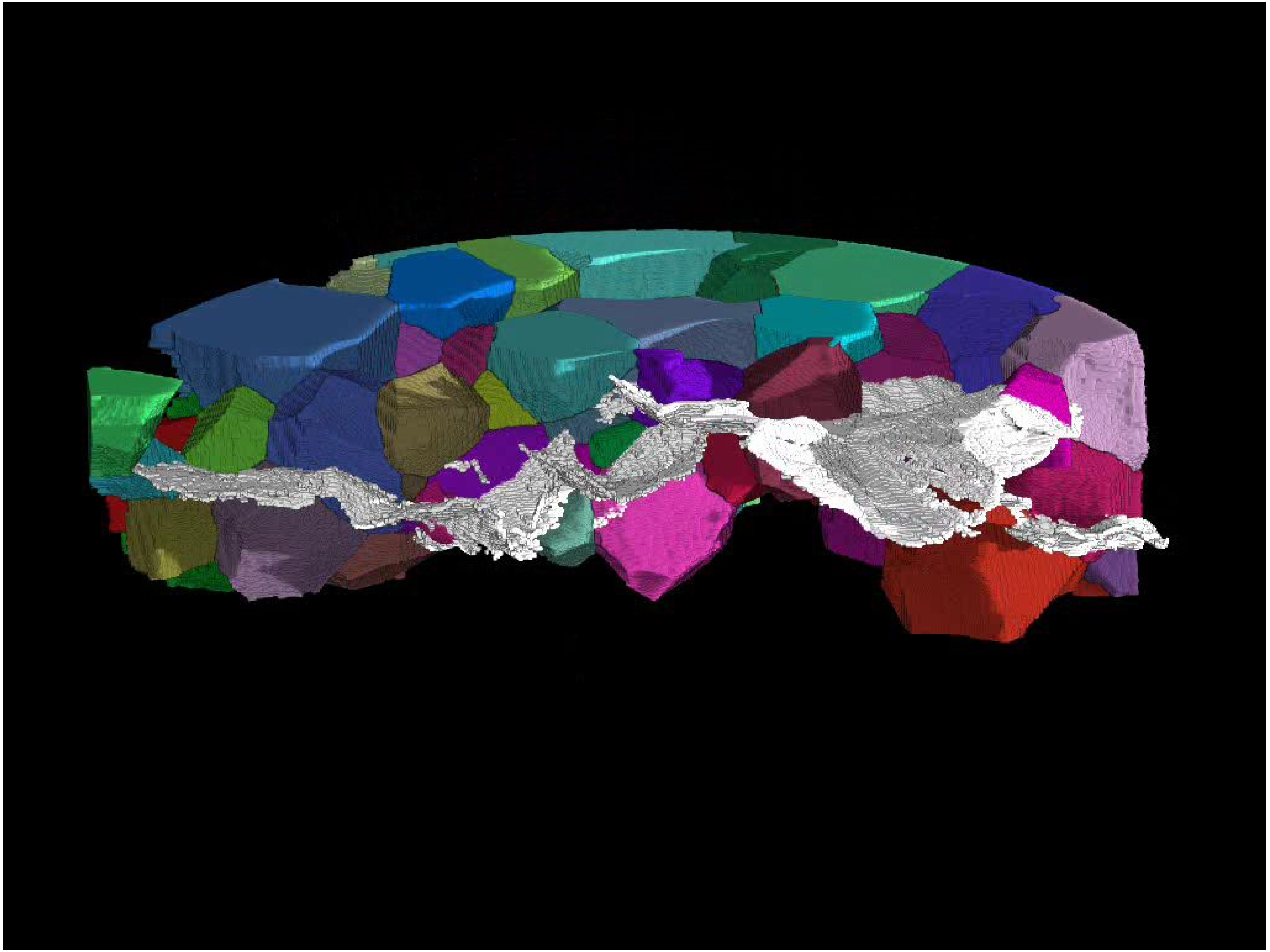

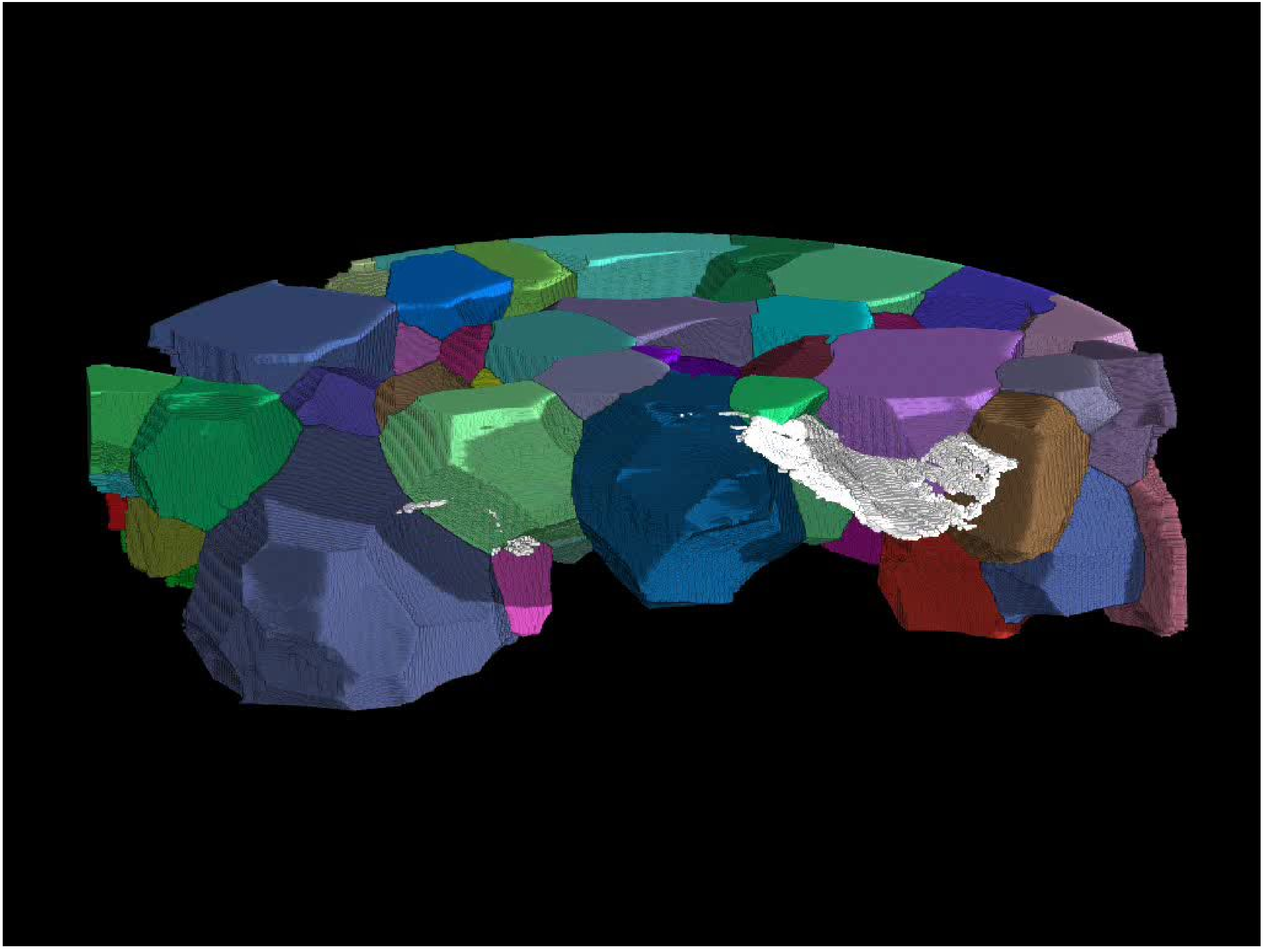

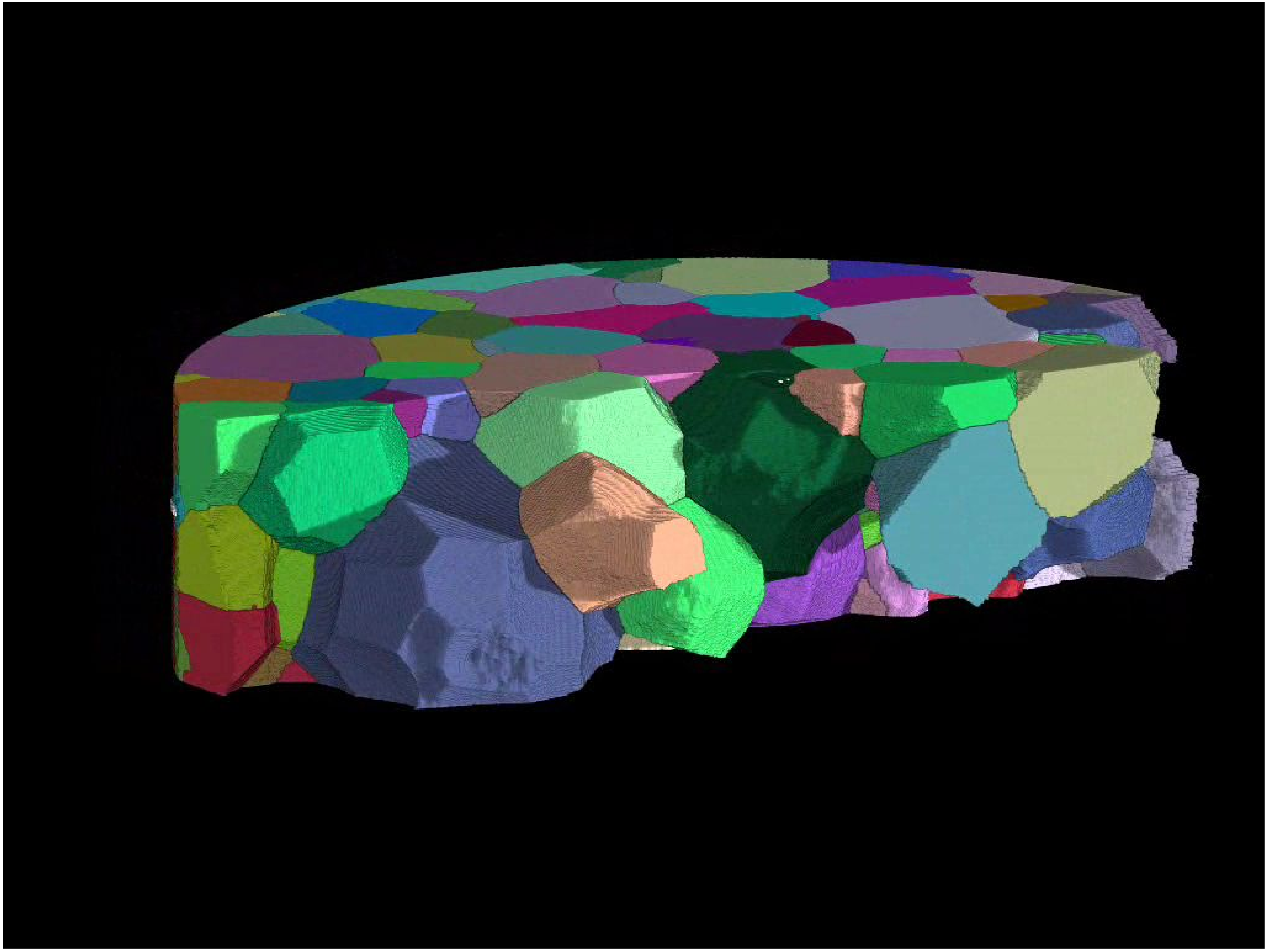

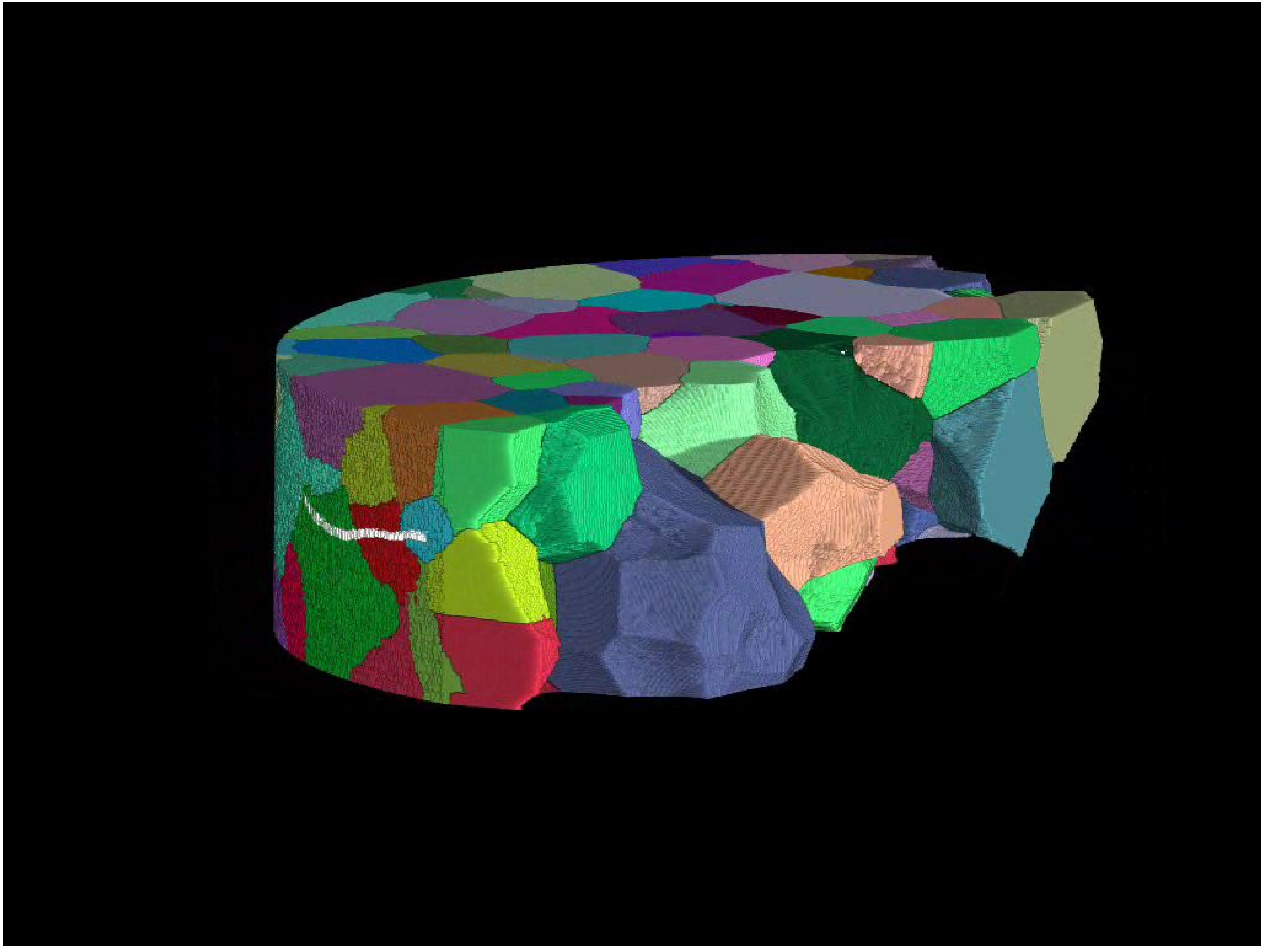

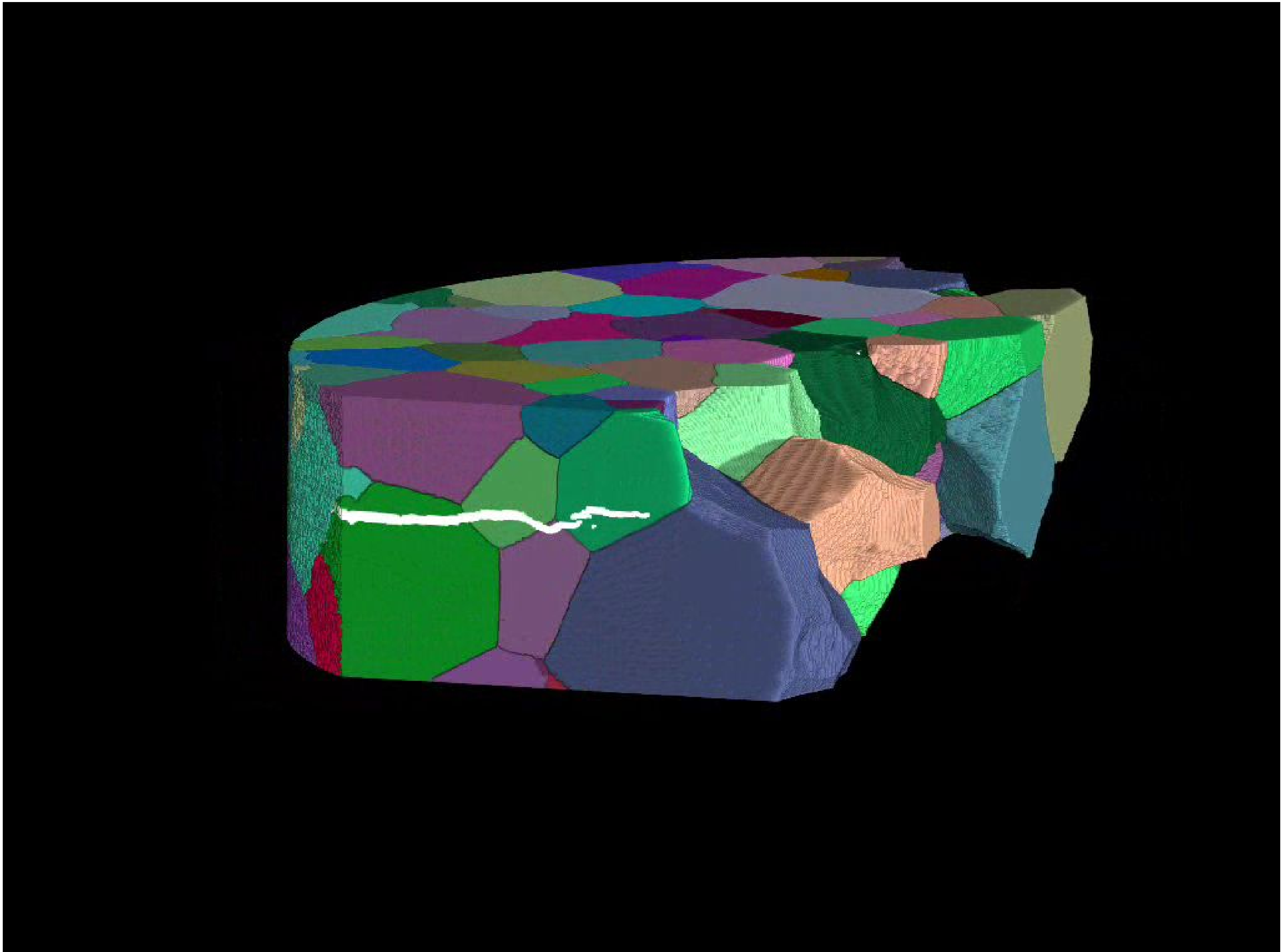

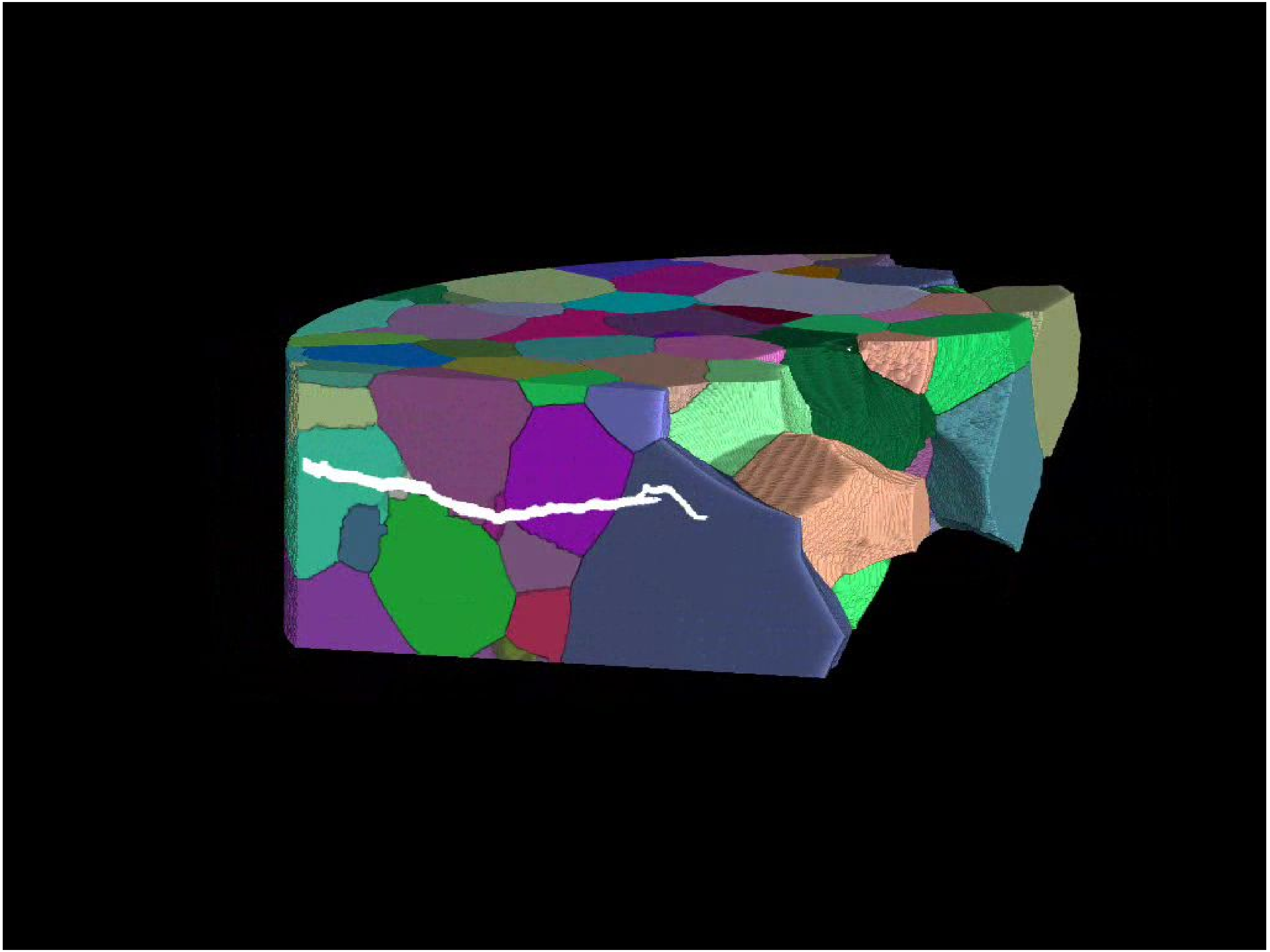

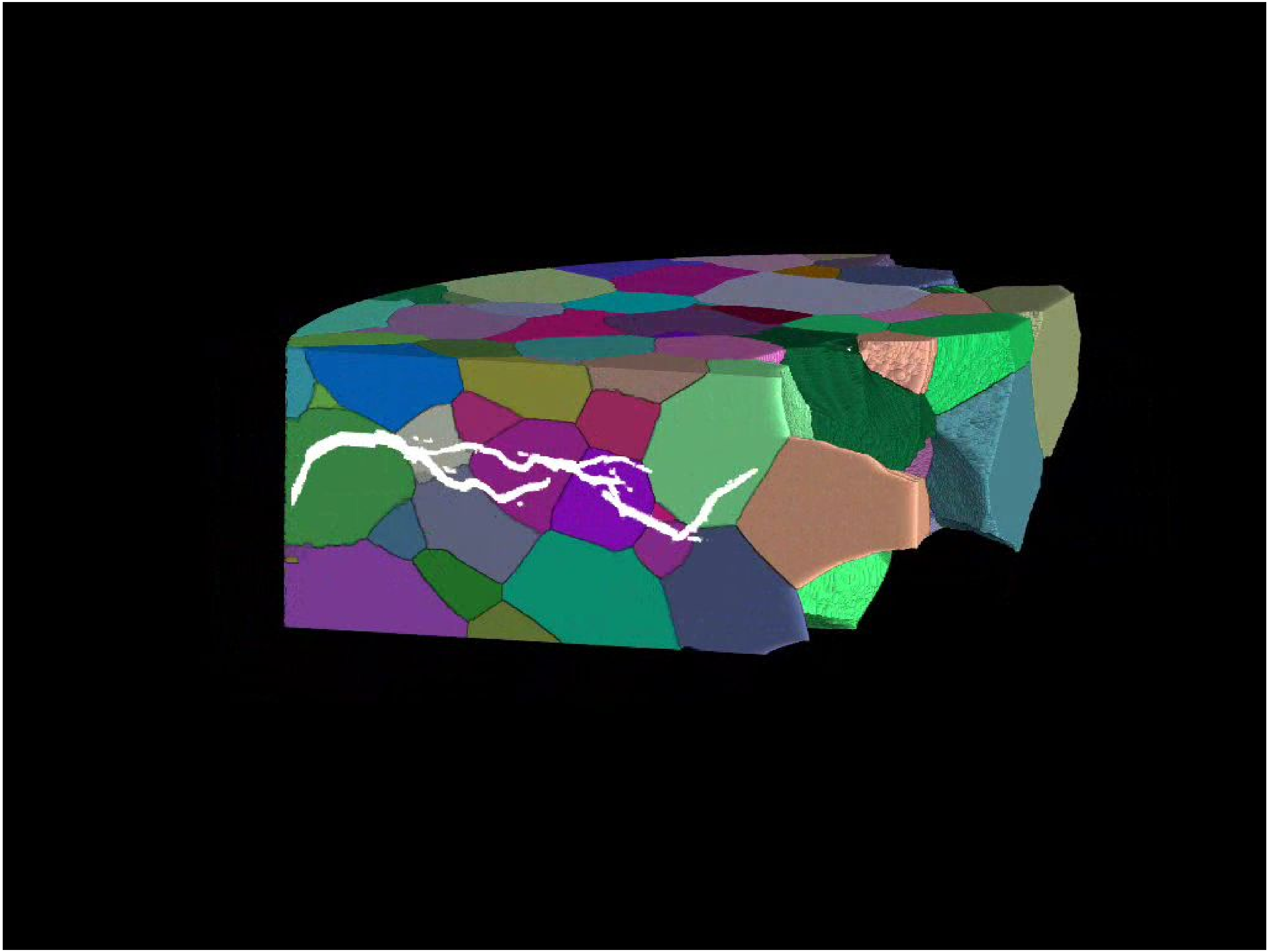

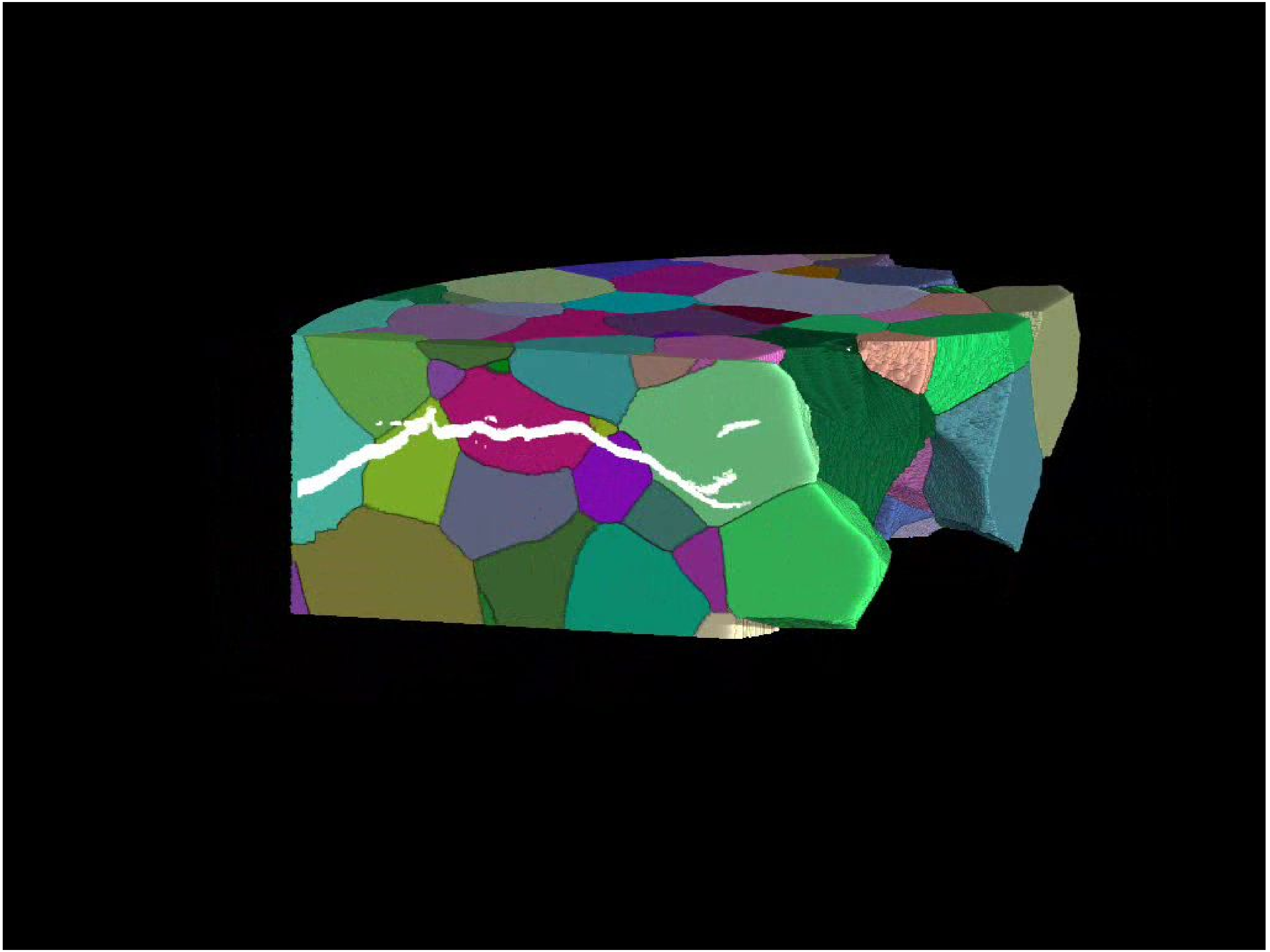

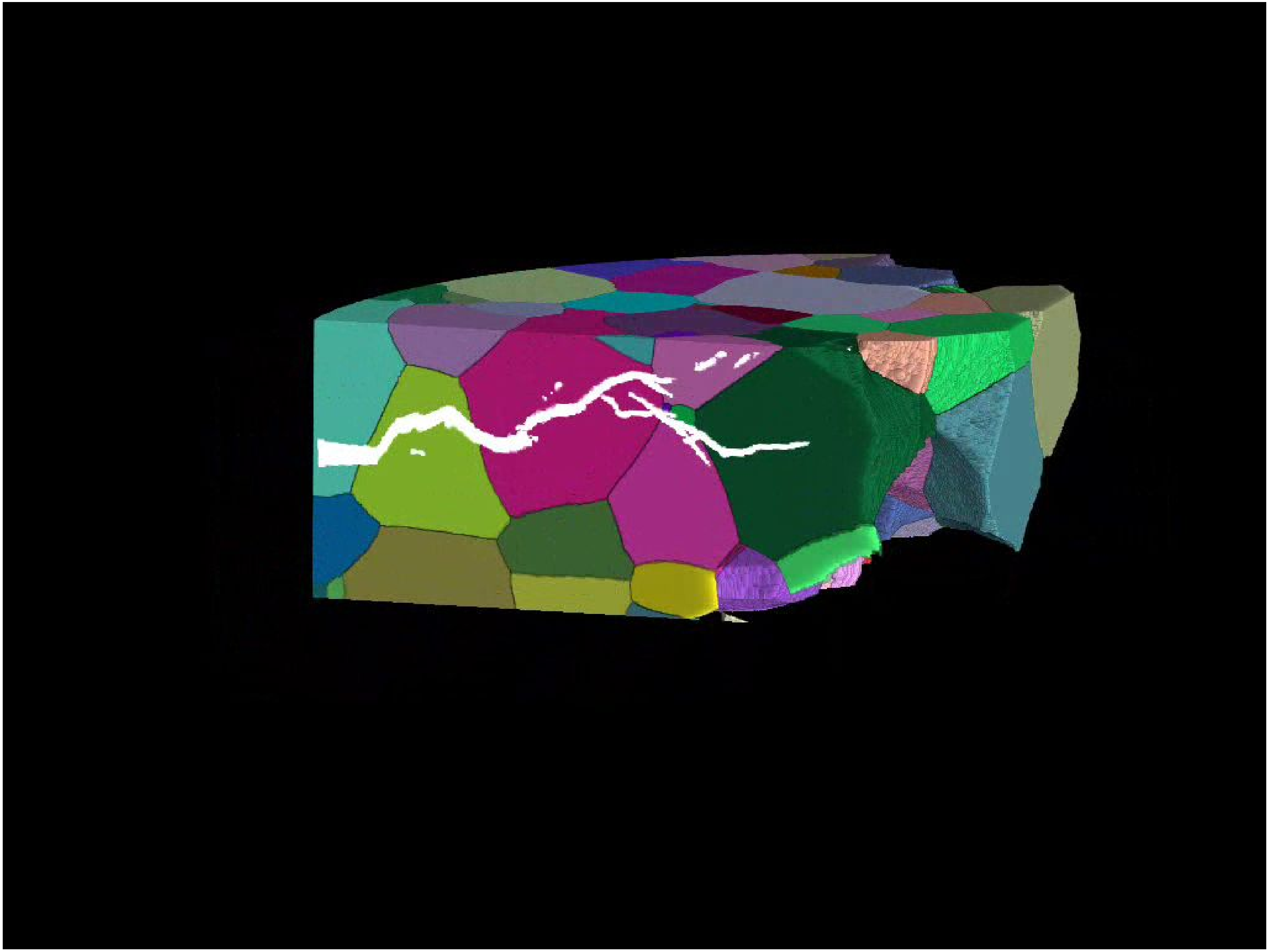

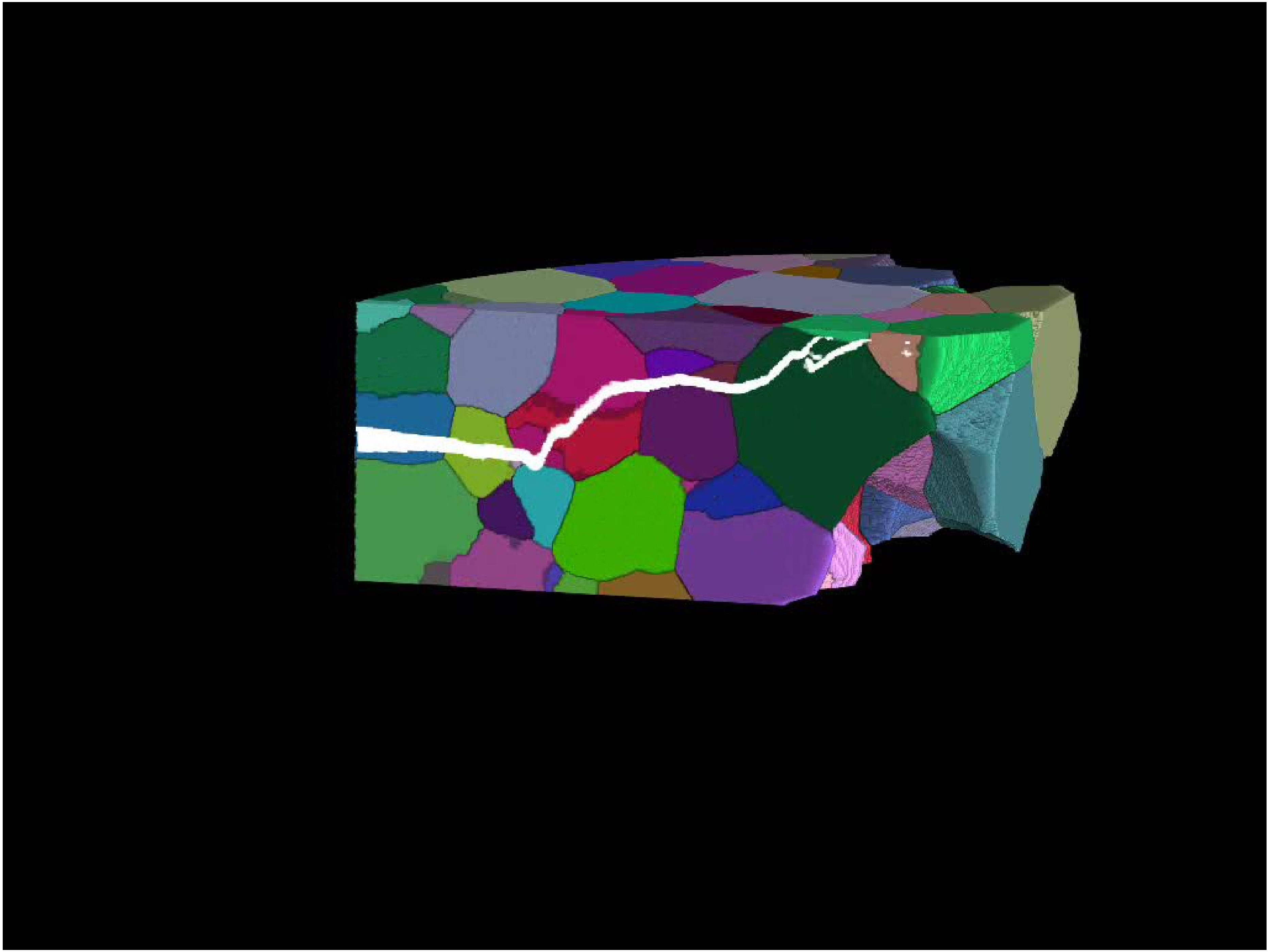

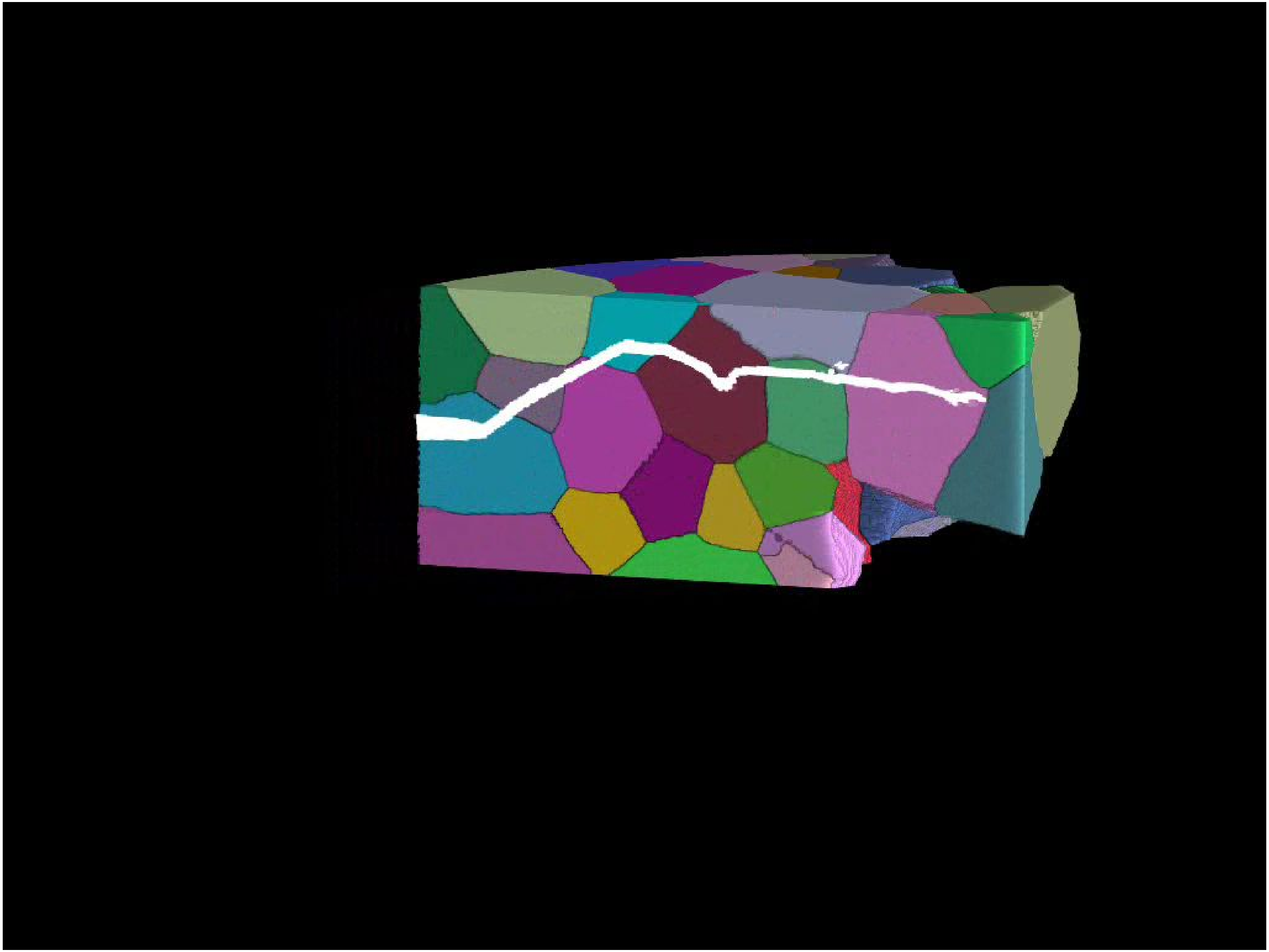

Visualisation of Fracture Surface in "21S"

Crystallographic orientation distribution

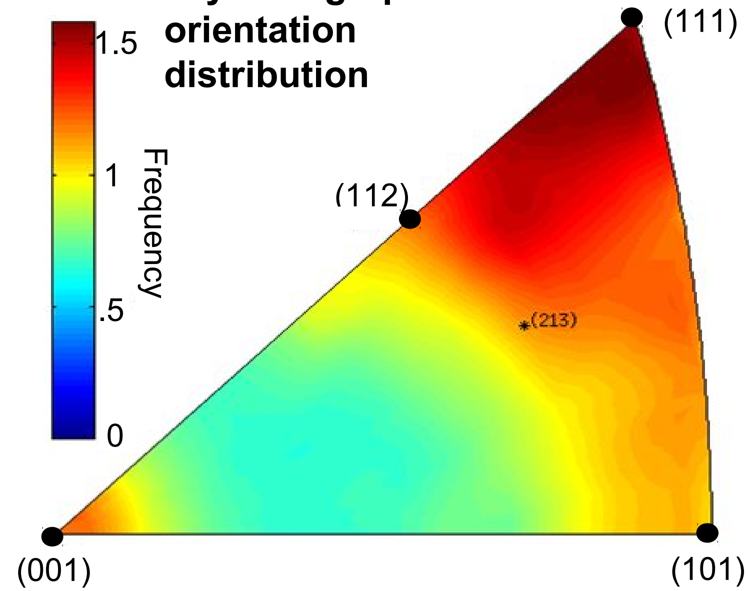

Crystallographic orientation

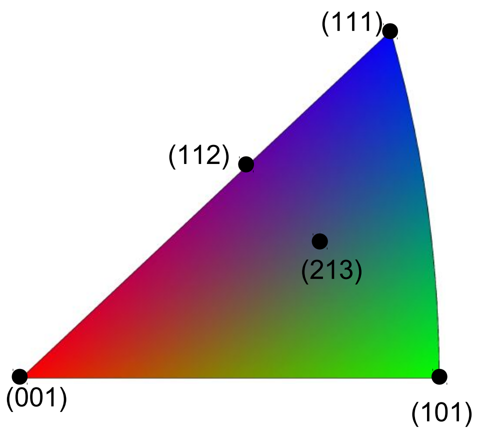

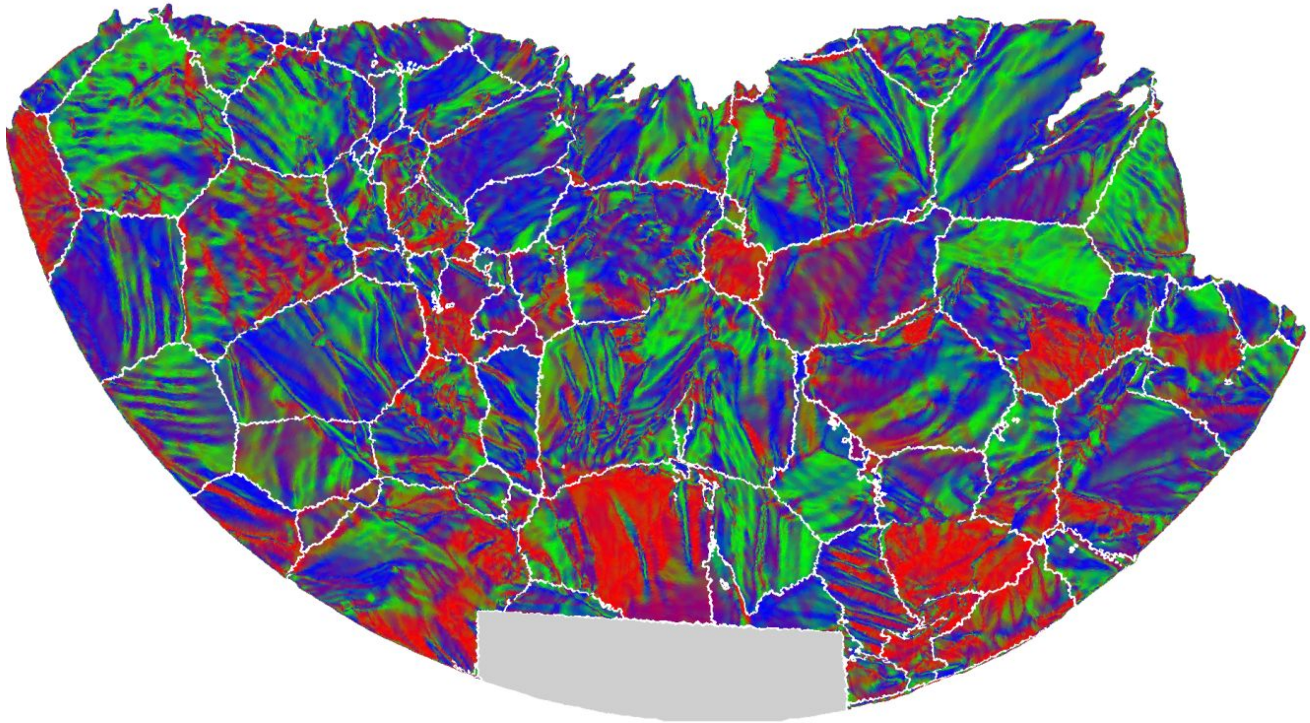

Real *v.s.* Measured Fracture Surface

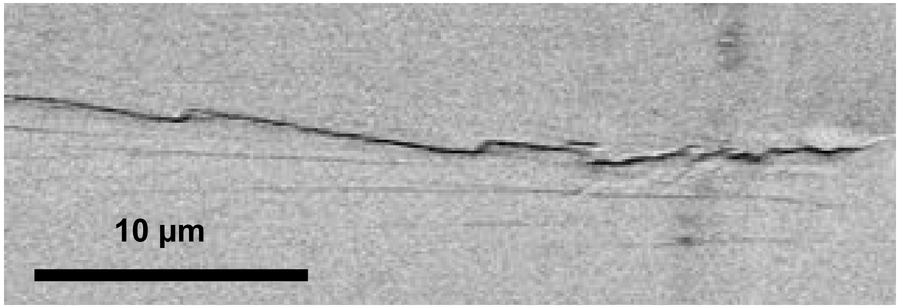

SEM micrograph: Real crack morphology

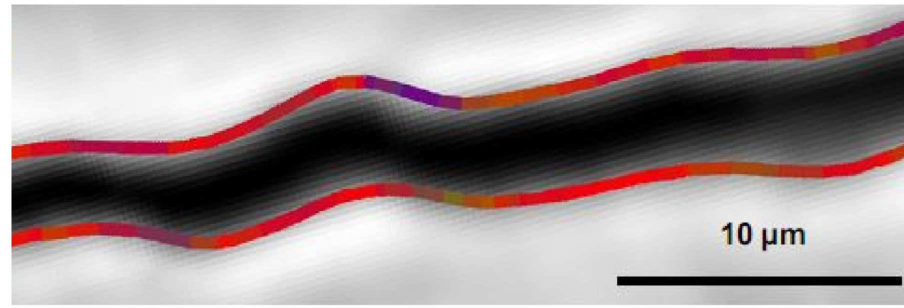

Tomographic reconstruction: Measured crack morphology

➡ Relation between real and measured fracture surface orientation depends on ratio between frequency of plane changes and resolution

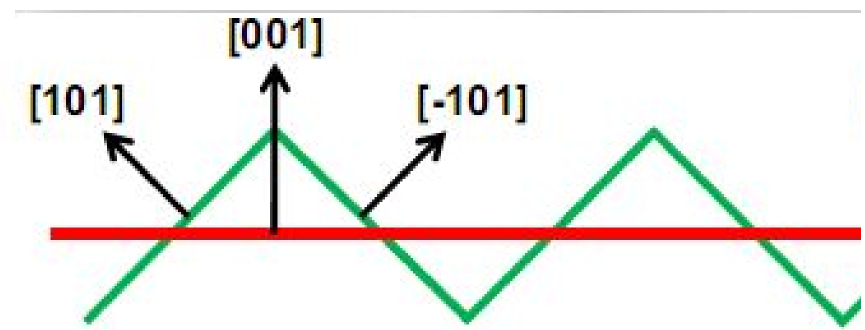

A measured {001} fracture surface might in reality be comprised of alternating {110} planes

Interpretation of Fracture Surface in "21S"

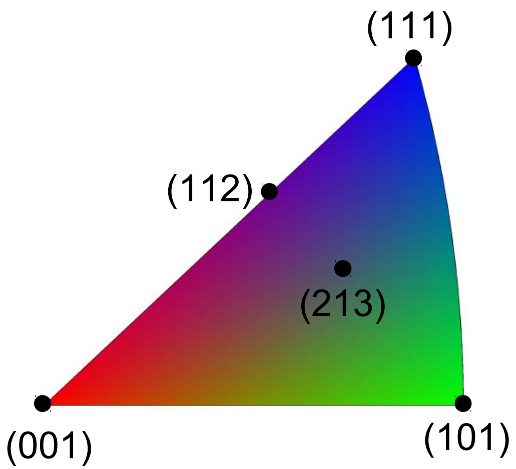

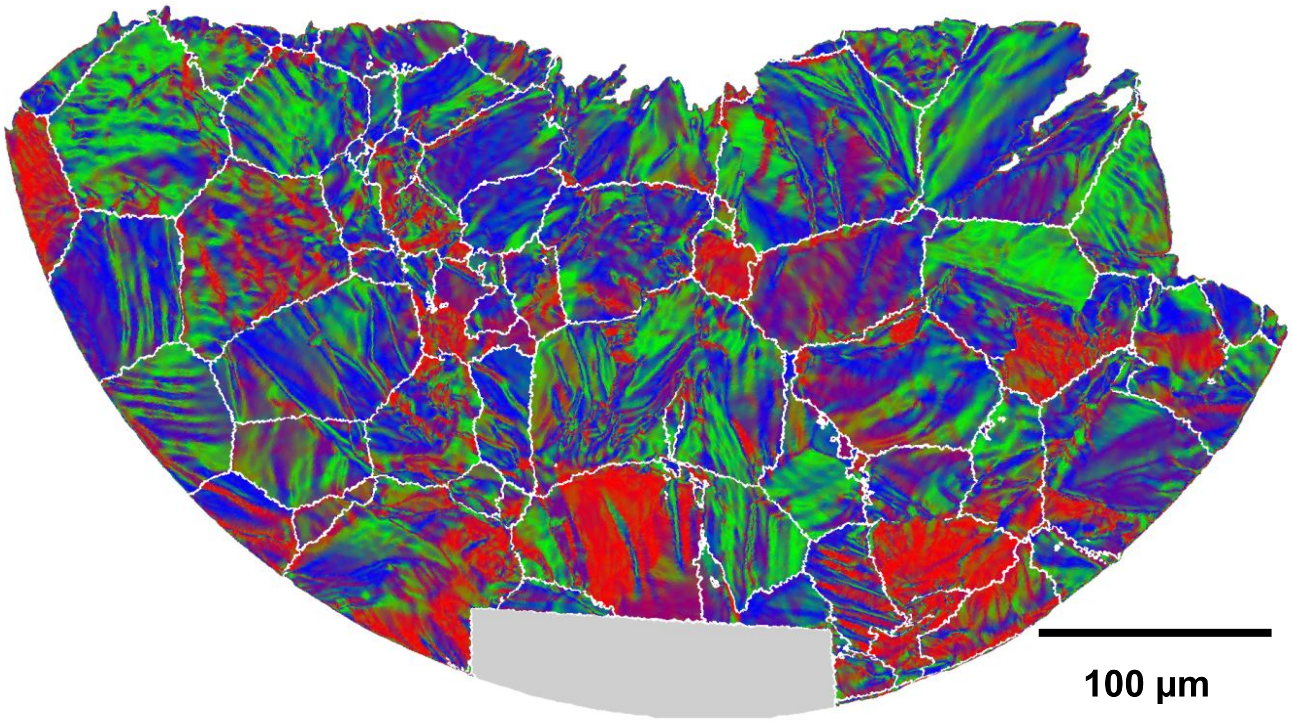

Frequency of plane changes	Measured surface orientation	Fracture surface color	Crack propagation
low	= real orientation	green, purple	"single slip"
intermediate	≠ real orientation	striped pattern	"double slip"
high	≠ real orientation	red, blue	"double slip"

M. Herbig et al. Acta Mater 2010.

Crack Fronts

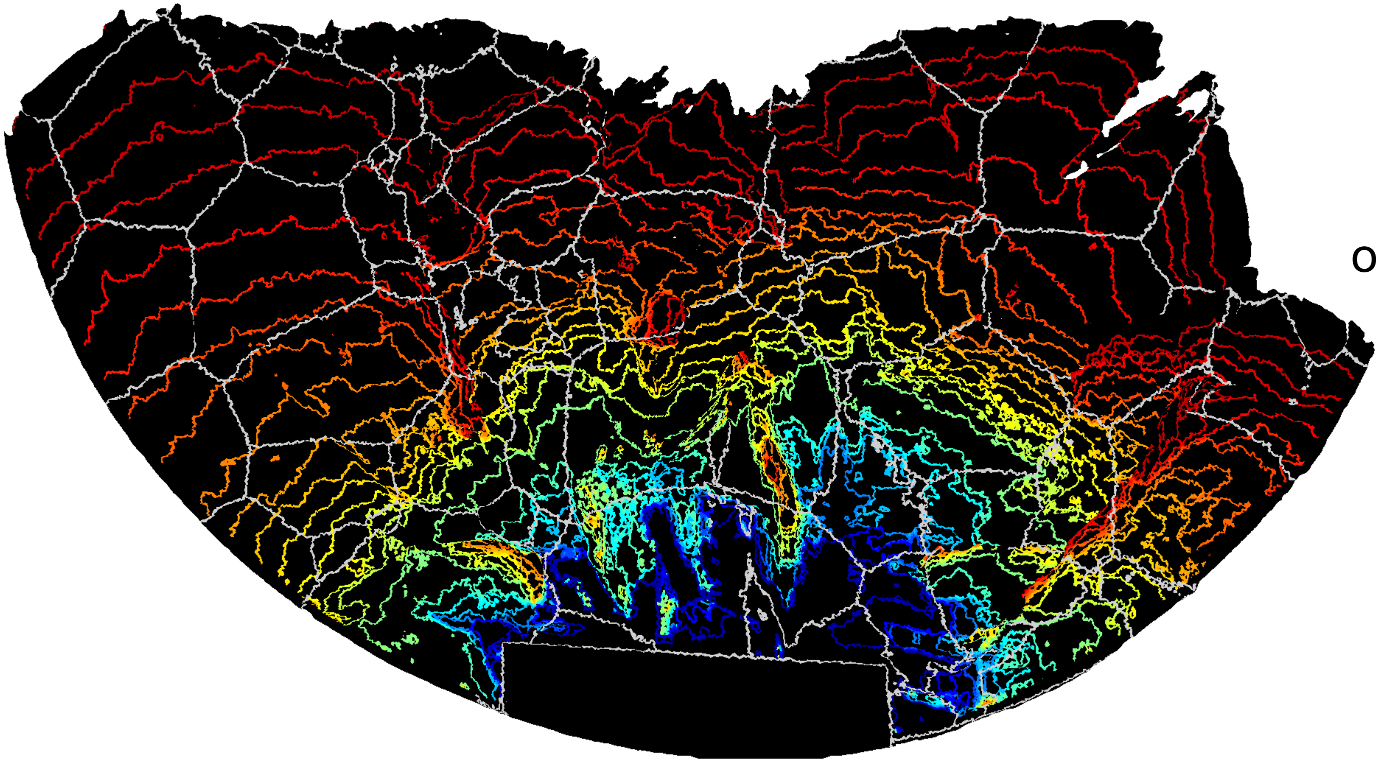

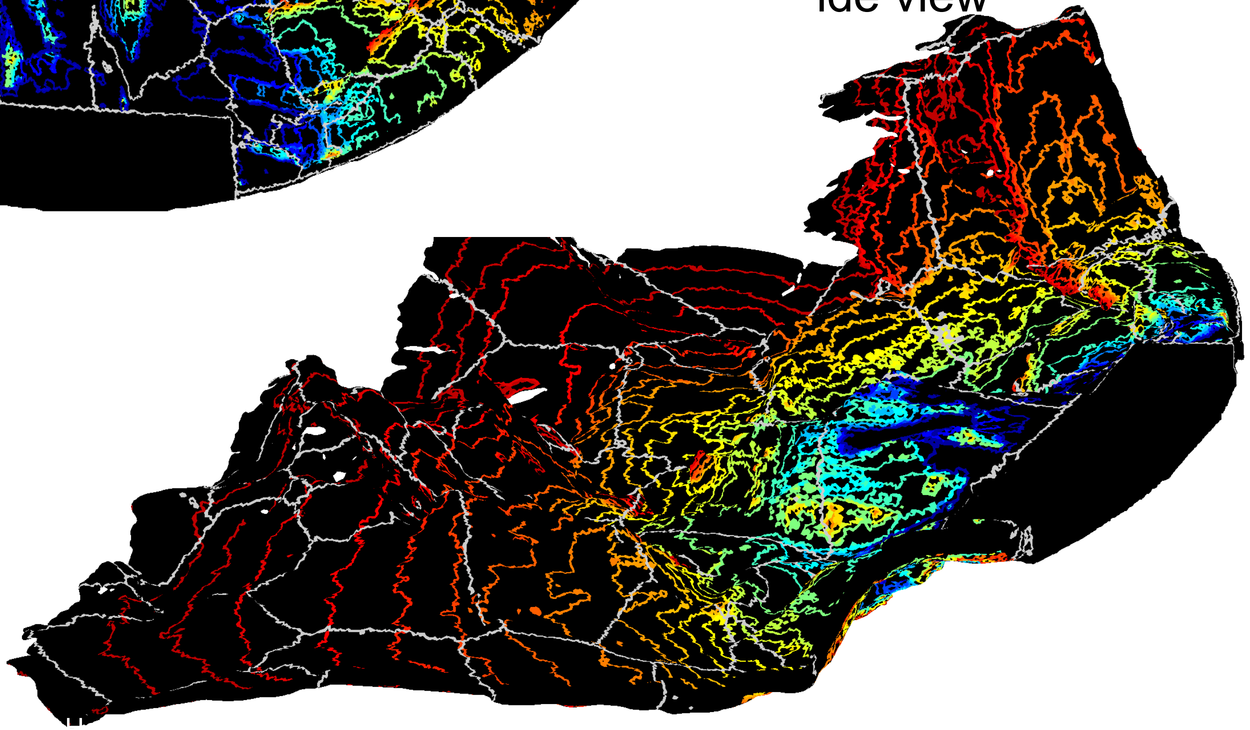

Plot of crack fronts.

Blue: 46 k cycles,
red: 75,5 k cycles

Extraction of Local Growth Rate

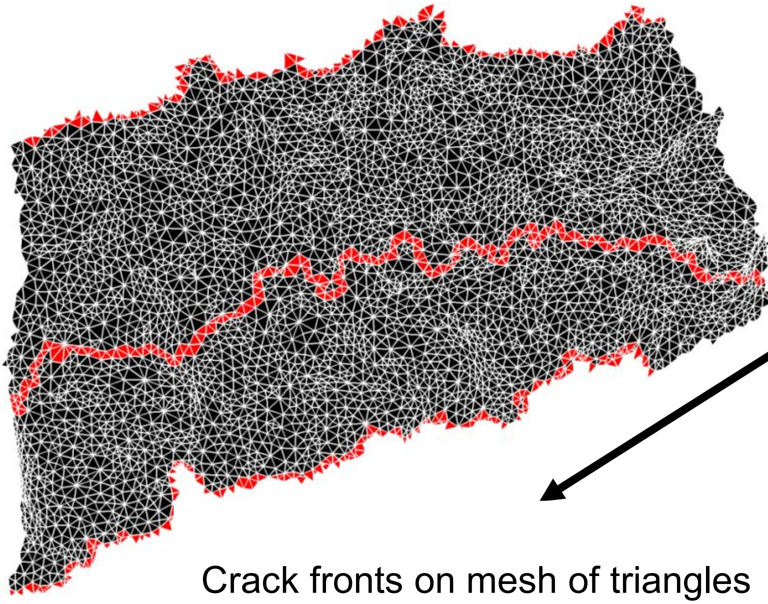

Crack fronts on mesh of triangles

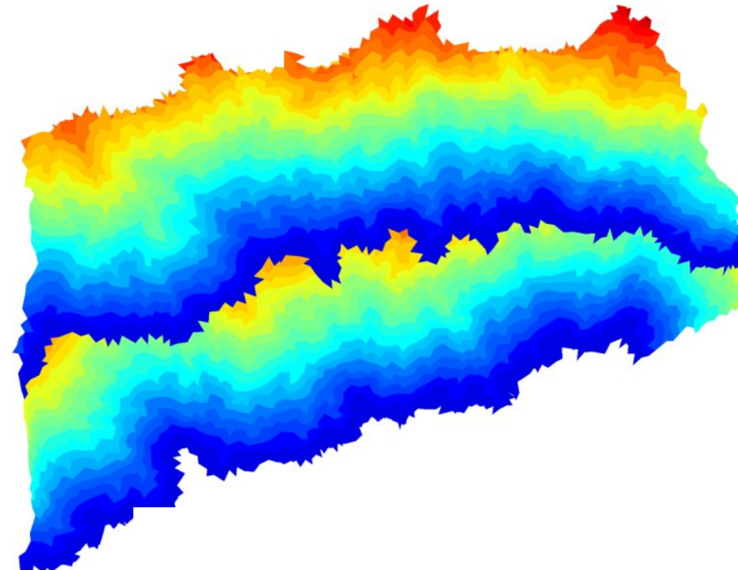

Finding stepwise nearest triangles

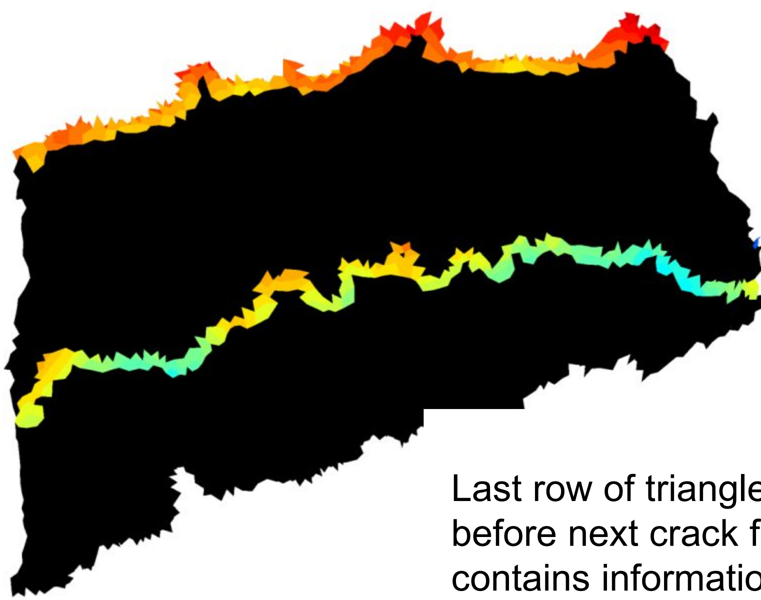

Last row of triangles before next crack front contains information on local growth rate

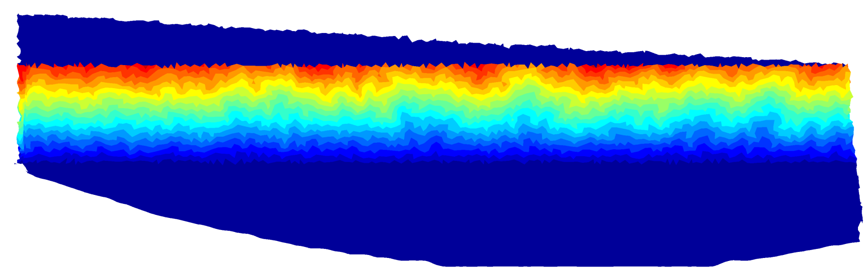

Calibration on notch

M. Herbig et al. Acta Mater 2010.

3D Local Growth Rate

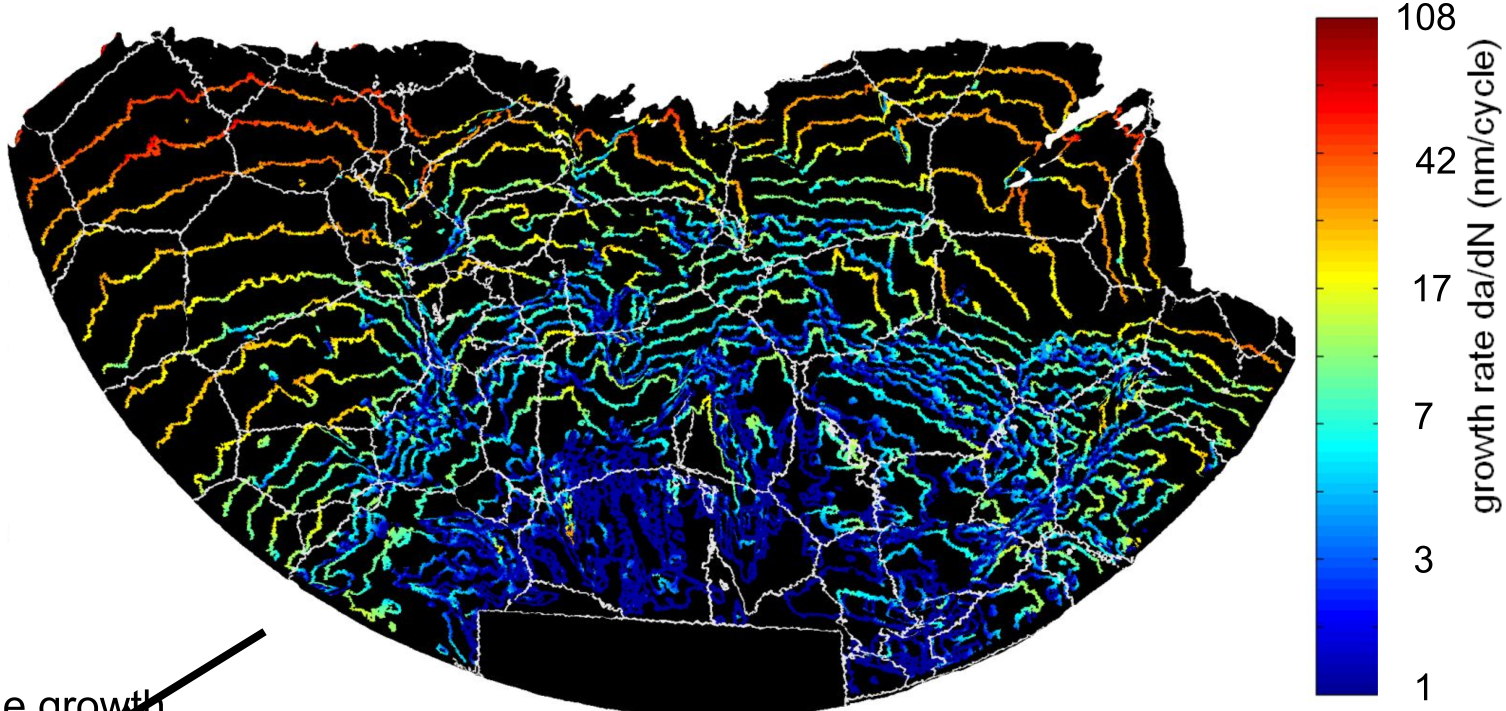

Average growth rate per grain

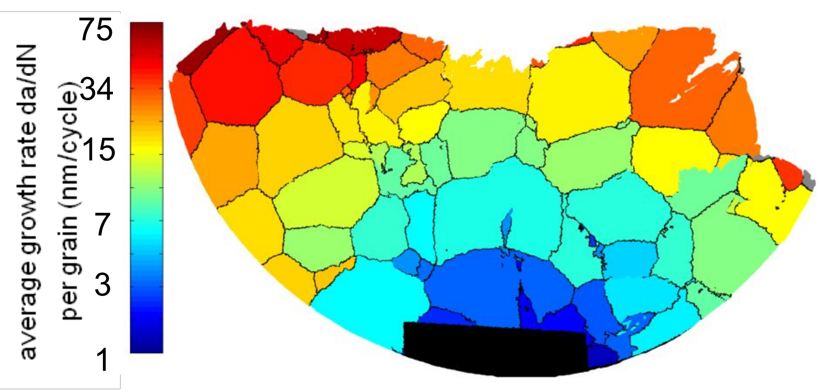

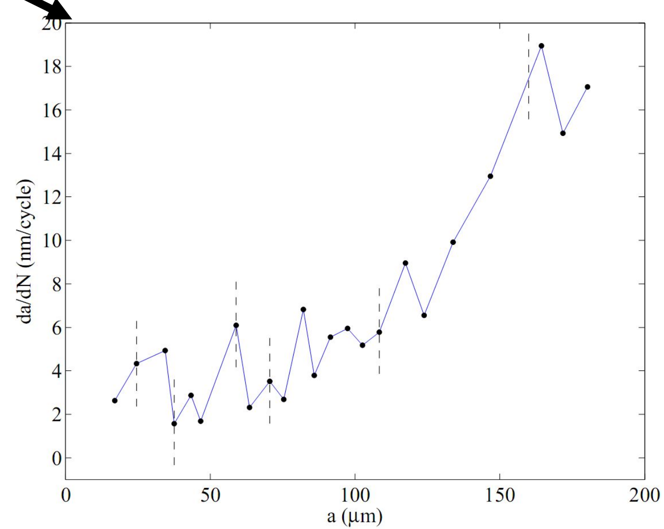

Local growth rate along 2D section

Stripes ↔ Crack Growth Direction

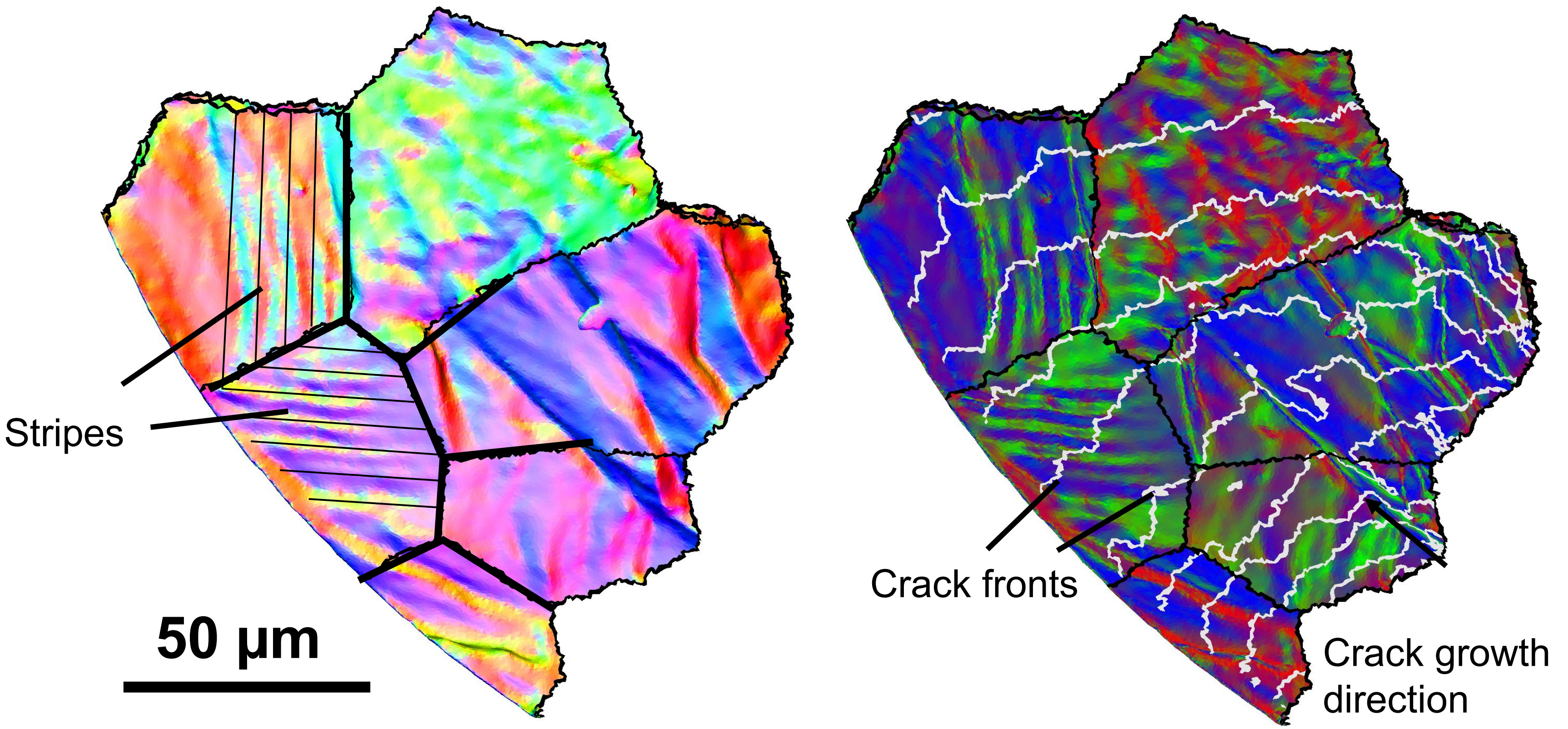

Physical orientation

Crystallographic orientation

Fatigue Mechanisms

Crack propagation through grain boundaries

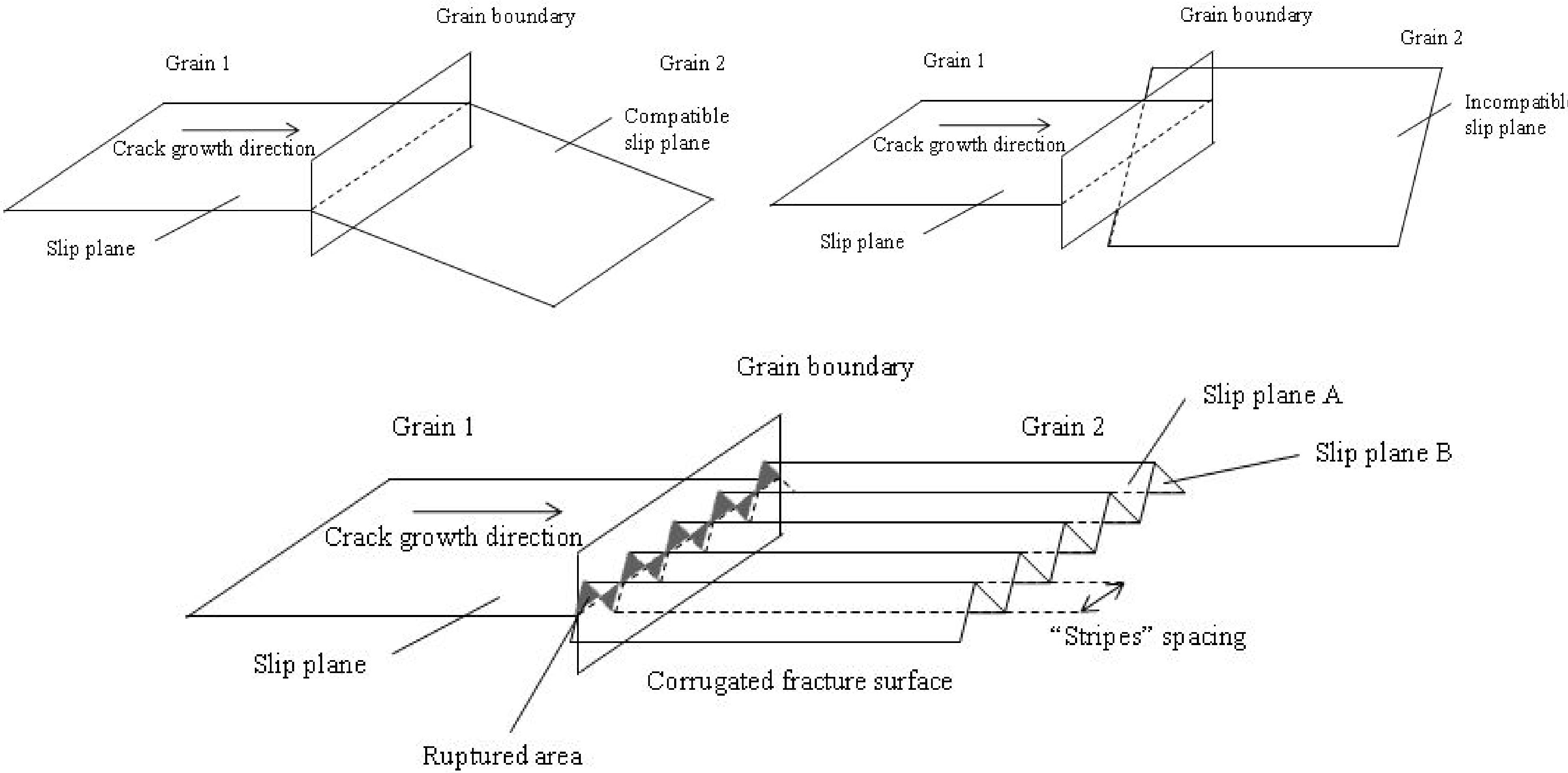

Zhai et al., Int. J. Fat. Eng. Mat. 2005], [Schaef et al., Acta Mat. 2011]

Stripes ↔ Crack Growth Direction

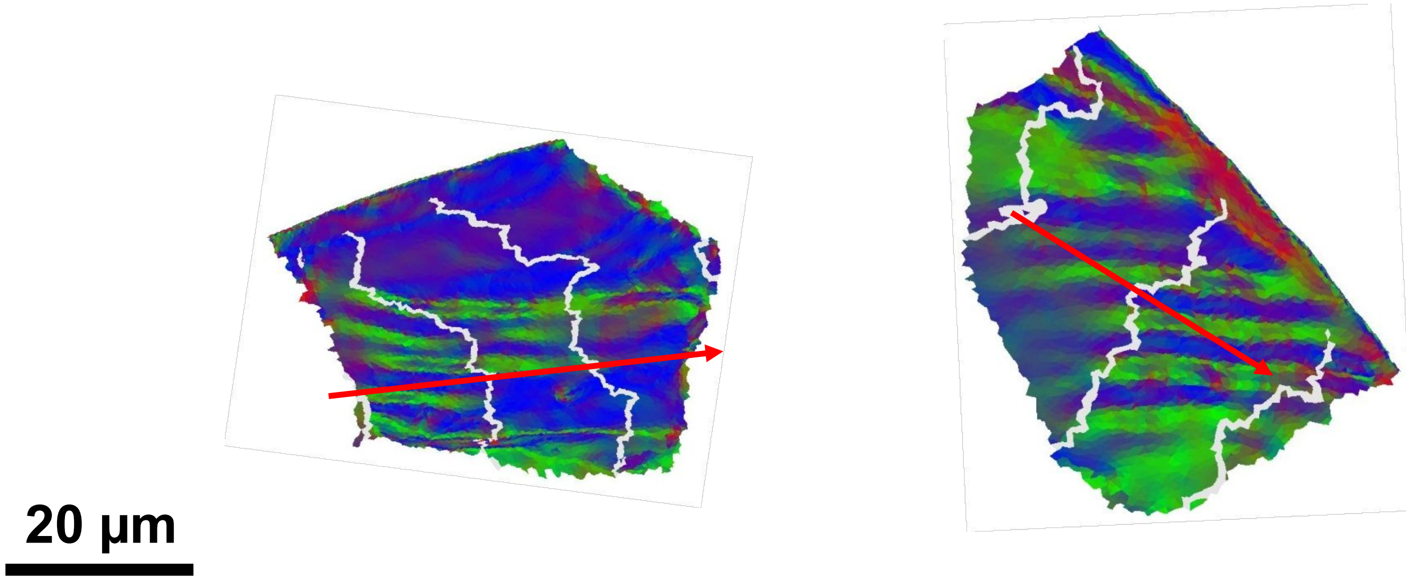

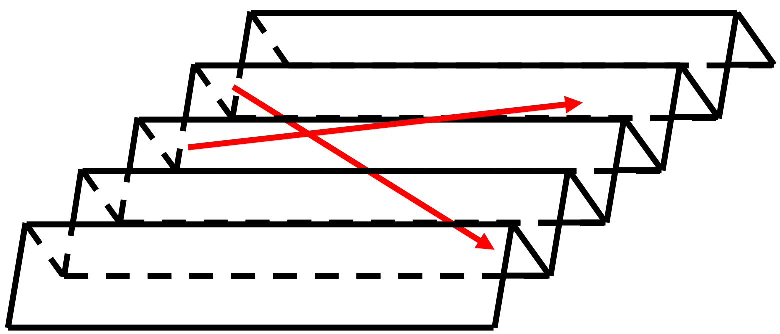

Measured crack growth directions

Crack fronts and stripe directions don't necessarily match

Crack plane v.s. Schmid factor

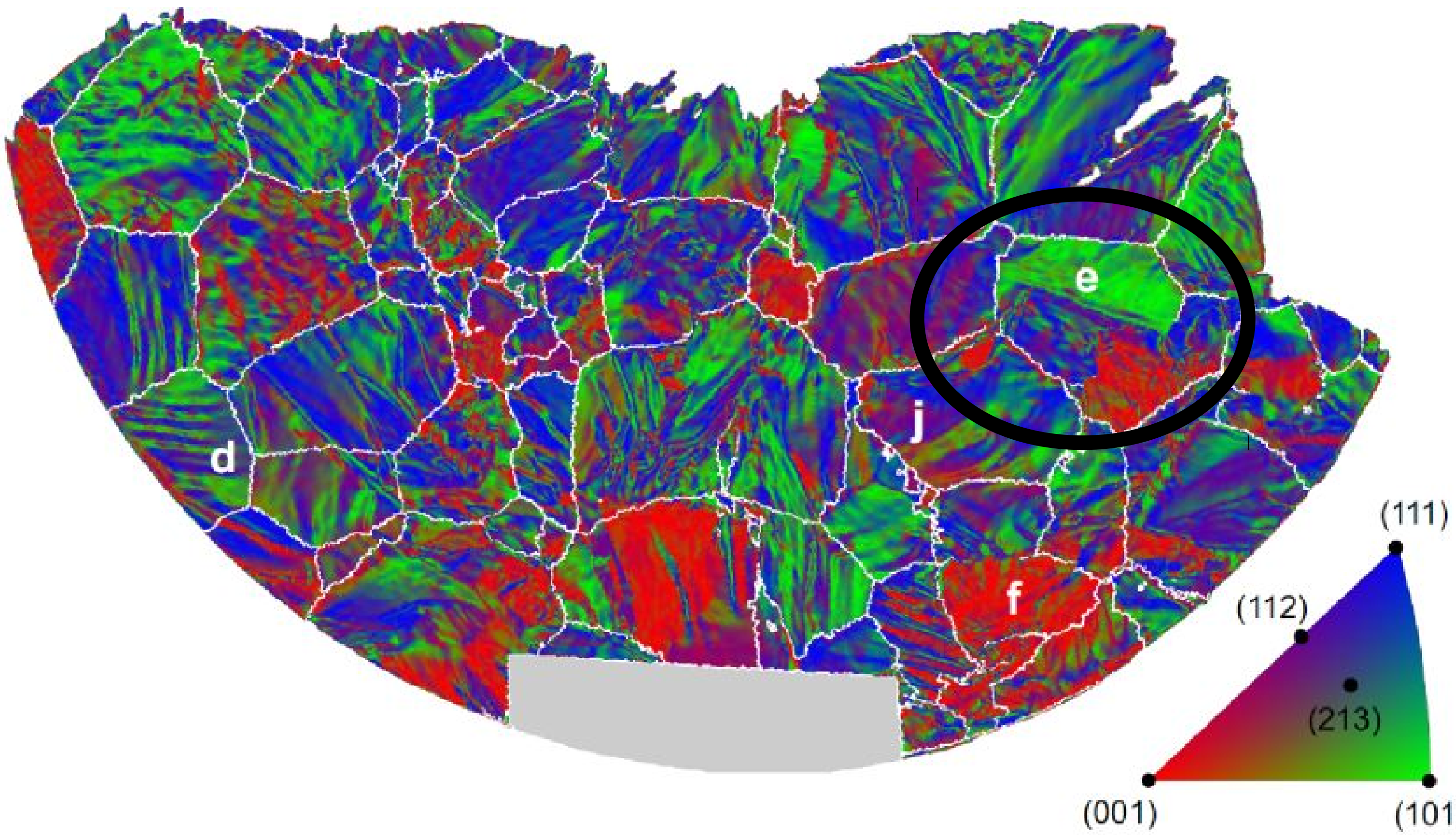

Crack plane v.s. Schmid factor

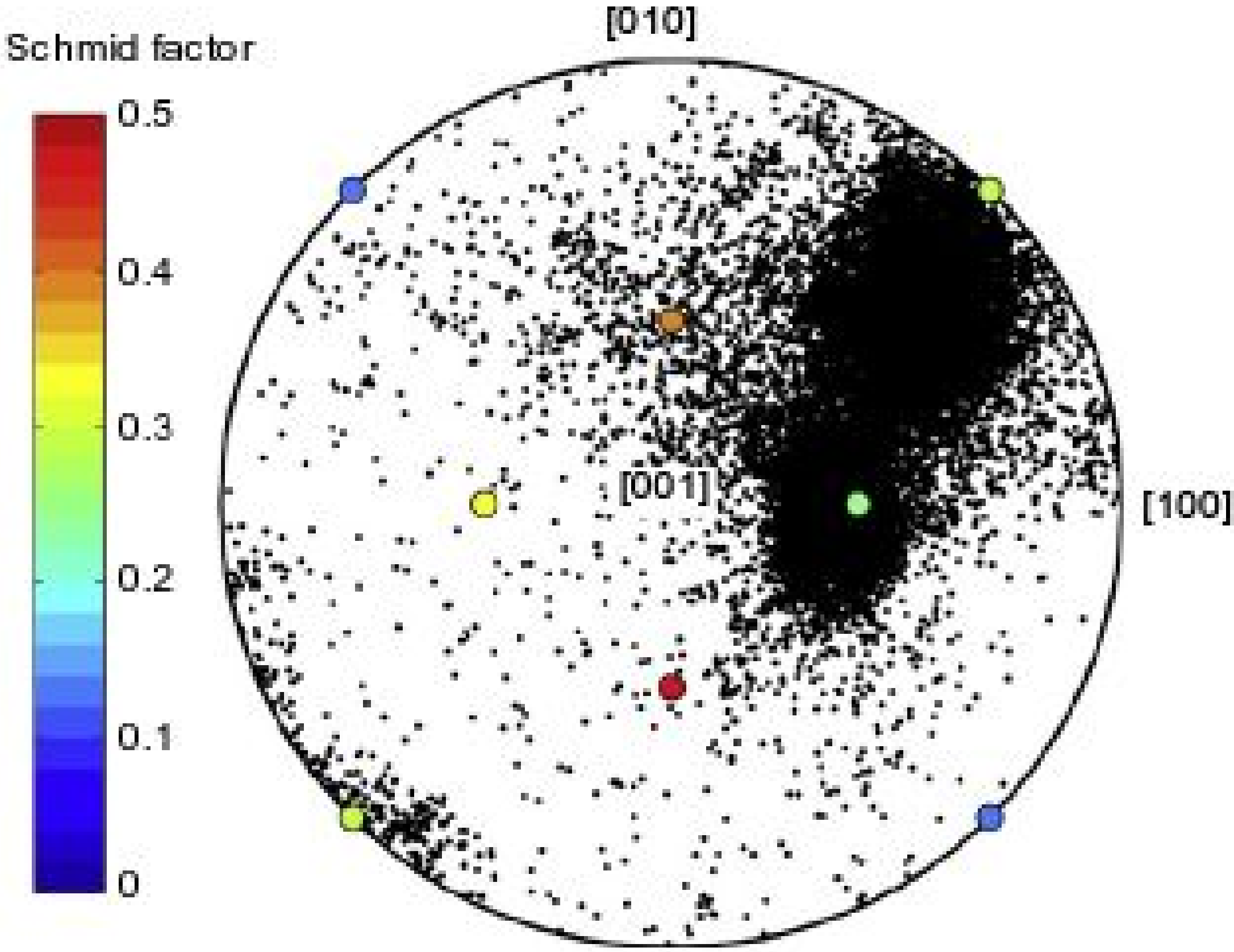

Schmid factors + uniaxial tensile test → much too simple

Crack plane v.s. Schmid factor

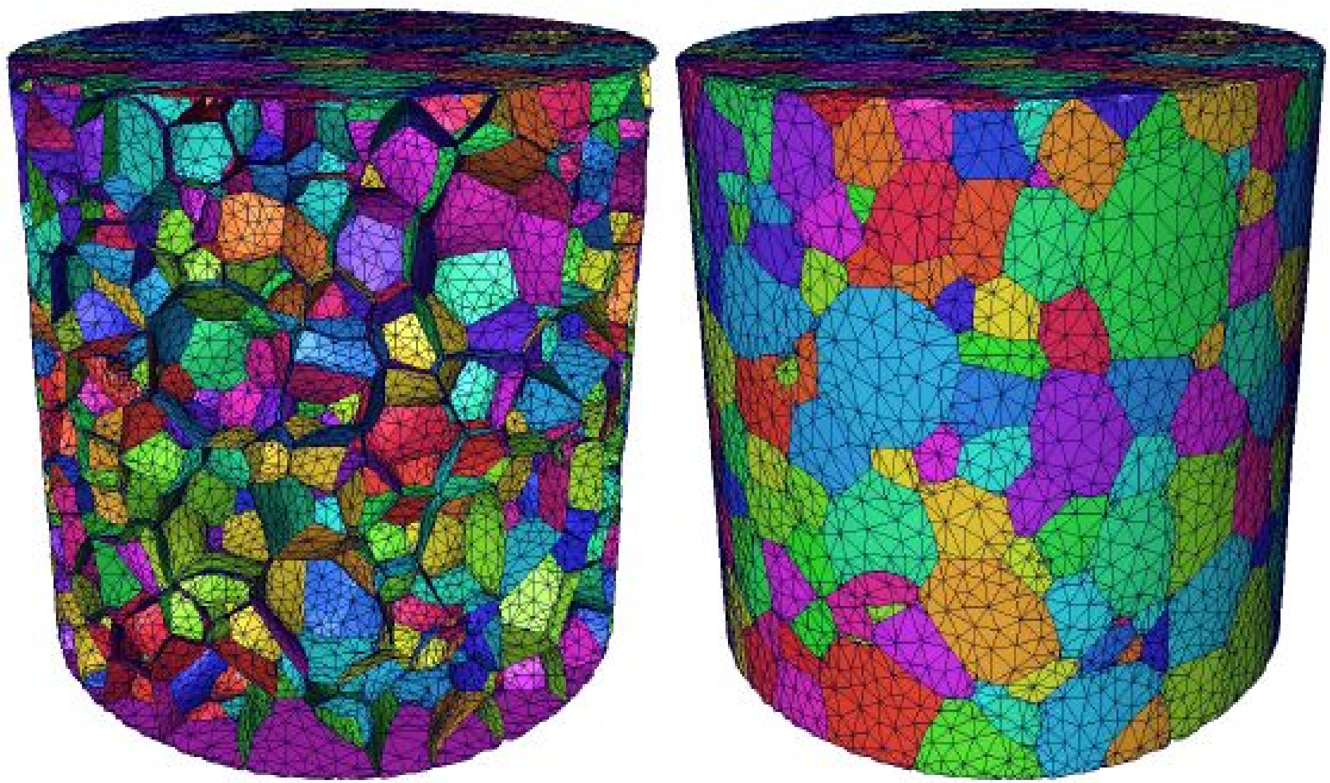

Courtesy. Henry PROUDHON ENSMP Paris

Crack plane v.s. Schmid factor

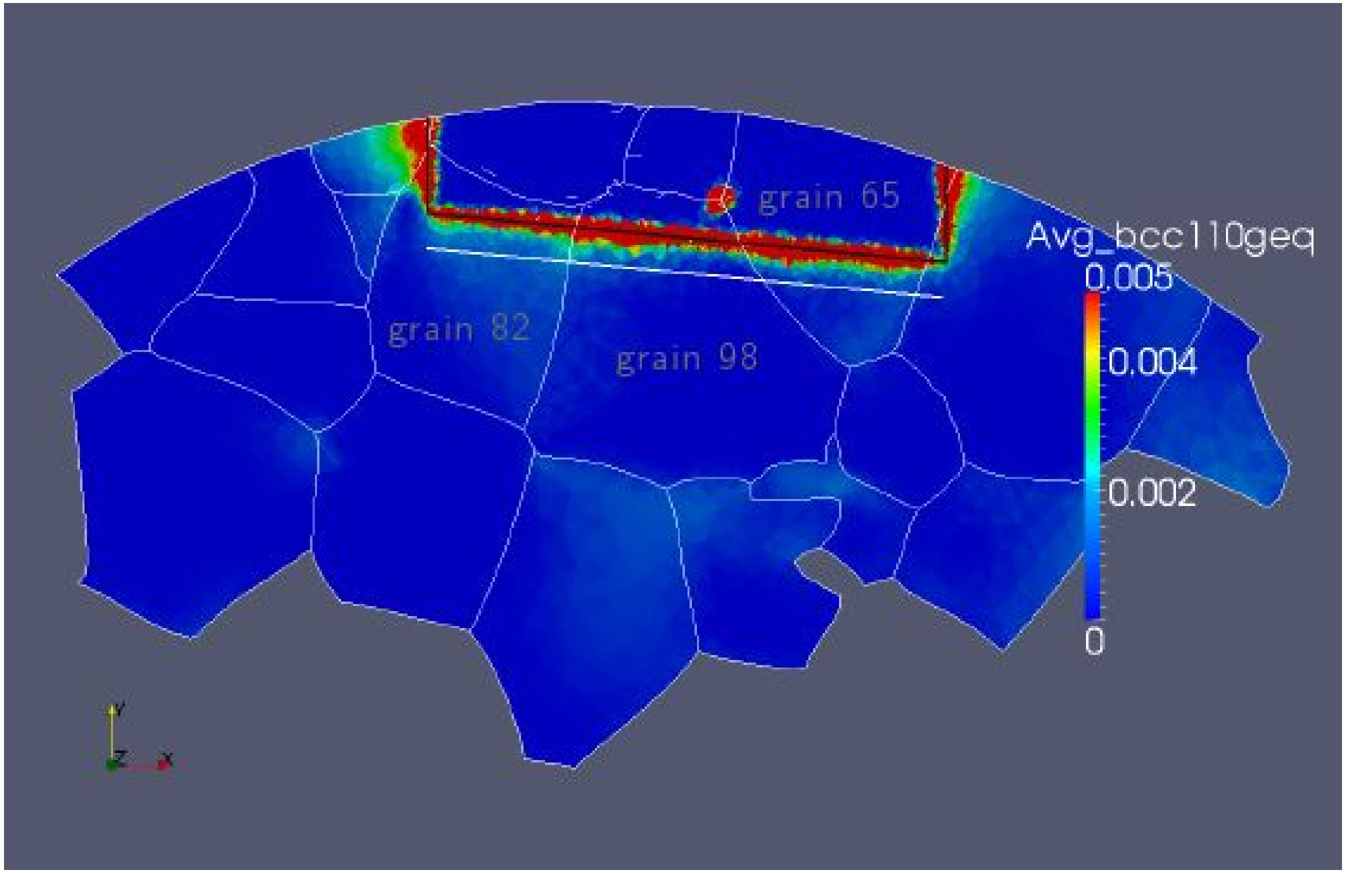

Accumulated plastic strain

- Microtomography to observe short fatigue crack growth in-situ in a grain mapped sample.
  - FIB notches placed in specific grains
  - In-situ fatigue using machine from INSA de Lyon
  - Use radiographs to monitor crack
  - Use tomograms to record crack evolution in 3D

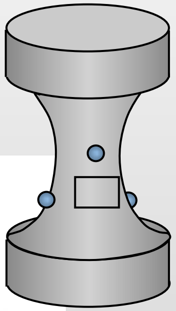

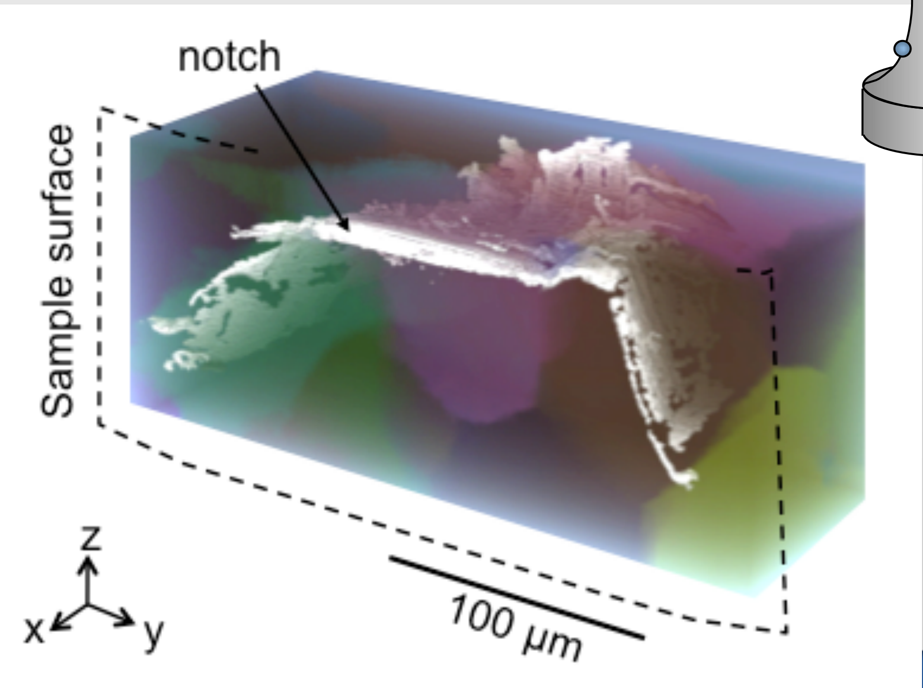

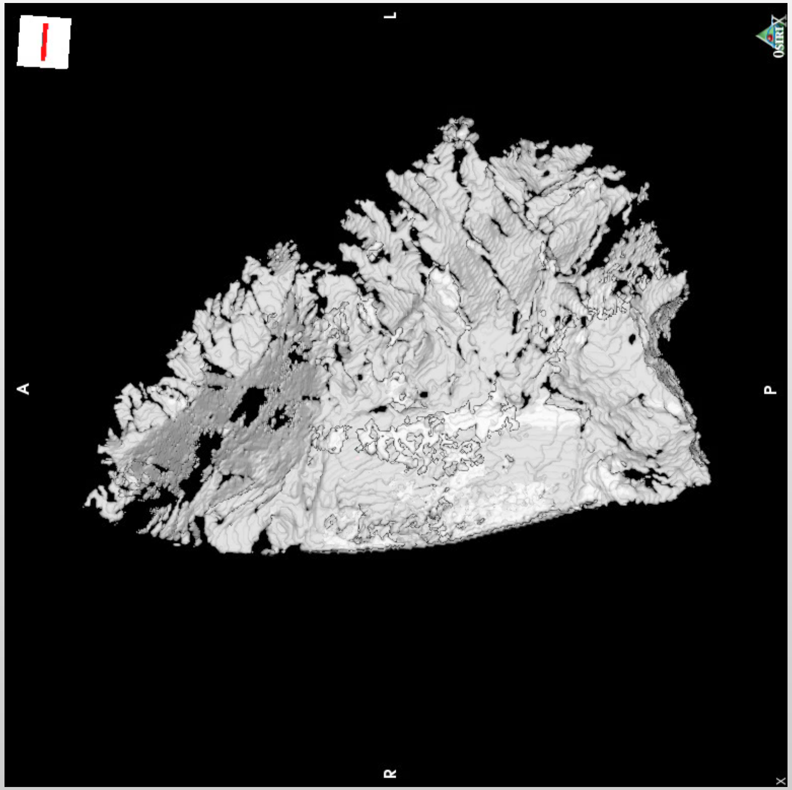

A. King *et al.*, *Acta Mater.* **59** (2011) 6761–6771

Crack growth rate

- Derive local crack growth rate from series of tomograms
  - Use projection of crack on x-y plane for ease of viewing

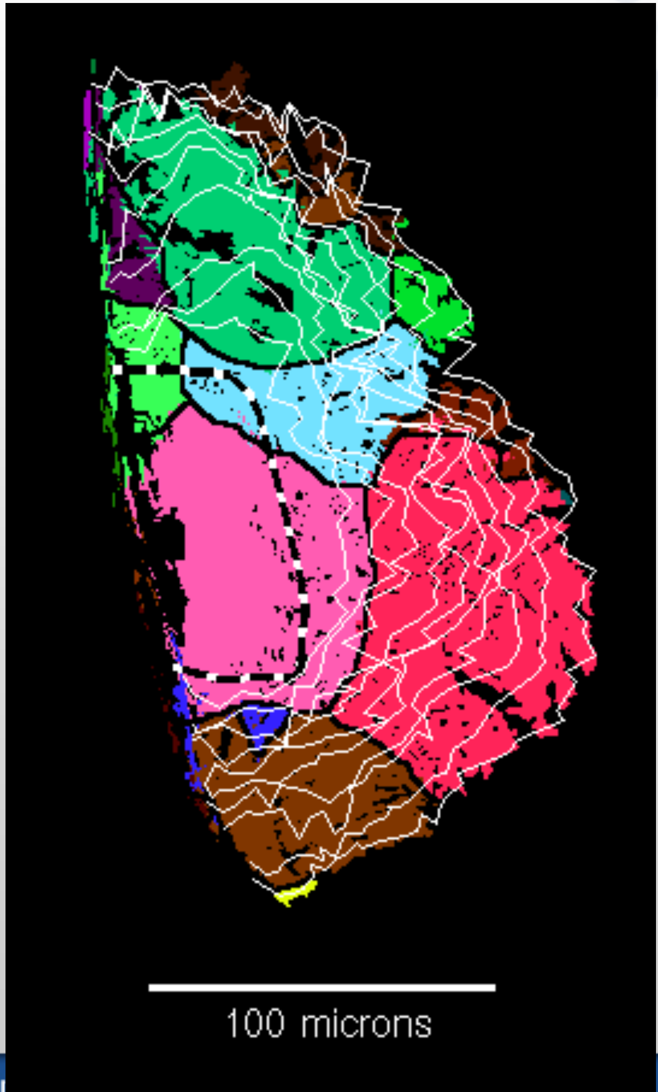

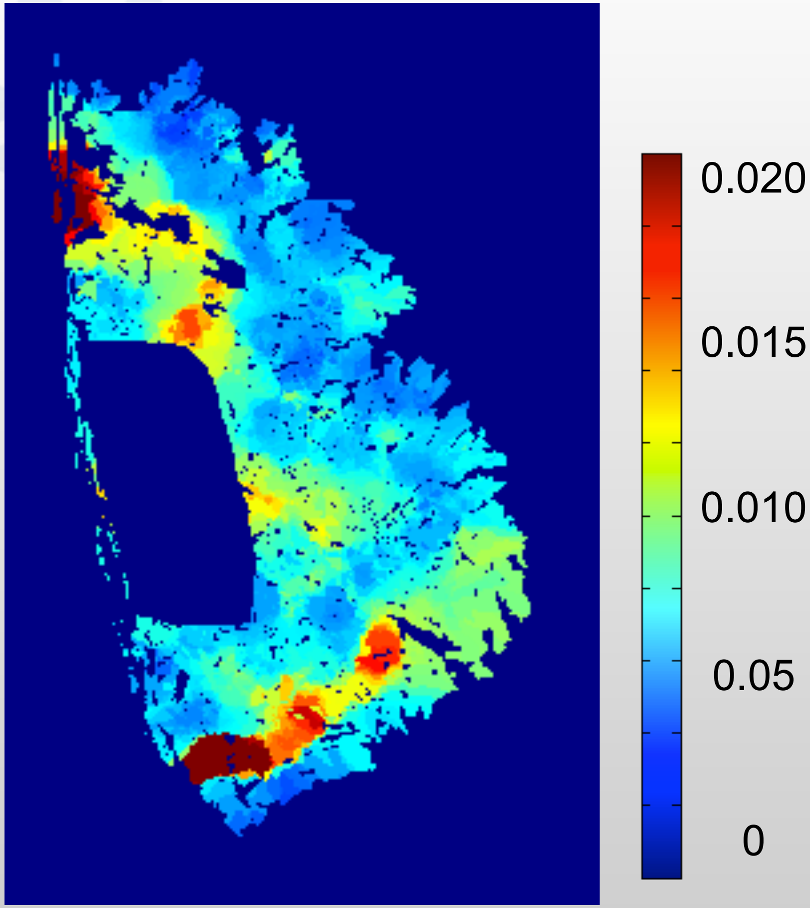

Crack growth rate (μ/cycle)

Crack and microstructure

- Look at final crack shape compared to microstructure

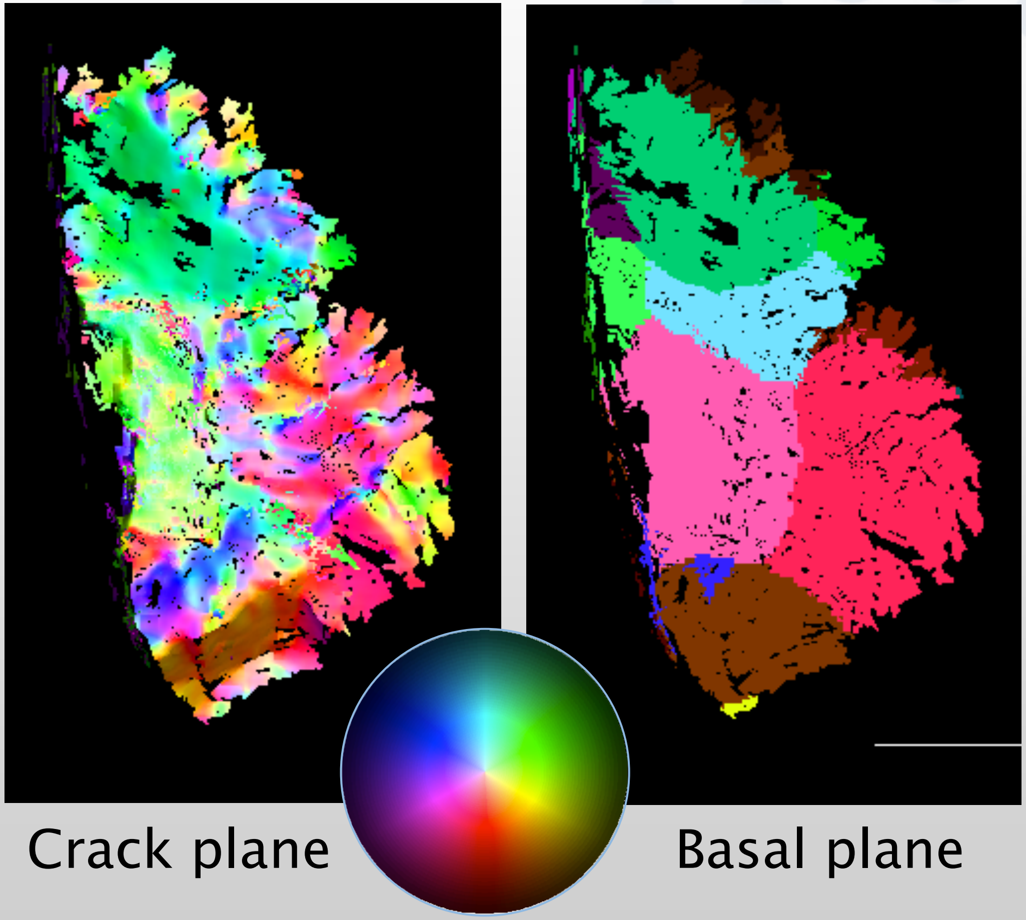

Crack plane

Basal plane

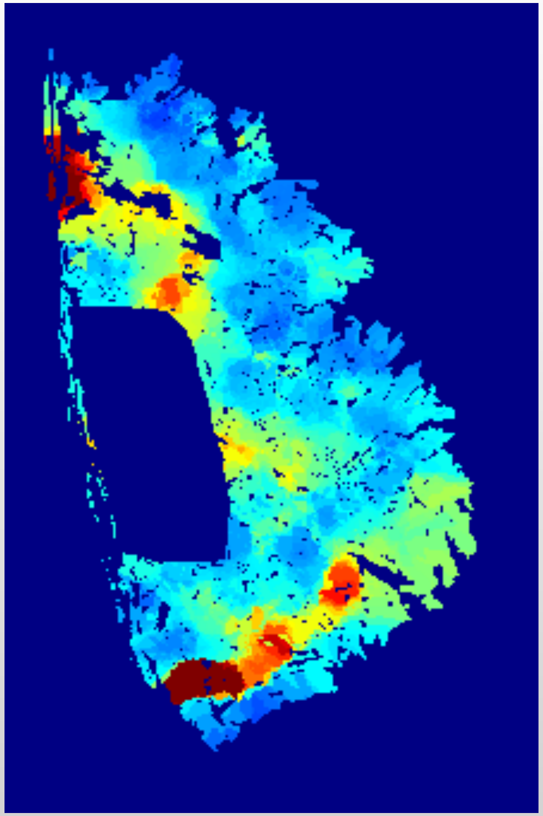

Crack growth rate

Microstructure analysis

- Schmid factor – assuming uniaxial tensile stress, calculate the shear stress resolved onto slip systems - ~driving force
- Tilt/Twist description of boundaries – how easily can a crystallographic crack reinitiate when crossing a boundary

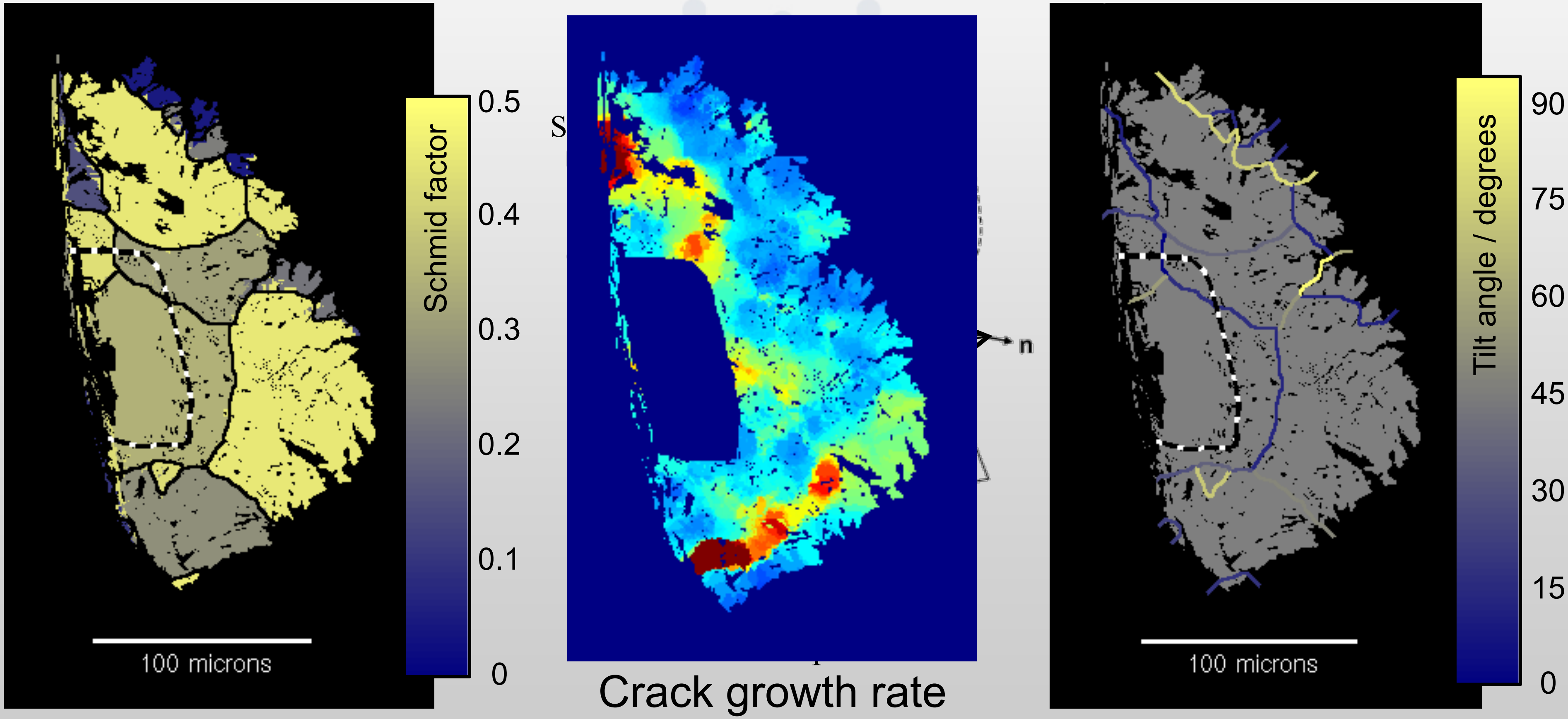

Neighbourhood factors

- Fast, non-crystallographic crack growth in a grain with low driving force
  - Need 3D neighbourhood and chronology to understand
  - Crack advances subsurface, leaving a ligament which then fails rapidly
  - Surface observations would be misleading

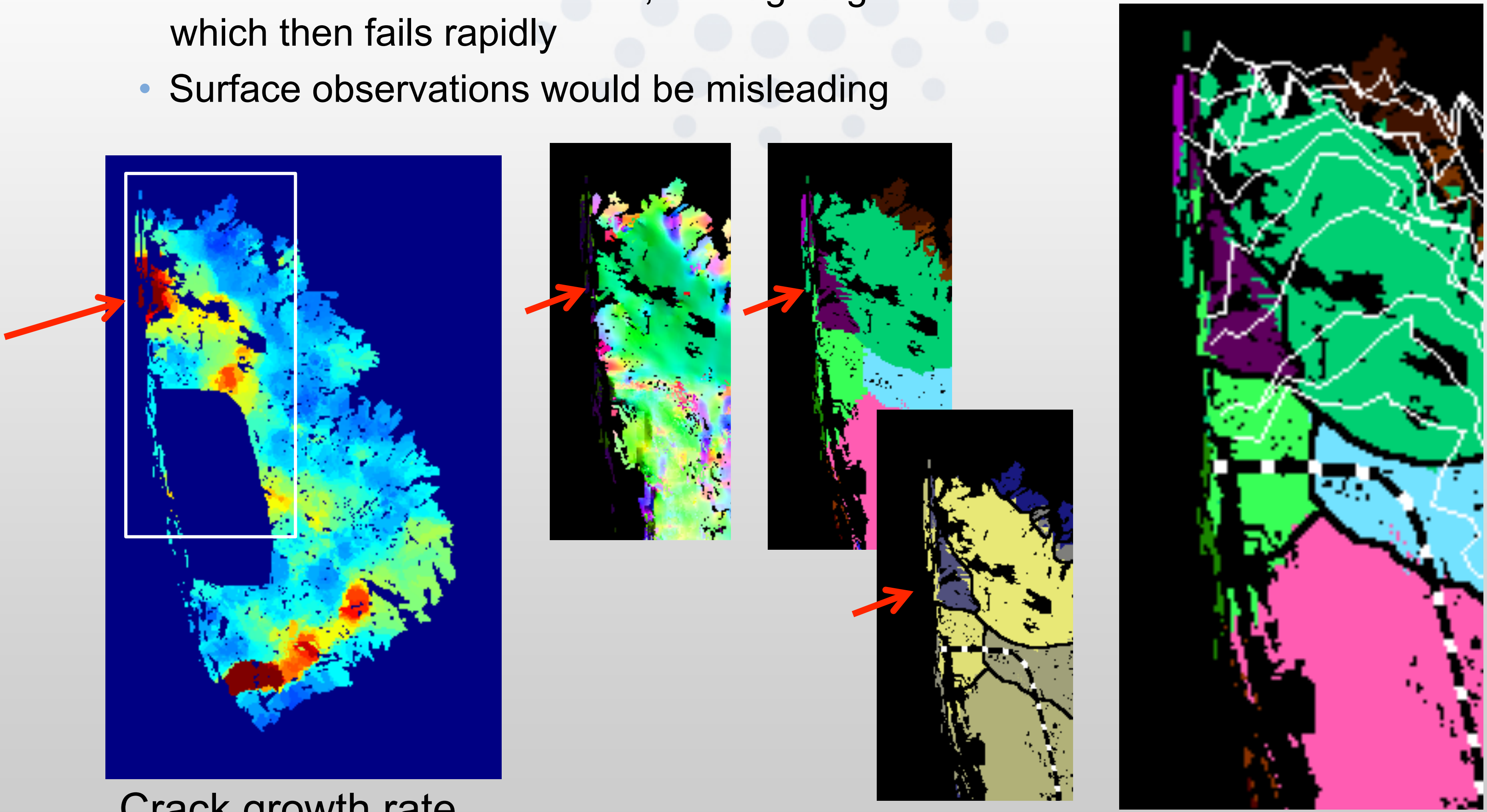

Crack growth rate

Compatibility to notch

- One more factor
  - The crack grows from the plane of the notch onto the slip planes
  - Somewhat like grain boundary twist, the compatibility of these planes is important

- Finally, seems that all the factors discussed influence behaviour
  - Challenging modelling problem
  - More data would be interesting
  - How does crack get past obstacles?

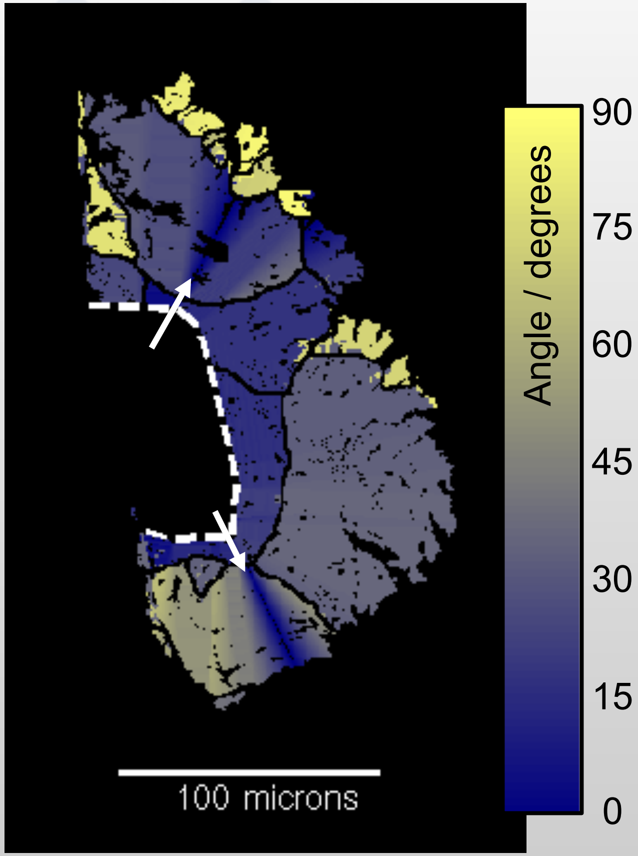

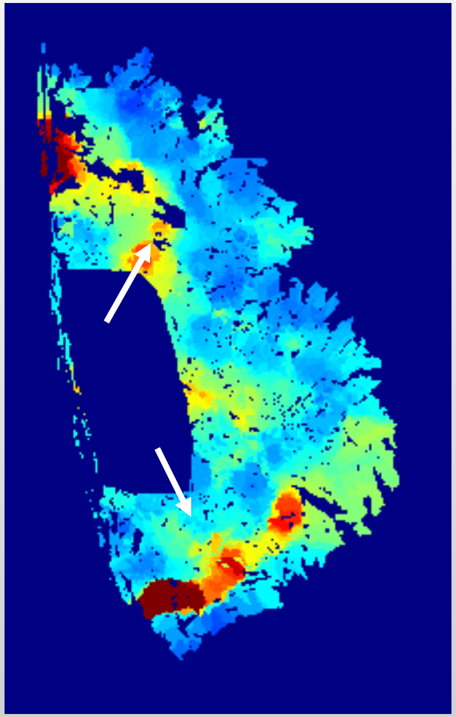

Crack growth rate

Limitations

- Spatial resolution too low for imaging fine crack details
- DCT only works for undeformed material
- Time sampling (GB crossing)
- Microstructure influence → Low stress levels
  → Long experiments
- SR experiments → low availability
- Artificial defects
- Modelling!!

What's next?

- Crystal plasticity analysis of short cracks
- Crack closure measurement + in situ cycling
- Fatigue test at (relatively) high temperature
- Fatigue test under vacuum
- Combine imaging with strain measurements

...